Morphology, Stratigraphic Distribution and Origin of Calcite Nodules from a Late Devonian Mixed Volcanic-Sedimentary Sequence, Southeastern Massachusetts

A Senior Honors Thesis for the Department of Earth and Ocean Sciences

Selva Marroquín

Tufts University, 2014

Acknowledgements

I would like to acknowledge the assistance of several individuals within The Department of Earth and Ocean Sciences. First, Jack Ridge and Molly McCanta for providing many resources and insight for this thesis; and Anne Gardulski for serving on my committee and taking the time to make valuable edits to the draft of this thesis. Finally, I would like to thank my advisor Jake Benner for his patience and commitment to my understanding of the material, for answering any and all questions, and thoroughly editing multiple drafts.

Table of Contents

Abstract

In 2008 a unique sedimentary unit of red sandstone with abundant calcite nodules was discovered within the northeast corner of the Narragansett Basin in southeastern Massachusetts. Although the outcrop of the calcite nodules examined in this paper was destroyed in 2010, the nodules collected in 2008 were interpreted preliminarily as calcite rhizoliths representing a preserved root horizon (Benner and Gardulski, 2010). The calcite nodule-rich unit lies stratigraphically below a dated rhyolite flow (Late Devonian, ~373 Ma; Thompson and Hermes, 2003) and is within the "lower portion" of the Wamsutta Formation, beneath an unconformity with the Carboniferous sedimentary rocks of the Wamsutta Formation. The outcrop area was investigated to determine whether the calcite features represent rhizoliths within a paleosol, possibly preserving an early, deeply rooted (~3m thick) plant ecosystem within a pyroclastic deposit. Petrographic analysis revealed an abundance of devitrified glass within the matrix of these samples as well as pumice and lithic fragments suggesting a volcanic origin of the deposit. Scanning electron microscopy revealed amorphous carbon fragments within all of the sample types, which supports a biogenic origin of the calcite nodules. Combining this microscopic data with stratigraphic fieldwork it was confirmed that most of the calcite nodules are preserved rhizoliths within a pyroclastic deposit from at least the Late Devonian.

Chapter 1 : Introduction

Within the Wamsutta Formation of the Narragansett Basin in southeastern Massachusetts lies a unique sedimentary unit containing calcite nodules discovered during fieldwork in 2008. Preliminary research on the calcite nodules within this unit has been presented at a professional meeting (Benner and Gardulski, 2010) but has not been subjected to peer-review or published. The calcite features were initially interpreted as calcite rhizoliths representing one or more preserved root horizons. The outcrop of the calcite nodules examined in this paper was destroyed by urban development in 2010 and rocks previously collected in 2008, as well as further outcrop investigation of the area, are used for analysis in this study. The area of interest is located west of MA Route 1 on the west limb of a northeast plunging syncline (Maria and Hermes, 2001). The age of the sedimentary units of interest are constrained by an overlying rhyolite flow dated at ~373 Ma (Thompson and Hermes, 2003), and by their intimate association of other volcanic deposits of similar petrologic characteristics. The age of the sedimentary unit containing the calcite nodules, therefore, dates to at least the Late Devonian, a period of rapid evolution of terrestrial plant ecosystems to include anatomy that can be recognized in present-day plants (i.e. seeds and deep root systems). If the unit is a paleosol, or ancient soil horizon, it may have preserved some of the earliest deeply rooted plant ecosystems of the Late Devonian.

The objectives of this thesis are threefold:

1) Establish whether the calcite nodules are biogenic or inorganic
2) Establish whether the horizon of interest is a paleosol
3) Describe the stratigraphic distribution of this calcite rich horizon

Methods of inquiry to address these objectives included fieldwork, hand sample description, microscopic petrography, and scanning electron microscopy.

Chapter 2 : Geologic Setting

The material examined in this thesis came from what is currently known as the Wamsutta Formation within the Narragansett Basin of southeastern Massachusetts and eastern Rhode Island (Fig. 2.1). The smaller, coeval Norfolk Basin lies only a few kilometers

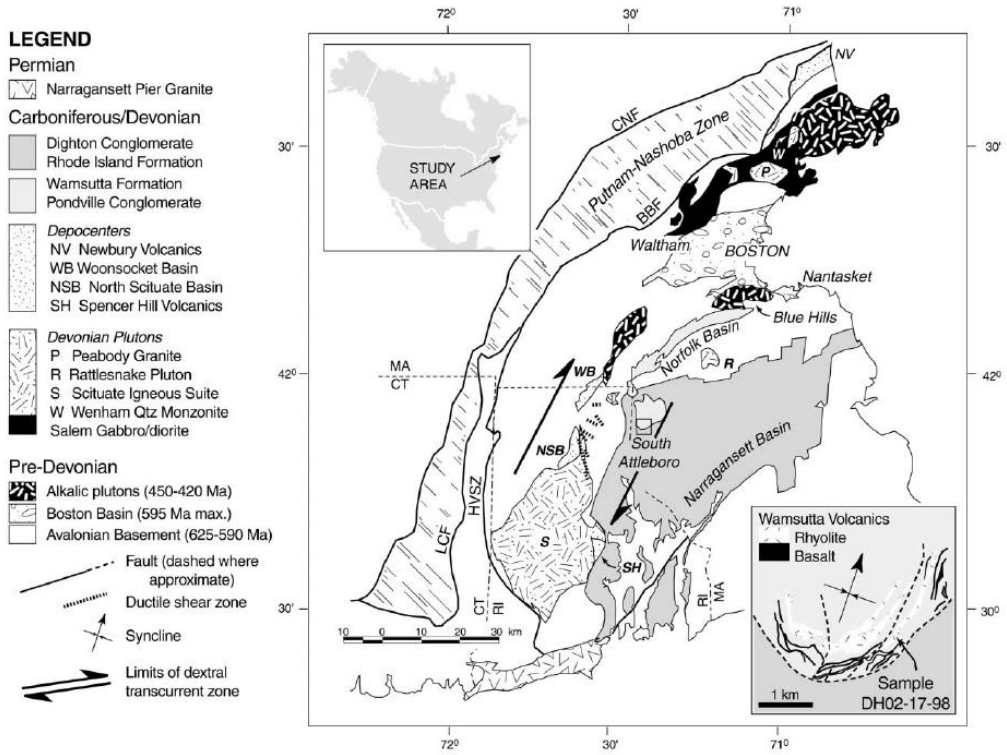

Figure 2.1: Volcanics are interstratified with sedimentary rock facies in the study area, which is located on the west limb of the north-plunging syncline. The box in the lower right corner is an expanded view of the field area, and shows the sample location for the dated rhyolite unit (Thompson and Hermes, 2003). The field area for this study is highlighted with a red star.

north of the Narragansett Basin; Precambrian basement plutonic rocks separate the two. The sedimentary rocks of the Narragansett and Norfolk Basins comprise several formations, in ascending order: Pondville Conglomerate (conglomerate and coarse sandstone), Sachuest Arkose (arkosic sandstone), Wamsutta Formation (mixed conglomerate, sandstone, shale and volcanics), Rhode Island Formation (predominantly gray shale with fluvial sandstones), Purgatory Conglomerate (conglomerate) and Dighton Conglomerate (conglomerate) (Murray et al., 2004).

The lower part of the Wamsutta Formation contains bimodal (rhyolite and basalt) volcanic flow deposits that are consistent with extensional tectonic activity (Thompson and Hermes, 2003). Interstratified with the volcanics are sedimentary units including sandstone, conglomerate and shale lithologies. Zircons from one rhyolite flow have been dated at 373 +/- 2 Ma, (See Figure 2.1; Thompson and Hermes, 2003), an age that infers sedimentation in the basin began in at least Late Devonian time. The upper part of the Wamsutta Formation is believed to be of Westphalian B and part of C age (Late Carboniferous) due to its relationship with the overlying Rhode Island Formation as well as evidence from plant remains (Lyons and Darrah, 1977) (Fig. 2.2). Therefore, within what is now known as the Wamsutta

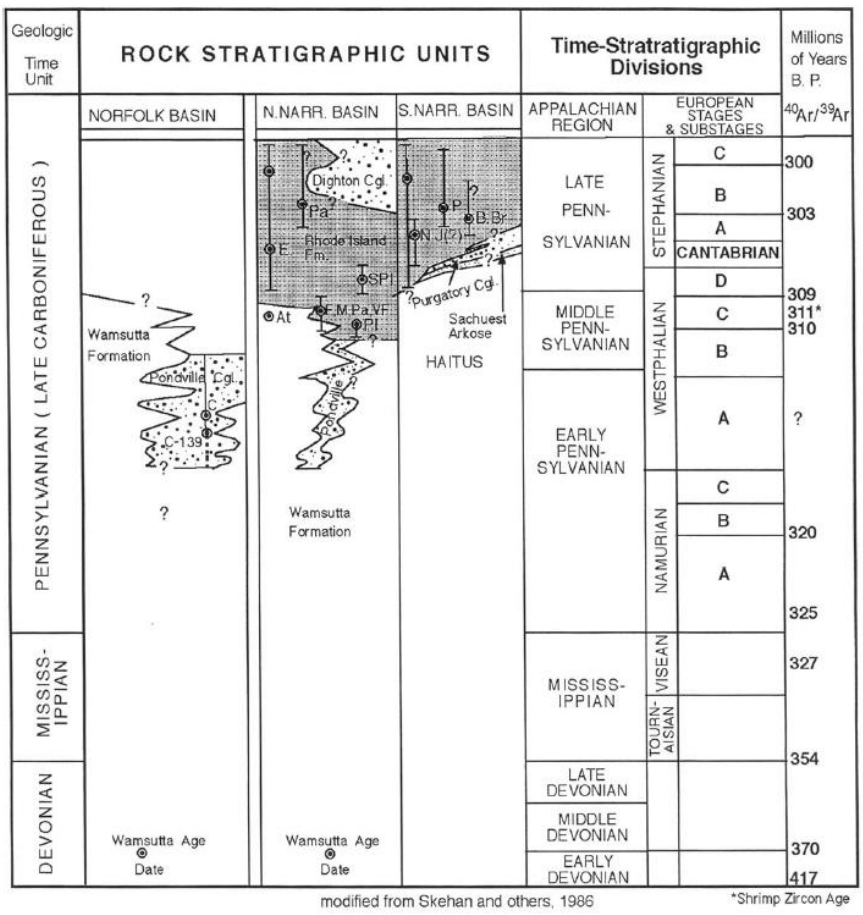

Figure 2.2: Stratigraphic columns highlighting the relationship between the facies within the Norfolk and northern and southern Narragansett Basin. The central column represents the northern Narragansett Basin and shows the dated lower portion of the Wamsutta Formation (~373 Ma) and the Carboniferous sedimentary rocks of the upper Wamsutta Formation. This figure highlights the 60 Ma unconformity that exists within the Wamsutta Formation (Murray et al., 2004).

Formation, an unconformity exists below the Westphalian sediments, representing a ca. 60 m.y. gap. The unconformity within the Wamsutta Formation may be correlative with a Westphalian unconformity in the Maritime Basins of Northeastern Canada (Murray et al., 2004) (Fig 2.3).

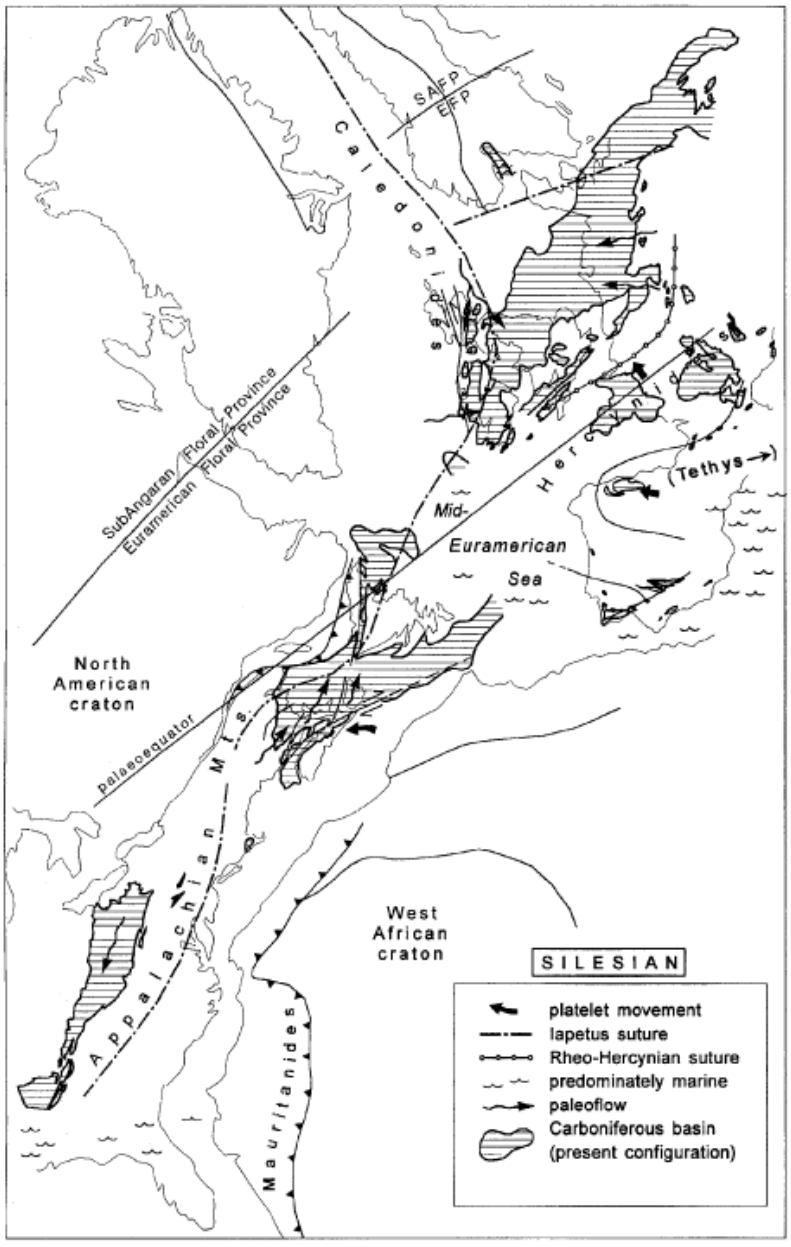

Figure 2.3: Locations of Carboniferous basins of Nova Scotia, as well as the eastern United States, which are underlain by Middle Devonian-Permo-Carboniferous strata (from Calder, 1998). These may be analogs of the Narragansett Basin investigated in this study.

The depositional environment of the upper Naragansett Basin Carboniferous lithologies has been interpreted as deposition on wet alluvial fans that formed along rift basin margins (Murray et al., 2004, Mosher, 1983, Cazier, 1987). These interpretations are consistent with the environment necessary to preserve the array of facies and fossil flora found in the Late Carboniferous section (Lyons and Darrah, 1978). The sedimentary rocks evaluated in this study lie below the unconformity, within the lower portion of the Wamsutta formation in the Late Devonian section between a prominent basalt flow and the dated rhyolite flow.

Chapter 3 : Field Relationships

The calcite-rich sedimentary rocks examined for this study come from one outcrop, site X1, located on the west limb of a northeast plunging syncline (Fig 3.1). Multiple northeast trending faults that cut across and offset the volcanic flows and sedimentary units within the field area (Figs. 3.1, 3.2). The outcrop of rocks at site X1 has since been destroyed but had been photographed extensively to provide sufficient field relationship information from the calcite unit and below to create a stratigraphic column (Fig. 3.3, 3.4).

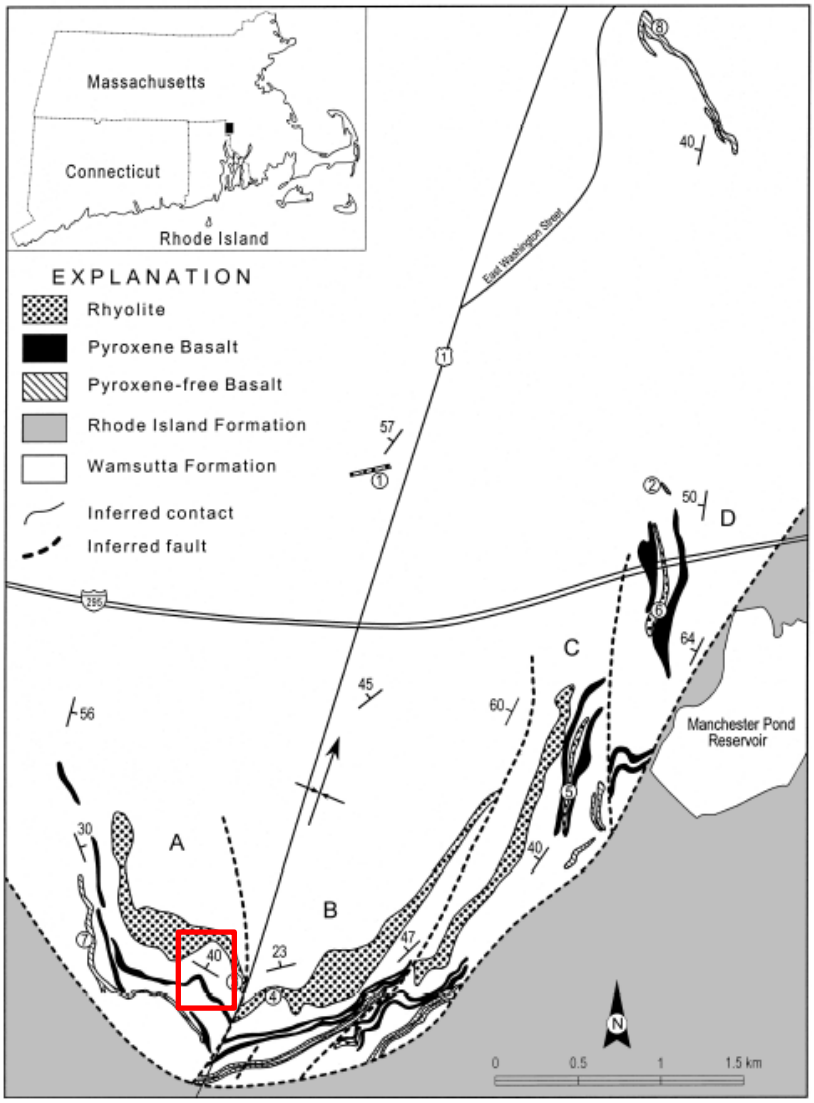

Figure 3.1: Geologic map of the field area displaying the volcanic units (rhyolite and basalts), inferred faults, and northeast 40 degree dip of the rock units (Maria and Hermes, 2001). Sites X1 and X2 fall within the red box that outlines the extent of the field area for this study.

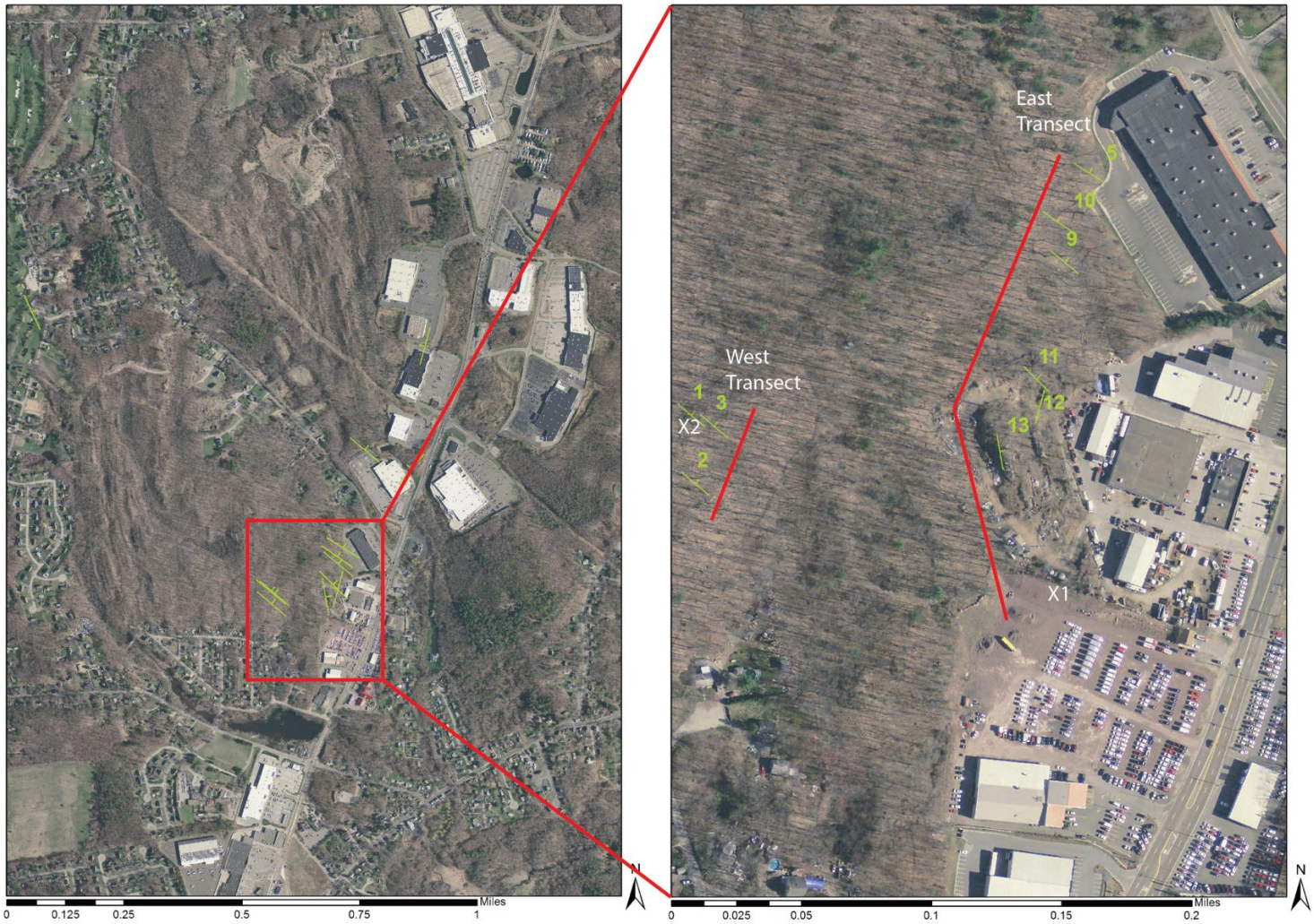

Figure 3.2: Aerial Photos of the field area with strike and dip symbols in green, most all pointing to a northeast dip direction. Enlarged area on right is the field area showing east and west transects (red lines) through the lithologic units of interest at sites X1 and X2. The east transect goes around an inferred fault through the area to avoid repeated units.

Figure 3.3: Photographs of the calcite rich outcrop at Site X1, before and after destruction of the site at a car sales lot in southern North Attleborough, MA.

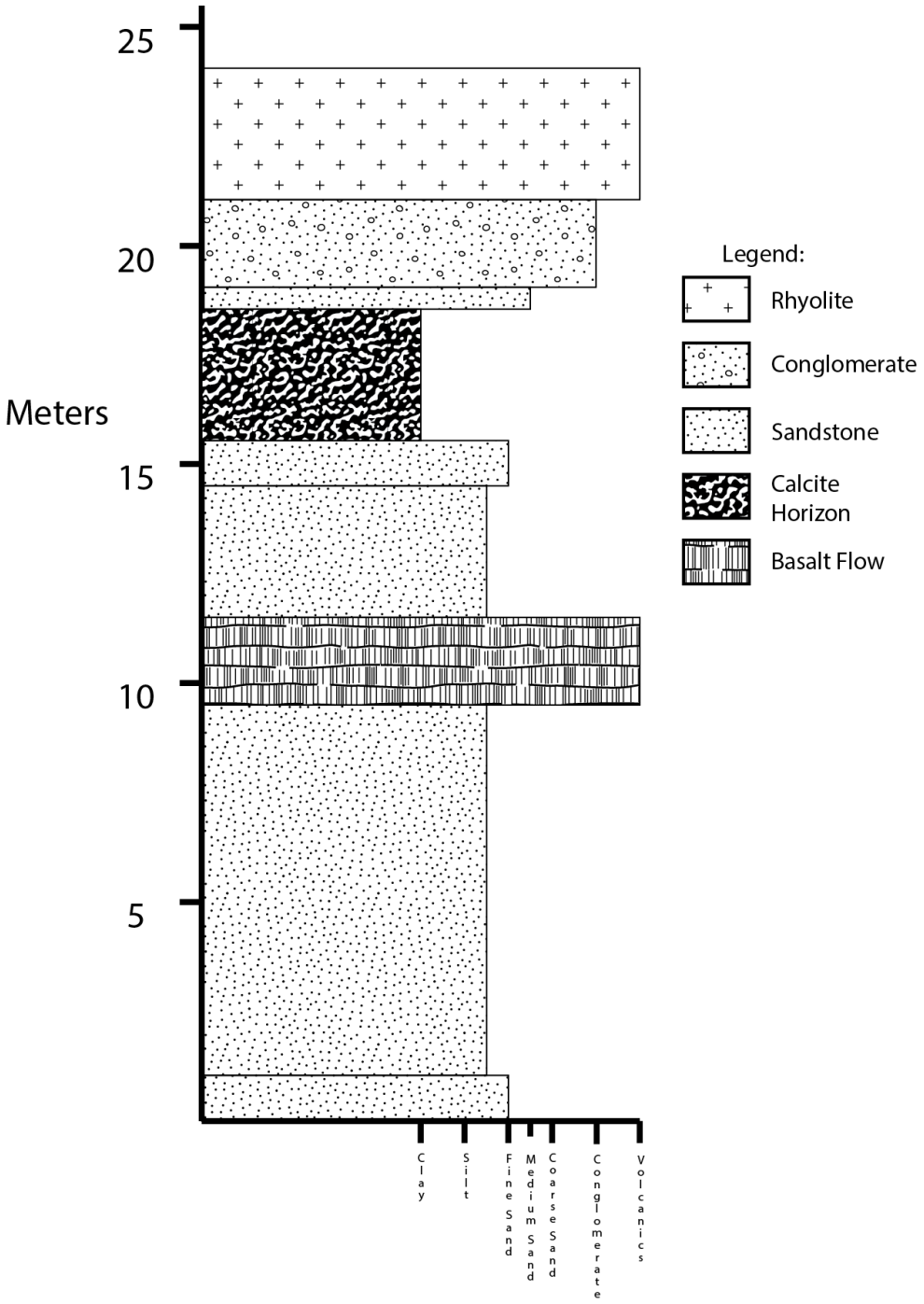

Figure 3.4: Stratigraphic column from units at site X1 shows the relationship of the calcite nodule horizon with the overlying rhyolite and underlying basalt.

The sedimentary and associated volcanic rocks examined in this study are constrained at their upper boundary by a thick (~5+ m) rhyolite flow correlative with the dated rhyolite flow, ~373 Ma (Thompson and Hermes, 2003). The rhyolite contains abundant flow banded layers oriented N58W 44NE (Fig 3.2, point 5), and smooth slickensided faces. The rhyolite flowed over a volcanically-derived conglomerate unit that contains abundant large (~20 cm) granite, rhyolite, and basalt matrix-supported clasts (Fig. 3.5). The contact between the two units is oriented at N55W 30NE and is noted on Figure 3.2 as site 10. The subangular clasts within the ~2 m thick conglomerate contain an abrupt contact with coarse sandstone (Fig. 3.6). A thin tuffaceous sandstone (~.5 m thick) is present just above the calcite-rich horizon. Within the thin sandstone sedimentary unit above the calcite-rich horizon are several regions

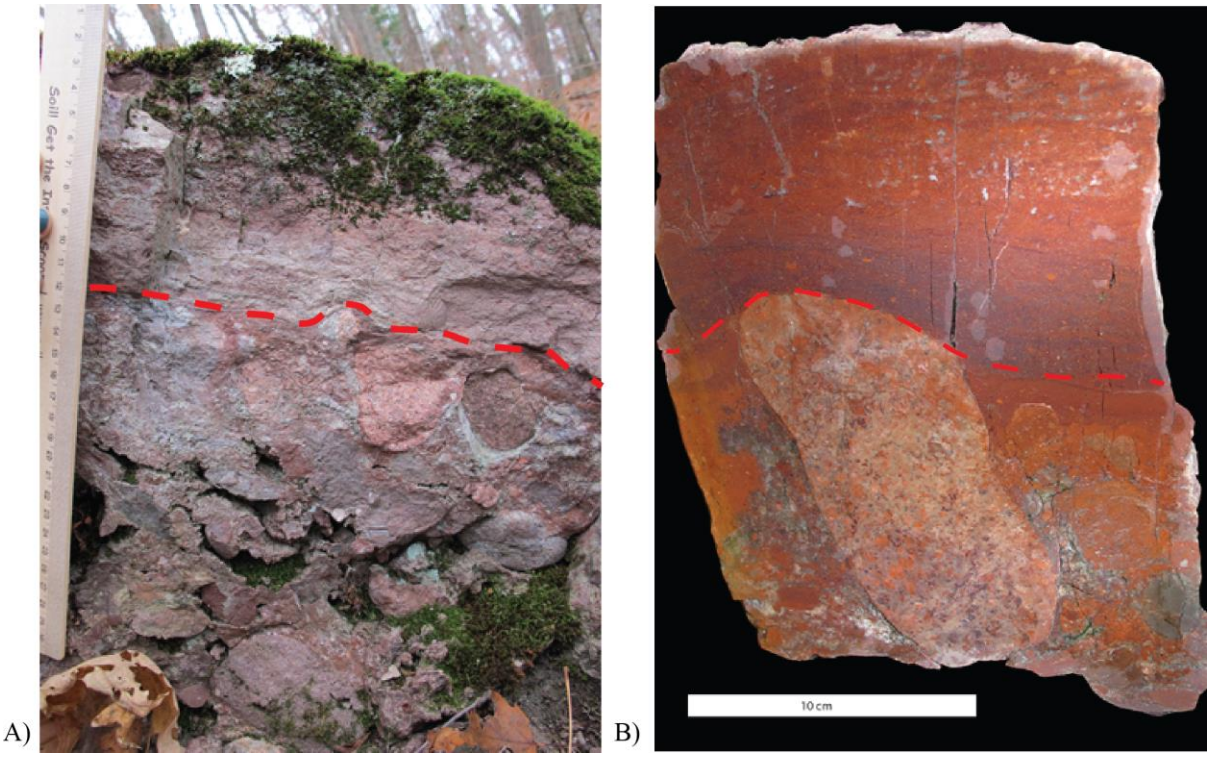

Figure 3.5: Dashed line represents the contact between the rhyolite flow and conglomerate. The sample on the right was taken from the field and cut and polished to enhance the detail of the contact. A large granite clast is within the conglomerate unit of the sample on the left.

Figure 3.6: Dashed line highlights the abrupt contact between the conglomerate and sandstone units within the east transect.

Figure 3.7: Weathered pits within a thin sandstone unit. Some of them are outlined in red.

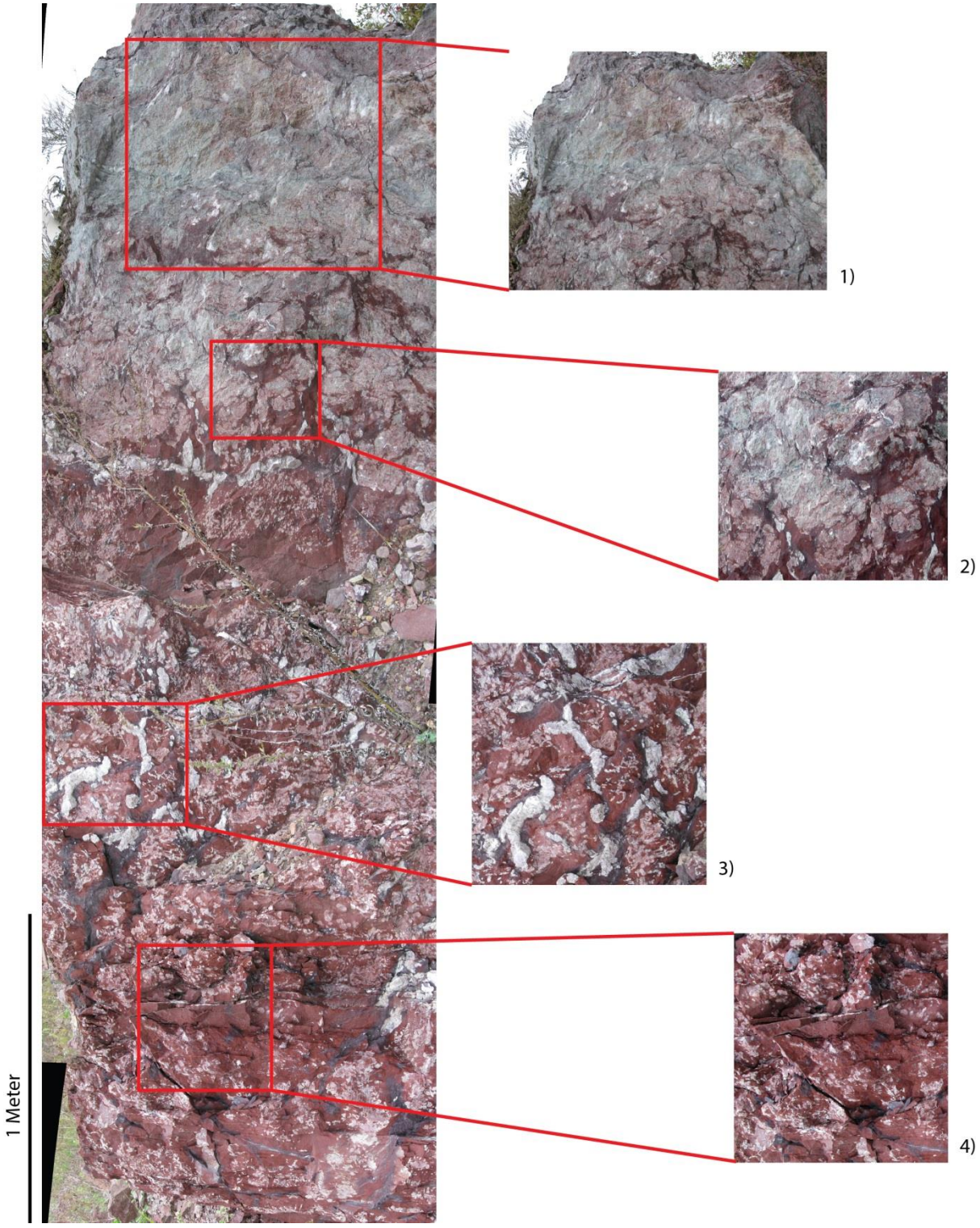

Figure 3.8: Stratigraphic column of the calcite-rich outcrop at Site X1. The expanded boxes highlight four different horizons within the profile. Box one is the massive carbonate that caps the unit. Box two is the nodular calcite while boxes three and four represent two different branching morphologies. Box three is thickly branching nodules while box four is thinly branching nodules.

The entire calcite-rich outcrop at site X1 illustrated varying morphologies of calcite nodules within its 3-meter thickness (Fig. 3.8). The top of the sequence contains a ~0.5 m thick bed of massive carbonate with little to no shale or find sandstone matrix. The massive calcite grades vertically into a pink nodular calcite horizon (~.5 m); the pink color being due to inclusion of red sediment within the nodules. Below this level, red fine sandstone matrix becomes volumetrically dominant with linked, branching thick cylindrical calcite, ~1-2 cm across; these branching structures stand out in the profile due to the lighter white color (Fig. 3.8). Below the thick branching calcite zone are distinct patchy regions, ~20-30 cm across, of thin branching cylindrical calcite that appear in cross section as distinct separate cylindrical nodules or compacted coalesced nodules in areas. The calcite morphology sequence described above is then repeated below the thin branching cylindrical nodules; pink nodules, thick branching cylindrical nodules and patchy thin branching cylindrical nodules at the base. The massive calcite zone is seen only once in this profile.

Photographs of this area show the four units that lie below the calcite rich outcrop at site X1, prior to removal of the outcrop (Fig. 3.9). A tan tuffaceous unit (~1 m) separates the base of the calcite unit from ~3 m of red sandstone and a dark ~2 m thick basalt flow. The basalt flow overlies ~7.5 m of red sediment and ~1 m thick unit of tuffaceous tan sandstone with planar cross beds. All four of these units are dipping north and the stratigraphic relationship among the units is shown on Figure 3.4.

The rhyolite (373 Ma) and basalt flows that bracket the calcite-rich unit at site X1 have been used to correlate it to a secondary outcrop (~0.15 miles west), site X2, containing similar calcite nodules within a dark red shale matrix (Fig. 3.2, point 1). The calcite-bearing unit at site X2 is a thinner unit along strike of the thicker calcite-rich outcrop found at site X1. Beneath this calcite rich unit at site X2 lays a more complete record of the rocks stratigraphically below the calcite-rich sedimentary unit (Fig. 3.10).

Figure 3.9: Beneath the calcite rich unit lay five additional units. Units one and five are a tan tuffaceous sandstone, units four and two are a thick red mudstone and unit three this a basalt flow. All of the units are seen dipping to the north.

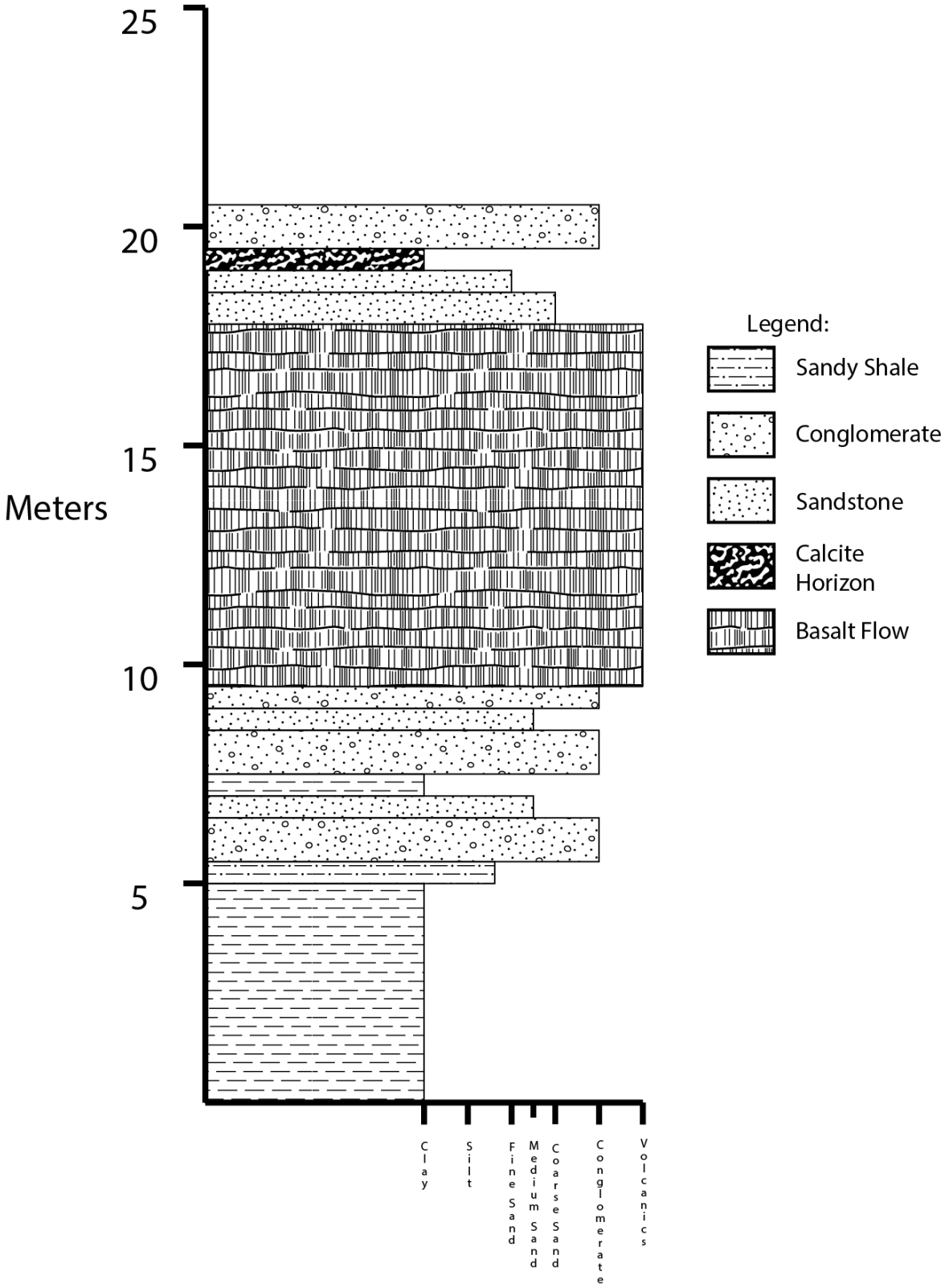

Figure 3.10: Stratigraphic column from units at Site X2 diagrams the relationship of the calcite rich horizon with the overlying rhyolite and stratigraphically lower basalt. Additionally there is a much thicker outcrop of basalt and thinner outcrop of calcite seen here than at Site X1.

Figure 3.11: Outcrop at site X2 with expanded boxes to highlight the differences in calcite on the east and west sides. The east side contains more lenses of calcite while the west side is more nodular.

Site X2 represents a wedged, depositionally discontinuous horizon that highlights the relationship between the different forms of preserved calcite-rich material and the depositional environment (Fig. 3.11). The morphology of the calcite varies from thin cylindrical calcite nodules and white lenses on the east side of the outcrop to more nodular white calcite on the west side of the outcrop (Figs. 3.12, 3.13). Within the east side of the outcrop the white lenses appear to have formed from coalesced thin tubes and are the result of soft deformation (Fig 3.13). This hypothesis comes from the association of these lenses with thin cylinders. If deformation took place after lithification to form the lenses, one would not expect to see undisturbed thin cylindrical calcite forms next to the lenses. The top of the unit contains an erosional contact between the calcite features and a sandy conglomerate cap that is similar to that found on top of the calcite unit at site X1. The sandy conglomerate capping the outcrop does not have cross bedding but does show some aligned grains that may indicate direction of flow. The aligned grains are not imbricate structures, but do show preferred alignment of grains.

Figure 3.12: Nodular calcite within a shale bed on the west side of the outcrop at site X2

Figure 3.13: Lenses of calcite with associated thin cylinders that are within a sandier matrix on the east side of the outcrop.

A unit of basalt, ~8 m thick, underlies the meter of thin sandstone that separates the basalt from the overlying calcite unit. The thick basalt may represent multiple flows, and the top of the unit shows a mixing relationship between the volcanic flow and red streaks of sediment preserved within the basalt. Abundant concentric bands of basalt mixed with red sediment are interpreted as lava pillows within the top of the unit. The pillows represent subaqueous volcanism, which implies that there was a standing body of water in the area. This find is evidence of active volcanism during sedimentation into a body of water (Fig 3.14).

Below the basaltic flow is a large outcrop that exposes 2.5 repetitive sequences, each sequence comprising (from base to the top) shale, conglomerate, and sandstone. Within the upper conglomerate of these sequences, coarse subangular pebbly sandstone lenses are present. The sandstone are thin to medium bedded with thin, discontinuous layers of shale (30 cm) (Fig. 3.15A). The only indication of current flow within these units is imbricated pebbles in the middle coarse sandstone (Fig. 3.15B). The basal conglomerate of this outcrop shows an abrupt transition at its top to sandy shale.

The repeated sequence of conglomerate-sandstone-shale could be interpreted as a fan supplying sediment to and interacting with an aqueous environment. Below the base sandy shale of this sequence is a thick unit of platy dark red shale, the thickness of which, ~79.5 m, was inferred from aerial photos, considering extent of the unit and the dip. No additional units were discovered below the very thick platy shale unit.

A)

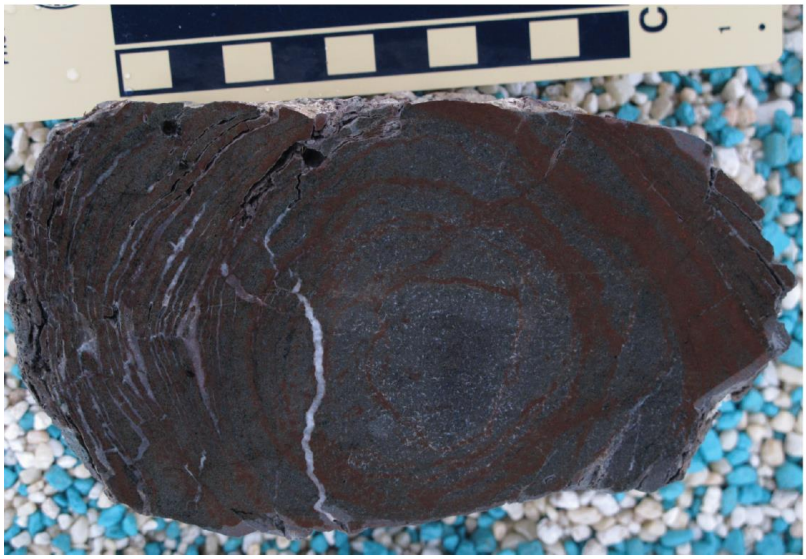

B)

Figure 3.14: Pillow basalts out in the field with concentric bands of basalt and red sediment. A sample was taken from the field and cut and polished to view the bands in greater detail.

A)

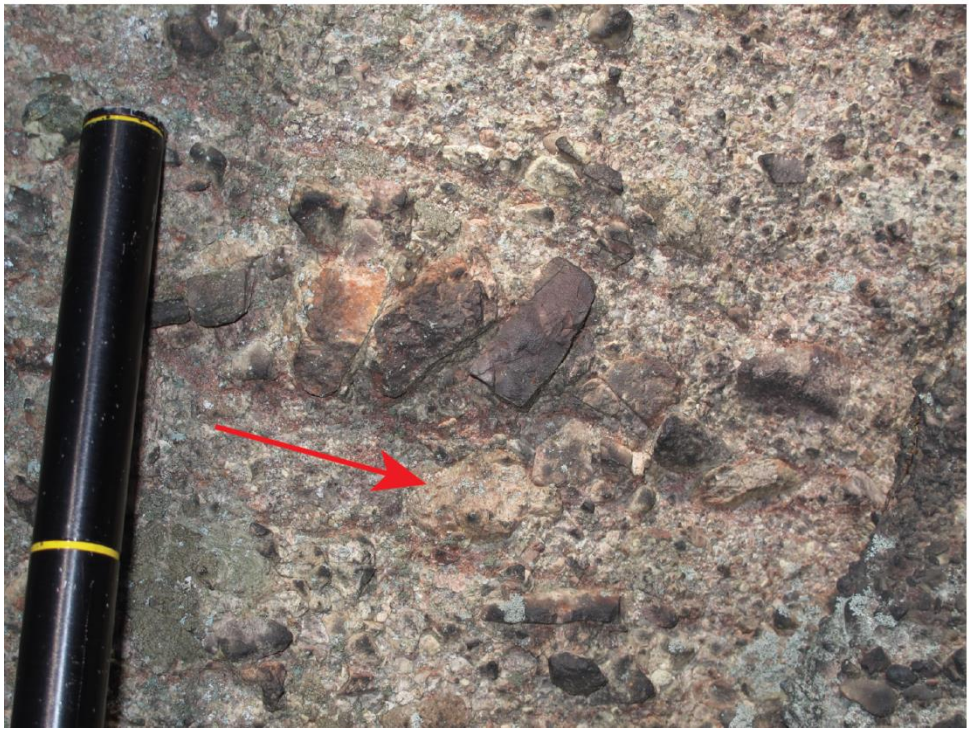

B)

Figure 3.15: A photograph of a portion of the repeating sequences of sedimentary units, highlighting the transition from conglomerate to thin shale (outlined in red dashes) to sandstone at the top of the sequence. Within the conglomerate unit were imbricate structures.

Chapter 4 : Hand Sample Observations

Four unique morphologies of calcite nodules were identified and analyzed to determine the cause of differences in occurrence, shape, and mineralogy. Types examined in this thesis are hereafter referred to as types A, B, C and D. This chapter is a description of rock samples and cut slabs that contain each type of nodule. A dissecting scope was used to examine the samples, which were described as bulk and cut samples.

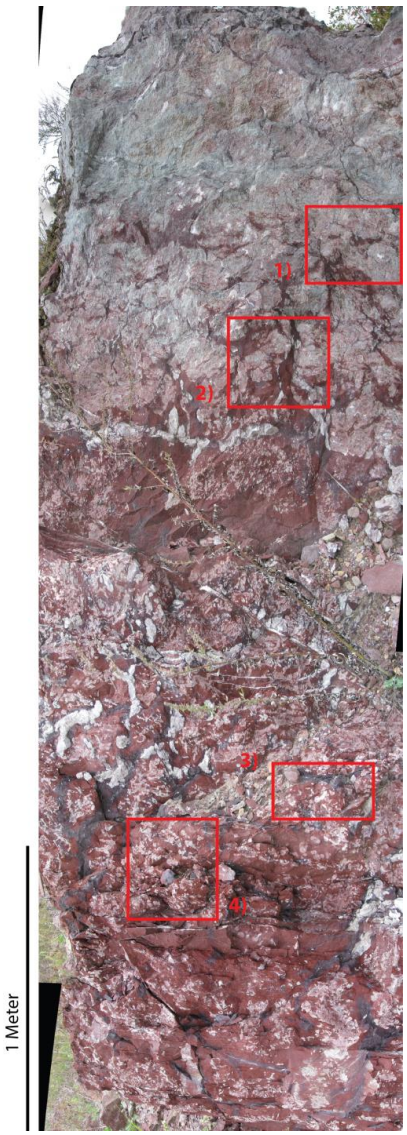

Figure 4.1: Site X1 outcrop profile showing rock sample horizons. Box 1 represents sample type B; box 2 is sample type A; box 3 is sample type D and box 4 represents sample type C.

Sample Type A

Sample Type A was sampled from the nodular horizon within the stratigraphic section, and has distinctive lobes of calcite that differentiate it from other sample types (Fig. 4.1). The bulk sample has a dark red matrix with ellipsoidal concretions that coalesce into larger calcite lobes. Lobes of calcite have an elongate/stretched appearance that is present over the entire sample in one preferred orientation, perpendicular to bedding (Fig. 4.2).

Figure 4.2: Cut slab of sample Type A, with elongate lobes of calcite and minimal red matrix

Type A cut samples consist of mostly white/pink calcite concretions (>50% by volume) within a deep dusky reddish matrix with some small areas of slightly lighter red matrix. Concretions look flattened and elongate in one direction, indicating shearing across the concretions. In cut pieces, white rings of calcite (~1 cm across) encase pink calcite and multiple rings are coalesced within larger pink calcite lobes (Fig. 4.3). The elliptical rings seem to be cylinders that have fused (coalesced?). In portions a complete cross section is not visible and only a crescent shaped calcite fragment is visible. An acid test with hydrochloric

acid (10% HCl) reveals that both the white calcite annulus and the inner pink calcite portion both effervesce (although the annulus does not react as much as the pink interior).

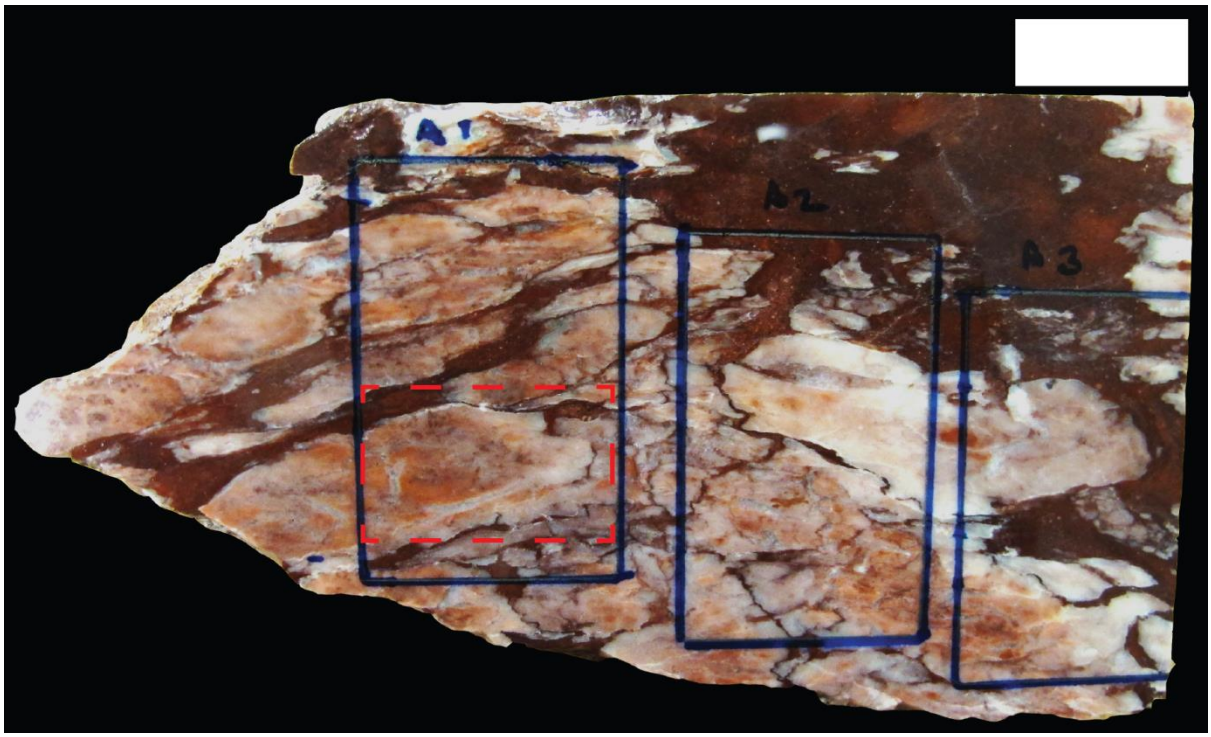

Figure 4.3: Cut wet slab of sample Type A, the red box outlines a white ring of calcite within the pink lobe of calcite. The blue boxes outline the thin section regions, A1, A2, A3 (not made into a thin section) and the white bar in the corner represents 1 cm in length.

would effervesce while a majority of the matrix was non-reactive. The result was a pitted fibrous appearance of the surrounding matrix. The Munsell's soil chart was used to describe the red and purple matrix color of the cut wet slab (Table 4.1).

Table 4.1: Shows the Munsell's Soil Chart designation of the matrix colors noted on each sample type

Sample Type	Matrix Color One	Matrix Color Two
A	Dusky Red: 10R 3/3	Purple Color: 10R 2.5/2
B	Deep Purple: 5R 2.5/1	N/A
C	Red: 10R 3/4	N/A
D	Dark Red: 10R 3/6	Maroon: 10R 2.5/2

Sample Type B

The sample rock for type B was taken from the nodular horizon of the outcrop profile, just below the massive carbonate from site X1 (Fig. 4.1). Type B is distinct in hand sample for its large masses of pink and green tinged calcite nodules with distinct margins between the nodules and matrix. Additionally, this sample type has dark purple red sediment that appears pinched between concretions (Fig. 4.4).

Slabs of sample B show alignment of the concretions that are isolated within the matrix and do not coalesce to form larger lobes of calcite. The concretions have pink, white, and green regions (Fig. 4.5). The pink may be due to calcite growing within the sediment and trapping red matrix grains within the calcite fabric. The green concretions, where the green color concentrates around the margins of the concretion, may be a result of clays or reduced iron conditions within the margin of the nodule.

The matrix in sample B is a much darker purple than that in sample A. There are bright red streaks and grains that appear to have been oxidized, as well as smaller pale green grains (Fig. 4.5). The matrix has a coarse texture with abundant pink feldspar grains and there is a higher abundance of large grains than present in the matrix of sample type A. The Munsell's soil chart was used to describe the dark purple sediment color of the cut wet slab, 5R 2.5/1 (Table 4.1).

Figure 4.4: Rock sample Type B with green and red concretions in deep purple sediment.

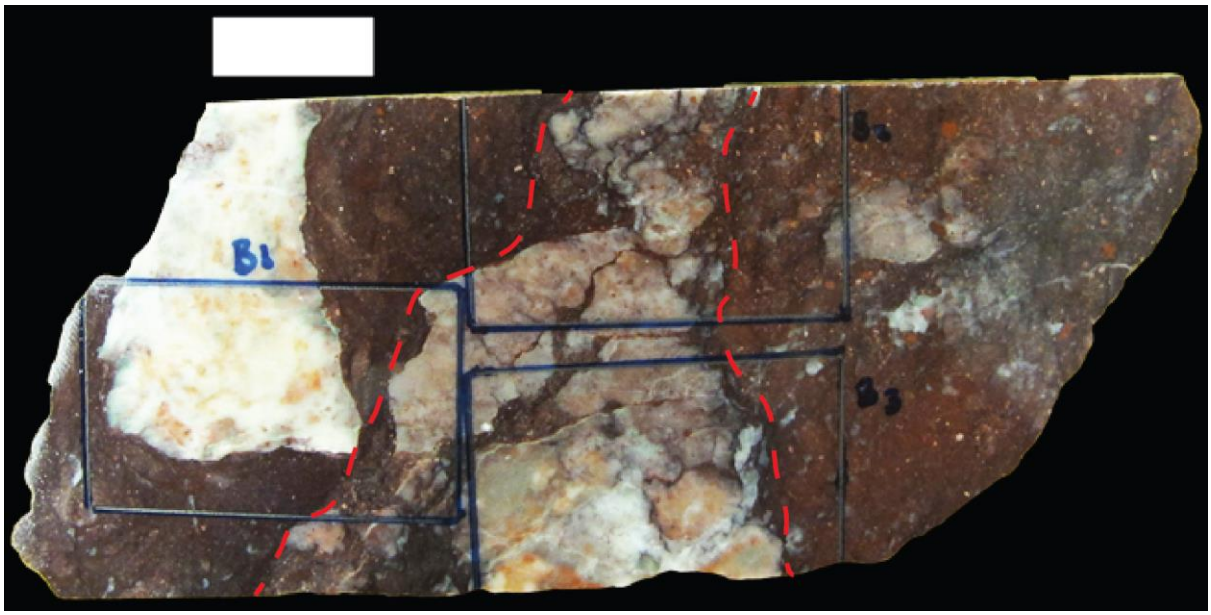

Figure 4.5: Cut wet slab of sample Type B, the red lines outline aligned concretions that are isolated within the matrix. The blue boxes outline the thin section regions, B1, B2, B3 and the white bar represents 1 cm in length.

Sample Type C

The sample rock for type C was taken from the thinly branching cylindrical patchy regions of the outcrop profile from site X1 (Fig. 4.1). In hand sample, type c illustrates thin curvilinear calcite cylinders that often appear coalesced (Fig. 4.6). These extremely thin calcite features (~2-3 mm thick) are more easily seen on cut samples than in the bulk rock sample. The cut section reveals curvilinear calcite and concretions that taper out into thin fibrous ends (Fig. 4.7). A high amount of sediment is incorporated into some of the denser calcite nodule areas contributing to the light reddish orange color of the nodules (Figure 4.7). In contrast, the thinner curvilinear calcite has less matrix/pink inclusions than the larger concretions. The thinner cylindrical calcite features appear as a darker Grey color. This sample contains areas with high concentrations of curvilinear calcite or concretions and other regions with only matrix.

The matrix in this sample is homogenous and a bright red color. There is very little mottling or variation in color within the matrix, apart from a few darker streaks in select areas. The Munsell's soil chart was used to describe the dusky red sediment color of the cut wet slab (Table 4.1).

Figure 4.6: Rock sample Type C with narrow concretions that branch into thin cylindrical nodules. The sediment is a bright red color.

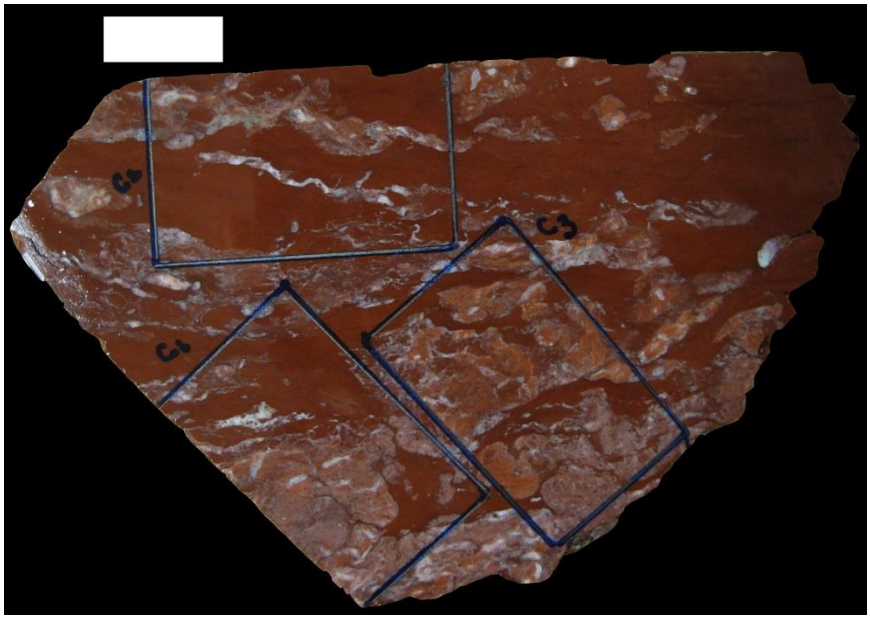

Figure 4.7: Cut wet slab of sample Type C, with thin curvilinear calcite cylinders. The blue boxes outline the thin section regions, C1, C2, C3 and the white bar in the corner represents 1 cm in length.

Sample Type D

The sample rock for type D was taken from the thinly branching cylindrical patchy regions of the outcrop profile, within the darker purple matrix from site X1 (Fig. 4.1). Sample

D in hand sample has concretions that look polygonal (similar to mudcracks). When cut, the white calcite tubes seem to taper into broad stubby ends, which could be due to the oblique angle at which they were cut, but also could be representative of the morphology in this sample (Fig. 4.9). Additionally there are small (~1 mm diameter) circular calcite concretions that are aligned horizontally on the slab, but are not attached (Fig. 4.9).

The matrix in type D seems to show a transition zone between bright red sediment, similar to samples A and C, to darker maroon sediment, found in Sample B. The matrix in Figure 4.9 also shows mottled appearance that looks like layering between the two types of sediment.

The matrix in this sample contains lighter rounded regions of matrix surrounded by darker red rings (~0.5 cm diameter). There are visible igneous lithic fragments that occur locally in the sample and abundant smaller grains that look like quartz with associated darker grains. The dominating feature within the matrix are the coarse grains that are in isolated areas, while other areas have very fine grains within the mottled regions of dark purple and bright red matrix. The Munsell's soil chart was used to describe the sediment color for both the dark purple and bright red color and can be found in Table 4.1.

Figure 4.8: Rock sample type D with calcite concretions that appear polyganol in hand sample within dark maroon sediment

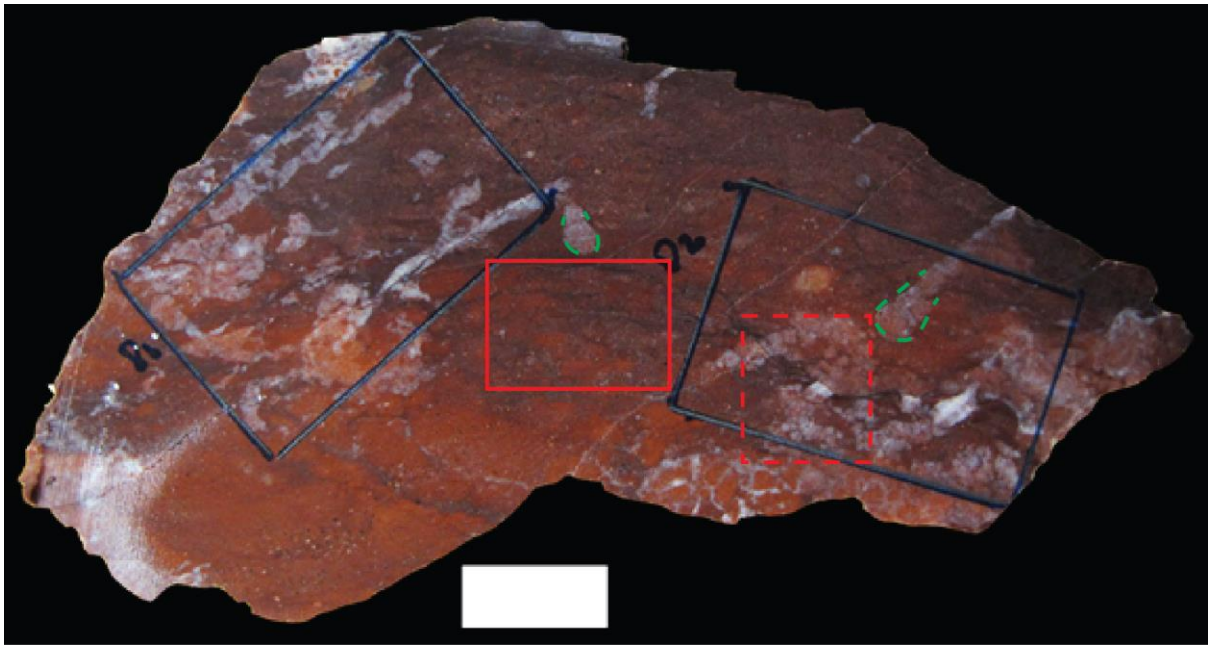

Figure 4.9: Cut wet slab of sample Type D, the red box outlines mottled area of red and purple sediment. The dotted red box highlights a region of small aligned calcite circles. The green dotted line outlines the blunt terminations to the calcite cylinders. The blue boxes outline the thin section regions, D1, D2 and the white bar represents 1 cm in length.

Chapter 5 : Petrography

Ten sample thin sections of carbonate concretions were studied under plane polarized light and cross-polarized light in order to compare and contrast the morphologies (A, B, C & D). The following sample descriptions were completed by observation of the samples under an Olympus petrographic microscope, under 40x magnification, unless otherwise stated. Additionally, dominant features observed on each sample type were boxed on a single representative thin section image, one for each sample type. The designation of calcite grain sizes are relative to each other on the sample and fall into three categories; micritic calcite (<0.0125 mm), medium coarseness (~0.1 mm), and sparry calcite (~0.25 mm). A table compiling the features observed for all sample types was created to indicate the presence or absence of distinctive features as well as the percentage of coverage of calcite or matrix on each slide (Table 5.1).

Table 5.1: The presence of unique features is noted with an, X, while the absence of the feature is an, -. The percentages of calcite and matrix are given where – imply 0.

Sample	Features									
	Micritic Calcite	Medium Coarseness Calcite	Sparry Calcite	Opaque Fine Matrix	Coarse Matrix	Transition Zones	Ellipsoidal Features	Circular Features	Horseshoes Features	Tubular Sparry Calcite
A1	X	X	-	X	X	X	X	X	X	X
A2	X	X	X	X	X	X	X	X	X	X
B1	X	-	-	-	X	X	-	X	X	-
B2	X	Minor	X	-	X	-	-	-	-	Minor
B3	X	X	X	-	X	-	X	X	-	X
C1	X	X	X	X	-	-	X	Minor	Minor	X
C2	X	X	X	X	-	-	Minor	Minor	Minor	X
C3	X	X	Minor	X	-	X	-	Minor	Minor	X
D1	X	X	X	Minor	X	X	-	-	-	X
D2	-	X	X	Minor	X	X	-	-	-	X

Sample	Micritic Calcite	Medium Coarseness Calcite	Sparry Calcite	**Total Calcite**	Opaque Fine Matrix	Coarse Matrix	**Total Matrix**
A1	70%	10%	-	80%	10%	10%	20%
A2	63%	7%	15%	85%	6%	9%	15%
B1	75%	-	-	75%	-	25%	25%
B2	58%	1%	6%	65%	-	35%	35%
B3	45%	15%	20%	80%	-	20%	20%
C1	40%	20%	15%	75%	25%	-	25%
C2	15%	5%	10%	30%	70%	-	70%
C3	20%	54%	6%	80%	20%	-	20%
D1	5%	15%	10%	30%	6%	64%	70%
D2	-	15%	25%	40%	3%	57%	60%

Sample Type A

Thin sections of sample type A contain ~80% calcite and ~20% sediment on the slides and are sheared elongate calcite nodules that contain inclusions of matrix and quartz grains within them (Fig. 5.1, 5.2). This sample type has minimal red matrix between concretions and the matrix contains an even mixture of fine opaques and coarse sediment. Within the matrix are small (~0.025 mm diameter) highly birefringent grains (olivine or pyroxene) that stand out against the predominant quartz grains (Fig. 5.3A). The calcite structures in this sample are micritic with curvilinear and ellipsoid medium grained calcite filled features within the calcite nodules (Fig. 5.3B, 5.3C). Transitions from the calcite nodules to the matrix are commonly intertonguing calcite and matrix regions (Fig. 5.3D).

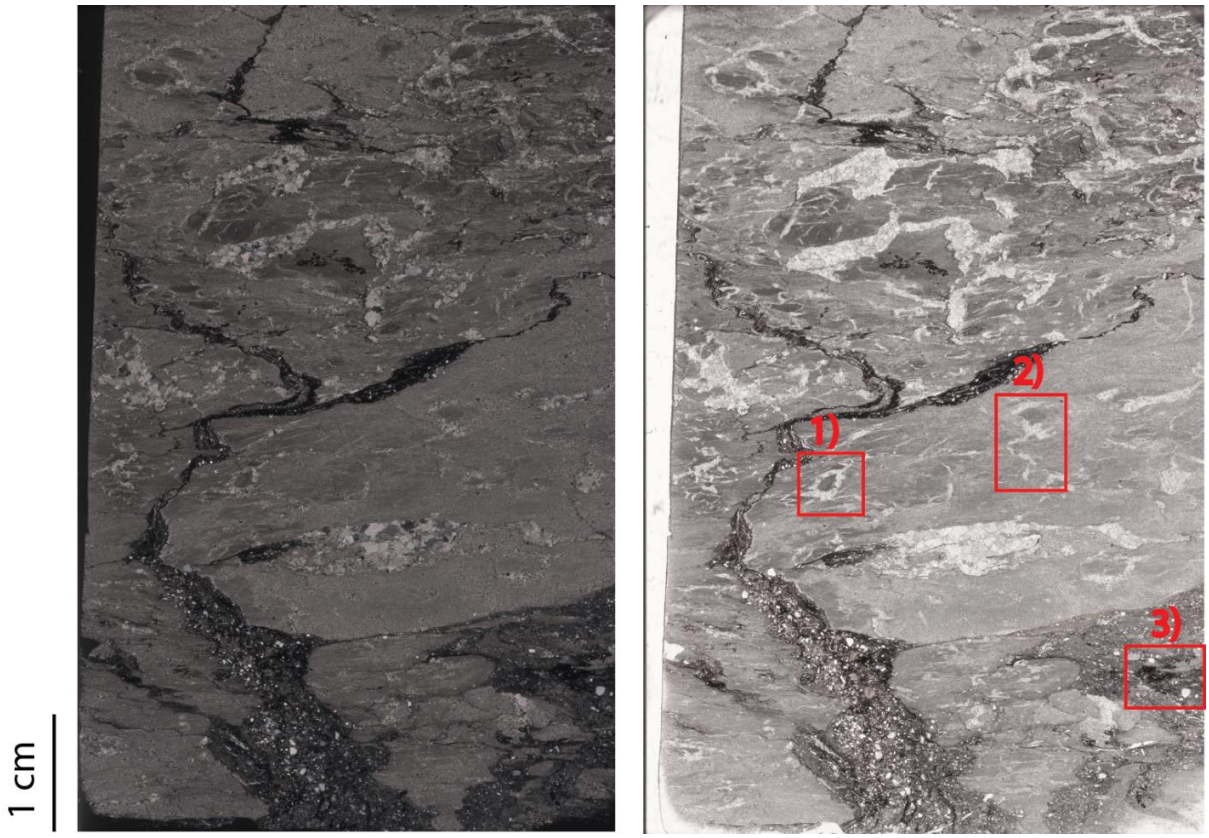

Figure 5.1: Scan of thin section for sample A2 which is shown in cross polars on the left and plane polarized light on the right. Box one represents an ellipsoid shape filled with medium grained calcite. Box two represents a curvilinear shape filled with medium grained calcite. Box three shows an area with intertonguing of calcite and matrix.

Figure 5.2: Engulfed quartz grain within the micritic calcite nodule.

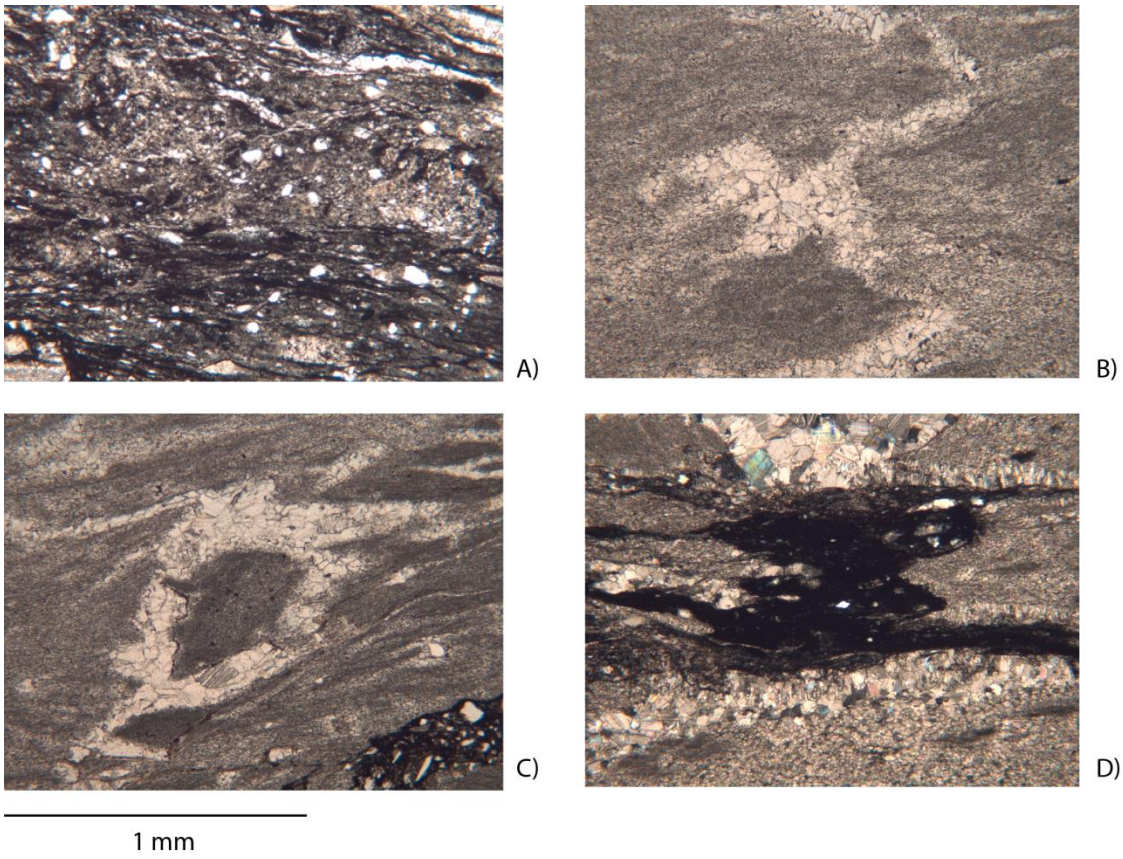

Figure 5.3: A) photograph of the matrix in plane polarized light with very small grains that are not birefringent in this image under plane polarized light, B) curvilinear medium grained calcite filled feature within the micritic nodule, C) ellipsoid medium grained calcite filled feature within the micritic nodule, D) intertonguing transition zone of calcite and matrix.

Sample Type B

Thin sections of sample type B contain between 65-80% calcite (predominantly micritic) and 20-35% coarse sediment (Fig. 5.4). The sample is composed of matrix-

supported micritic calcite nodules that are within coarse sediment and contain some quartz inclusions within the micritic nodules. A few grains within the margins of the calcite show evidence of compaction of the sample after nodule growth (Fig. 5.5). The matrix is predominantly larger subangular quartz grains and shards as well as minor highly birefringent grains (olivine and pyroxene) (Fig 5.6A). The matrix is coarse, but under cross polars is appears to parallel the margin of the calcite nodules (Fig. 5.4). A pumice fragment and shards of devitrified glass were identified within the matrix (Fig. 5.6B, 5.6C). There are no intertonguing transition zones between the calcite and sediment and more commonly you see abrupt transitions between the two, or grains of sparry calcite broken off during diagenesis of the nodule and included within the matrix (Fig. 5.6D).

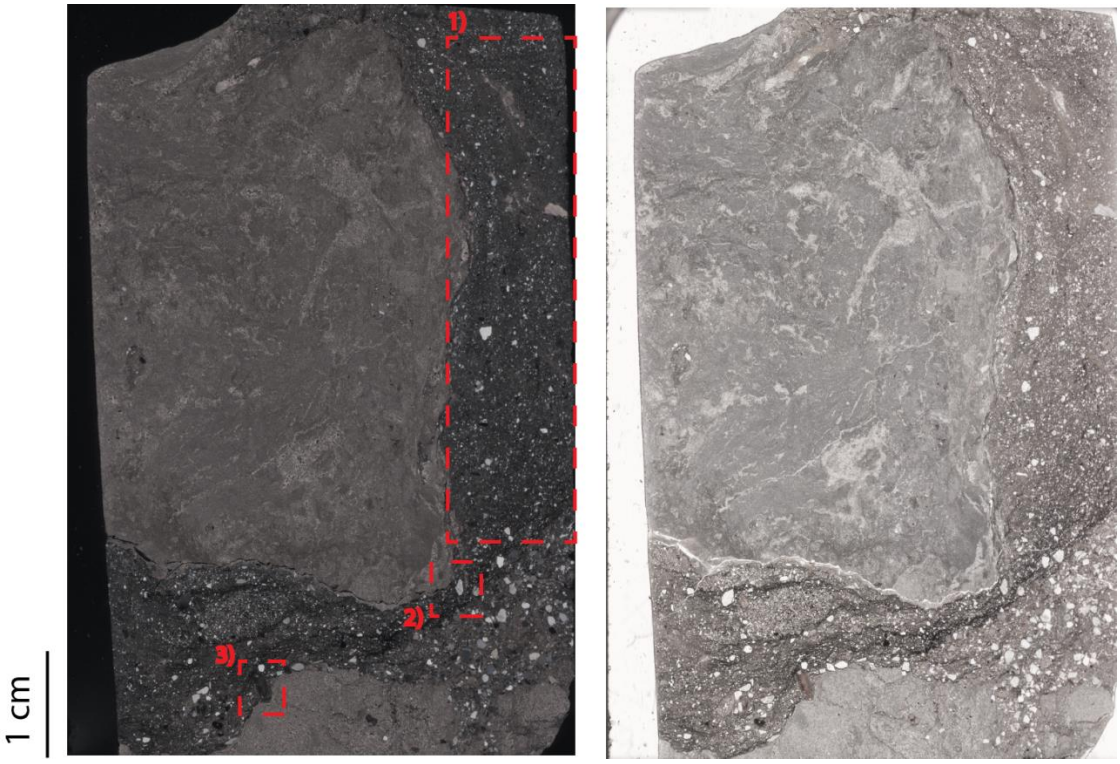

Figure 5.4: Scan of thin section for sample B1, which is shown in cross polars on the left and plane polarized light on the right. Box one represents alignment of matrix parallel to the calcite nodule. Box two represents contains a grain of quartz with calcite filled seams (Fig. 5.6D). Box three contains a region of the calcite nodule that is warped around a brown matrix grain (Fig. 5.5).

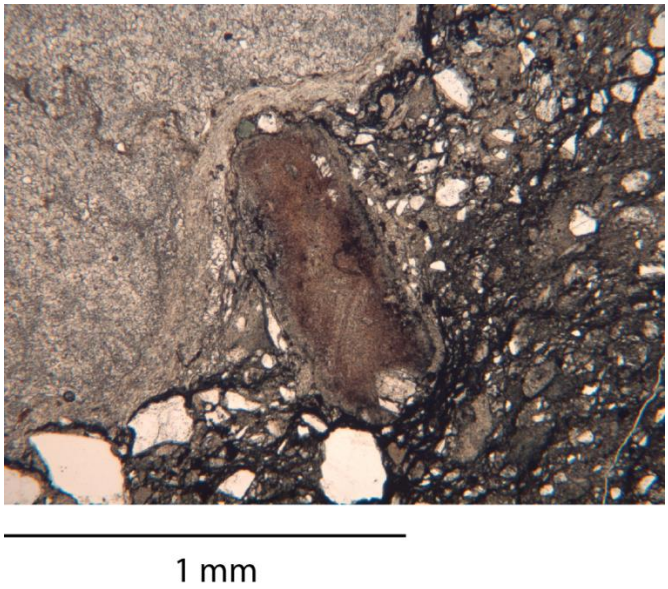

Figure 5.5: Compaction of micritic calcite grains within the nodule around a large brown matrix grain.

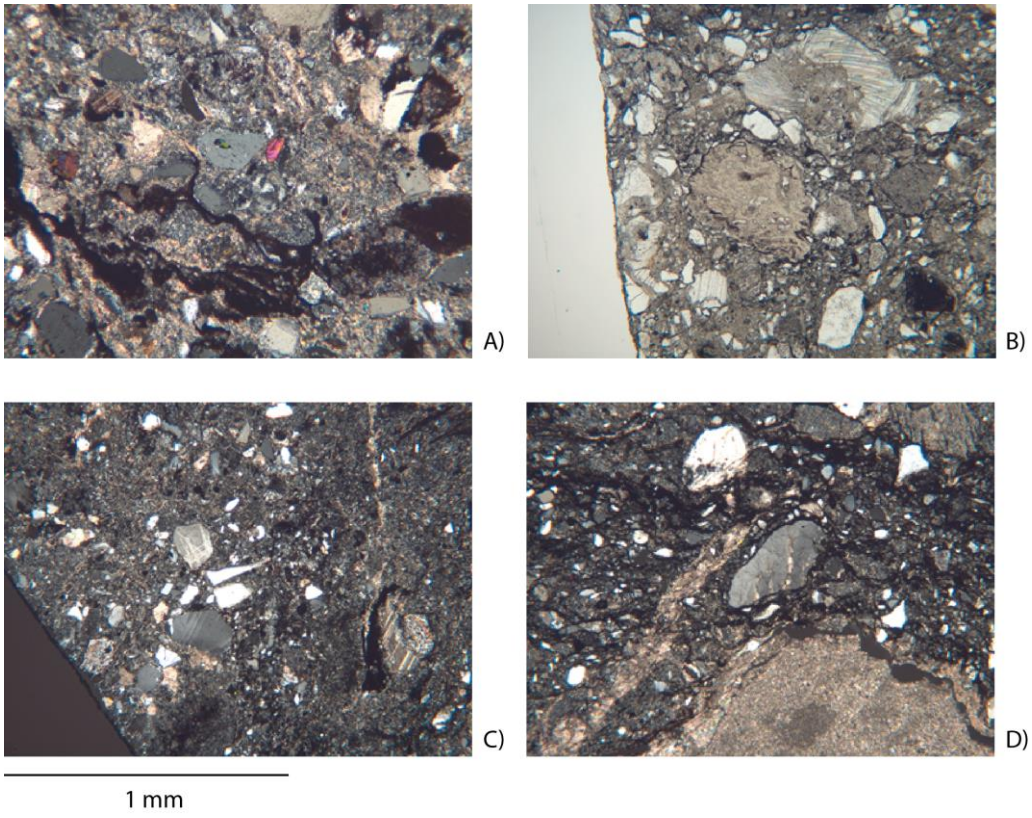

Figure 5.6: A) Matrix of the sample contains highly birefringent grains (pink and green) that are included within quartz grains as well, B)Light brown pumice fragment within the matrix and is located just below the rhombohedral calcite grain, C) Abundant devitrified glass shards within the matrix, D) Quartz grain that may have broken off from the nodule and contains calcite filled seams.

Sample Type C

Thin sections of sample type C contain between 30-80% calcite (predominantly micritic and medium coarseness) and 20-70% fine opaque sediment. The abundant curvilinear sparry calcite within the sample characterizes sample type C (Fig. 5.7). The few nodular regions appear to be coalesced curvilinear cylindrical features with many pockets of trapped matrix within the micritic calcite in these regions (Fig. 5.7). The isolated curvilinear cylinders of calcite appear to form with blunt rounded terminations as opposed to sharp pinching out (Fig. 5.7). Acicular calcite grains form spherulites within the nodular calcite and typically nucleate from a micritic calcite or quartz (Fig. 5.8A, 5.8B). The matrix on this sample contains minor highly biregringent grains and is made of predominantly fine opaques which give a black appearance (Fig. 5.8C). The transition zone between the calcite nodule and matrix is often abrupt or gradational with anastomosing channels of calcite separated by pockets of fine matrix (Fig. 5.8D).

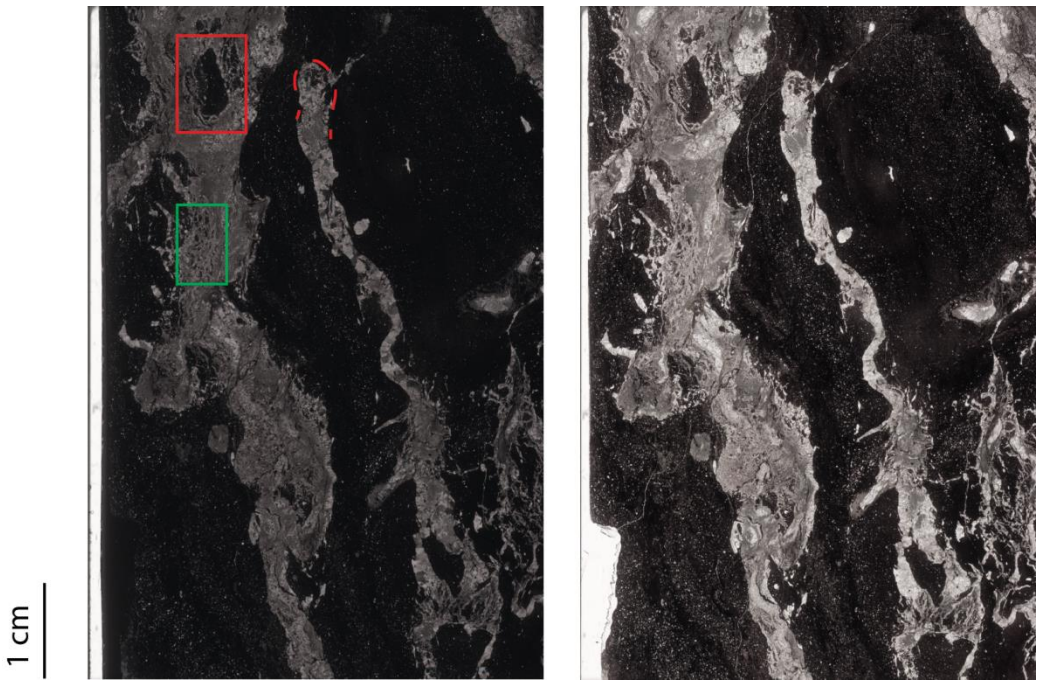

Figure 5.7: Scan of thin section for sample C2, which is shown in cross polars on the left and plane polarized light on the right. The red box represents an area of engulfed sediment within the calcite nodule. The green box represents an area with

anastomosing channels of calcite separated by pockets of fine matrix (Fig. 5.8D). The red dotted line outlines the blunt terminations to the calcite filled curvilinear cylinder.

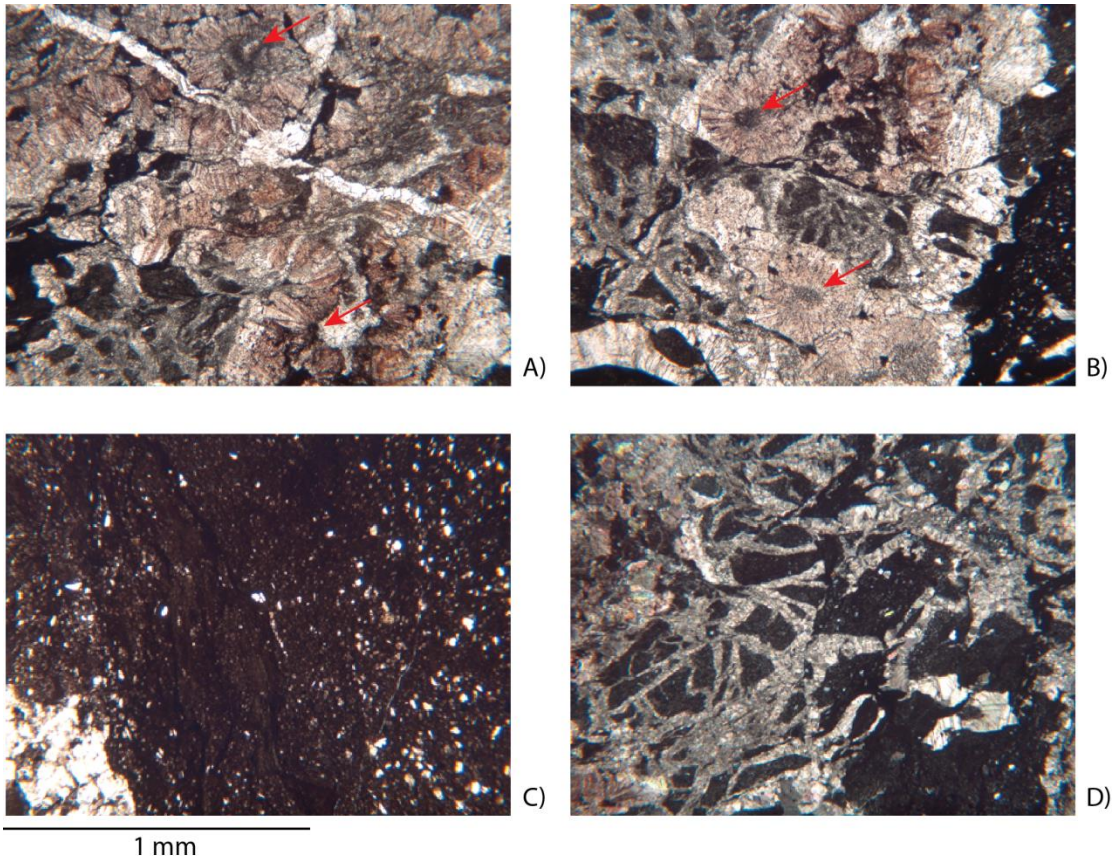

Figure 5.8: A & B) Red arrows point out the center circle within the calcite spherulites, C) Matrix of the sample is full of fine opaques, D) Anastomosing channels of calcite separated by pockets of fine matrix.

Sample Type D

Thin sections of sample type D contain ~30% calcite (predominantly sparry and medium grained) and ~70% coarse matrix. Sample type D contains palisade arrangement of calcite spars along the arcuate margins of the nodular calcite as well as bluntly terminating calcite cylinders that are filled with sparry and medium grained calcite (Fig. 5.9). The calcite cylinders contain engulfed quartz grains within their margins (Fig. 5.10A). Within the calcite nodules are acicular grains of calcite that form calcite spherulites (Fig. 5.10B). This sample type does not contain any curvilinear features within the calcite nodules and instead the nodules grade from sparry calcite at the margins to more micritic calcite inward (Fig. 5.9). The matrix is coarse with abundant small shards of devitrified glass and small birefringent

grains (olivines and pyroxenes) (Fig. 5.10C). The matrix is oriented along the margin of the larger calcite nodules and is cross cut by the bluntly terminating cylinder of calcite (Fig. 5.10).

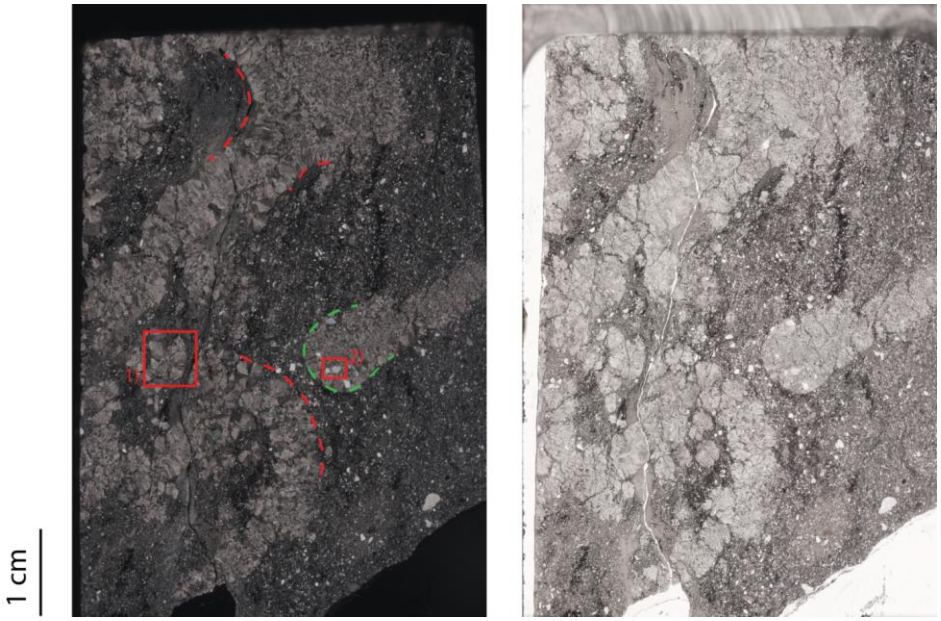

Figure 5.9: Scan of thin section for sample D2, which is shown in cross polars on the left and plane polarized light on the right. Box one contains a calcite spherulite which can be seen in greater detail in Figure 5.10B. Box two encloses two engulfed quartz grains within the micritic nodule (Fig. 5.10A). The red dotted lines outline the palisade arrangement of sparry calcite grains and the green dotted line outlines the blunt termination to the calcite nodule.

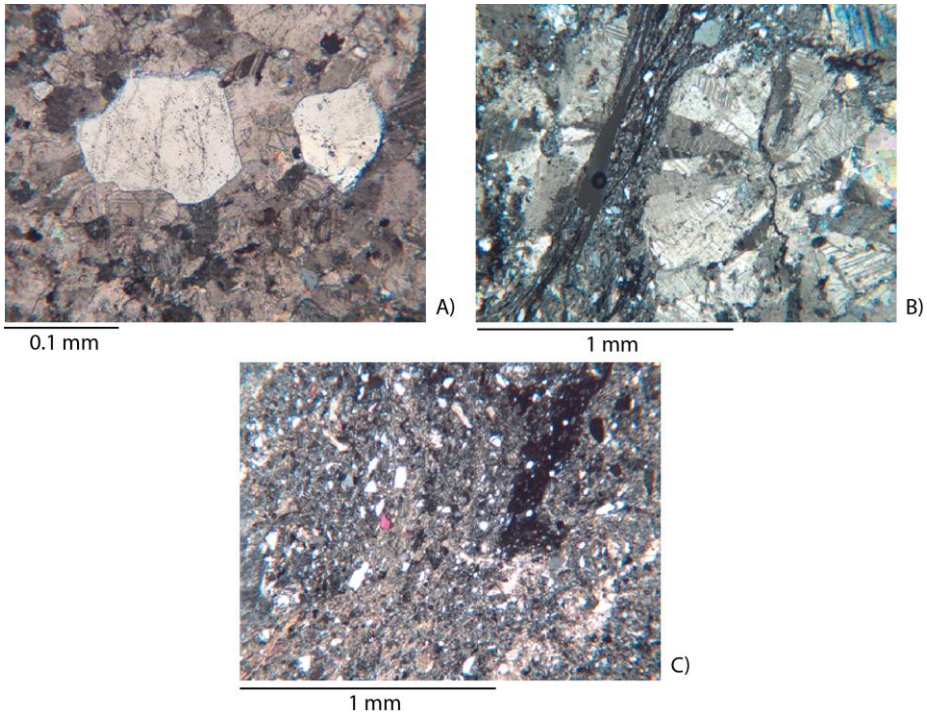

Figure 5.10: A) Engulfed quartz grains within the cylindrical calcite nodule, B) Calcite spherulite within the calcite nodule, C) Coarse matrix with highly birefringent grains as well as angular shards.

Chapter 6 : Scanning Electron Microscopy

All of the thin section samples described in this chapter have complementary rectangular slabs from the same rock sample that were coated with Au/Pd by spattering and analyzed under the SEM at 15 KV. EDX element maps were captured with a 4-pi Spectral Engine and Revolution software. Electron backscatter (BS) images were also captured to determine the location and abundance of low-density organic material within the sample.

Sample Type A

The organics found on this slab were found within either potassium and silica rich grains (possibly feldspar grains) or blocky calcium-rich grains. An electron backscatter image illustrates two dark organic masses that occur within the calcite (Fig. 6.1). Six organic fragments were selected for examination. The first form of organics appears to have small slits within the amorphous structure and occurs within the calcite grains that surround the carbon (Fig. 6.2). The second form looks similar to the first, but with less obvious slits and a more mottled appearance (Fig. 6.3). The third form appears to be a cast of an area that once held an organic piece; the carbon peak detected in this spot was likely due to minor residue organics (Fig. 6.4). The final form of carbon occurs as a mottled circular mass within a smooth circular region (Fig 6.5). A line scan through the organic form showed peaks of silica and potassium in the surrounding material and a peak of carbon throughout the circular organics region (Fig 6.6).

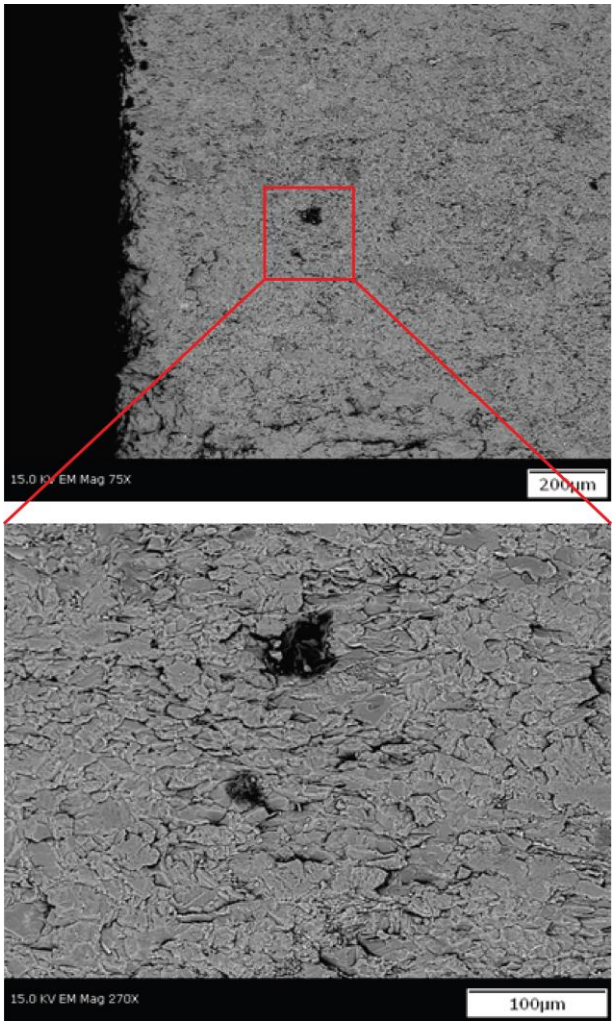

Figure 6.1: Electron backscatter image of two organic pieces that show up as dark circular features within light grey matrix minerals.

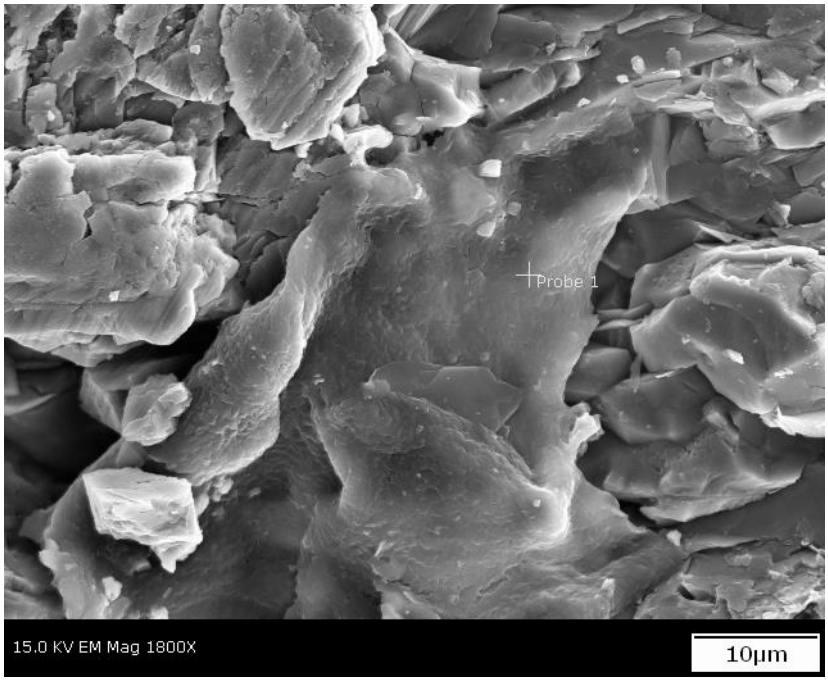

Figure 6.2: First form of organics with small curvilinear slits and an amorphous shape with a diffuse boundary.

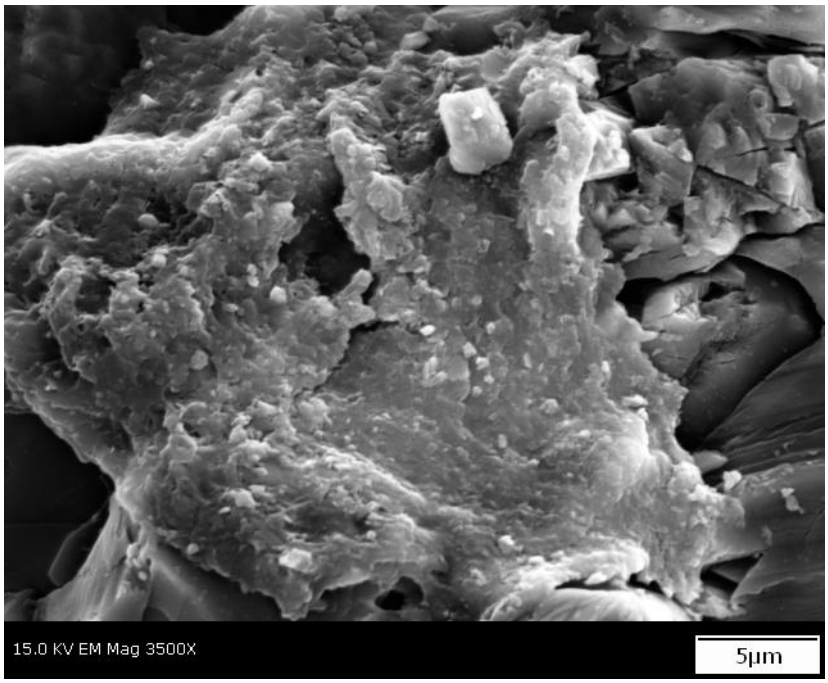

Figure 6.3: Second form of organics that is amorphous like the first form but with a mottled appearance lacking slits.

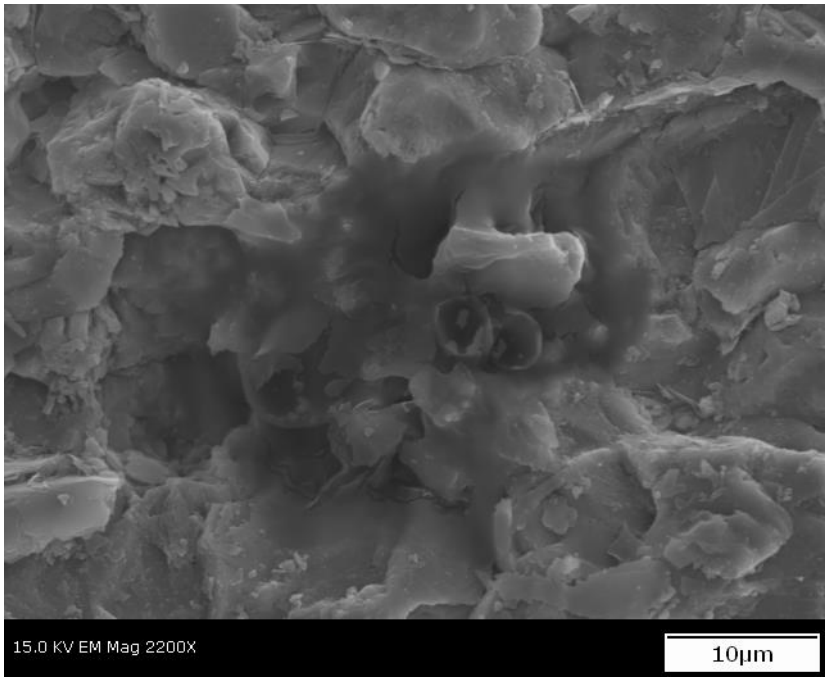

Figure 6.4: Darker central region (~40 µm in diameter) is a cast of an area that once contained organic material.

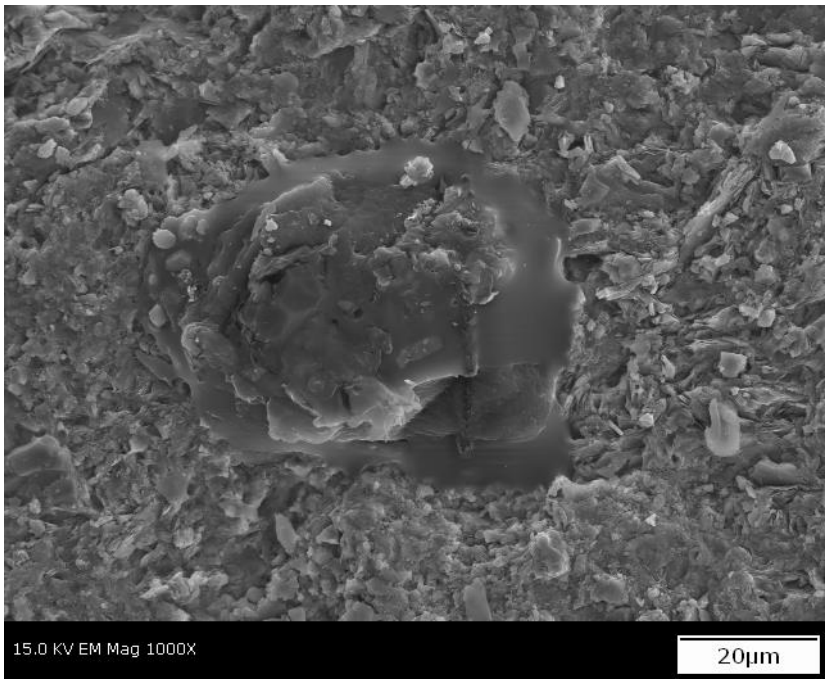

Figure 6.5: Final form of carbon identified that is a mottled circular mass within a smooth exterior ring that has a diffuse boundary with the matrix.

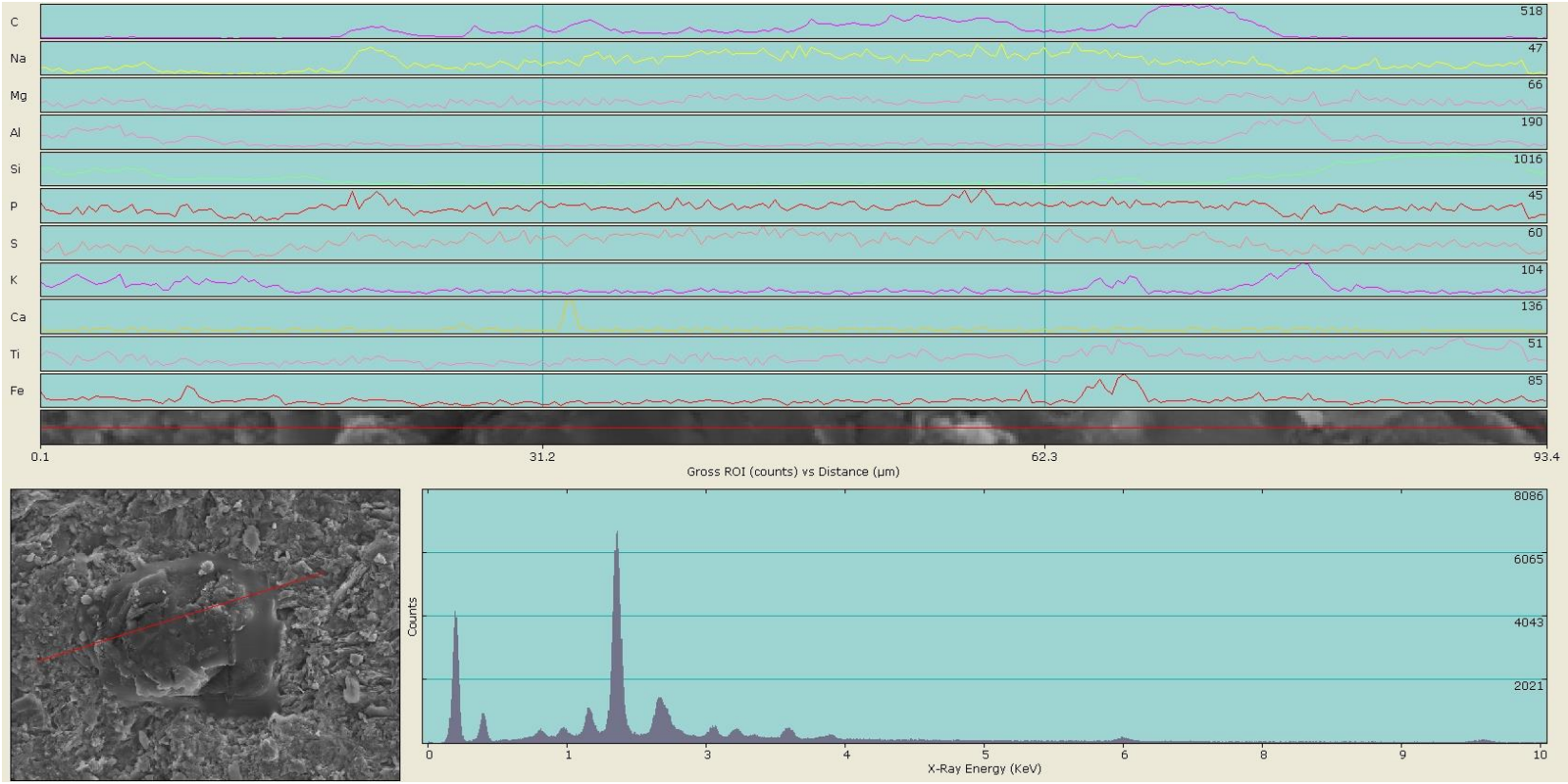

Figure 6.6: A line test through the organics shows from left to right through the matrix and across the carbon mass how the element peaks changed. The carbon spikes in the center and flattens on the edges while the silica spikes at the edges and flattens through the center of the scan, across the organics.

Sample Type B

The calcite within this slab are blocky, well defined grains that are approximately 15 μm across (Fig. 6.7). One type of organics had an elongate rod shape that occurs within the blocky calcite, but is unique from the round organics found in sample type A because of the rod, non-amorphous form (Fig. 6.8). A separate form of amorphous organic material seen in abundance on the slab appears to overlie blocky calcite (Fig. 6.9). This form of organic material also has characteristic small slits within the structure that are ~1 μm across.

An electron backscatter image was used to look for organics and six fragments of organics were identified that occur in four different forms (Fig. 6.10). One of the fragments of organics (Fig. 6.11) had the characteristic slits seen repeatedly on the organics of types A and B, and is surrounded by blocky calcite. The second form of organics appears as mounds of organics with curvilinear margins and variable topography (visible due to the difference in lightness or darkness) on the sample (Fig. 6.12A,B,C). The third form is a flat, rounded, amorphous form lacking slits within the structure. This fragment of organics also has a small rectangular rod of silica rich material overlying it (Fig. 6.13). The final form is a combination of the elongate rod form and mounded form with curvilinear boundaries between fragments of stacked organics that may have been stacked or moved during sample slab preparation (Fig. 6.14). All of the forms appeared within blocky calcite.

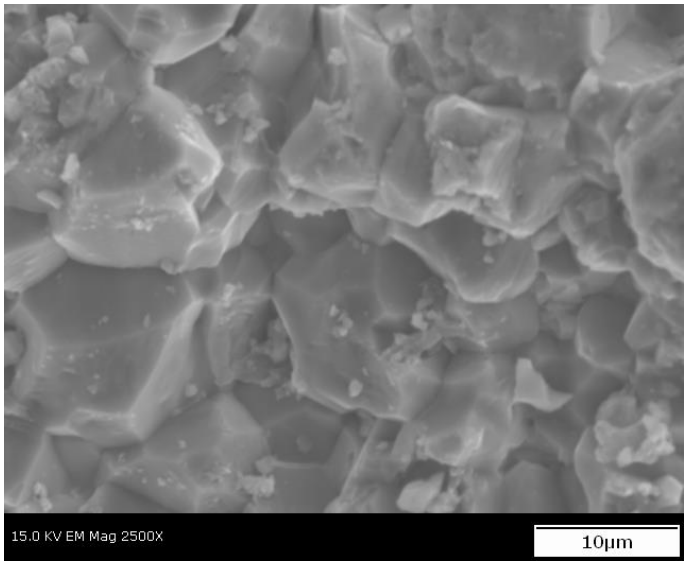

Figure 6.7: Blocky, well defined grains of calcite within the sample are approximately 15 µm across. The organics within this sample are commonly found within these blocky grains.

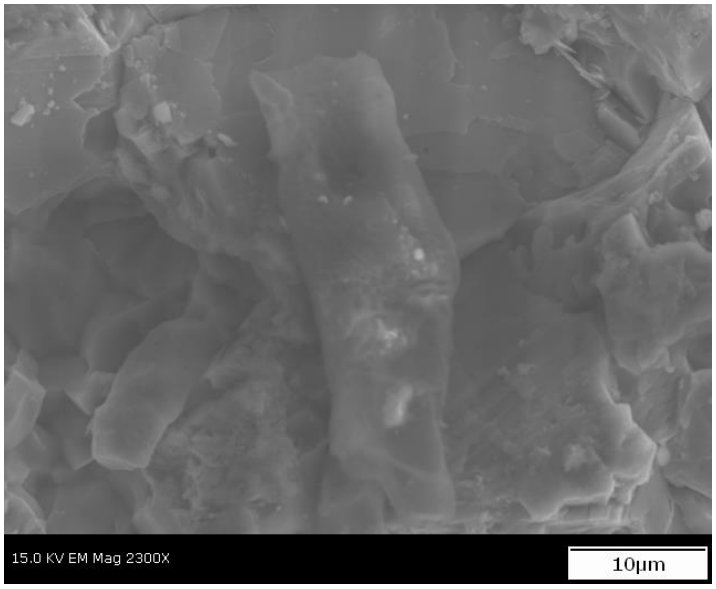

Figure 6.8: The rectangular rod structure in the center of the image is one of the forms of organics noted on this sample. It was one of the only non-amorphous forms.

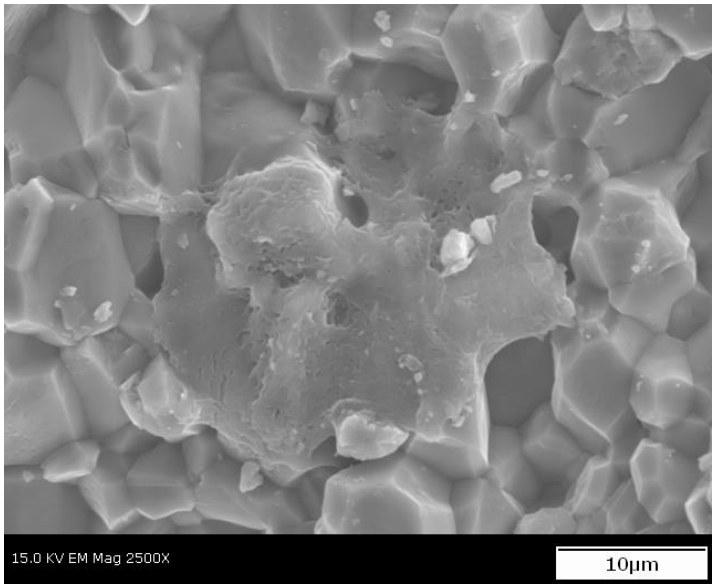

Figure 6.9: Amorphous carbon with abundant curvilinear slits that appears to lie on top of blocky calcite grains.

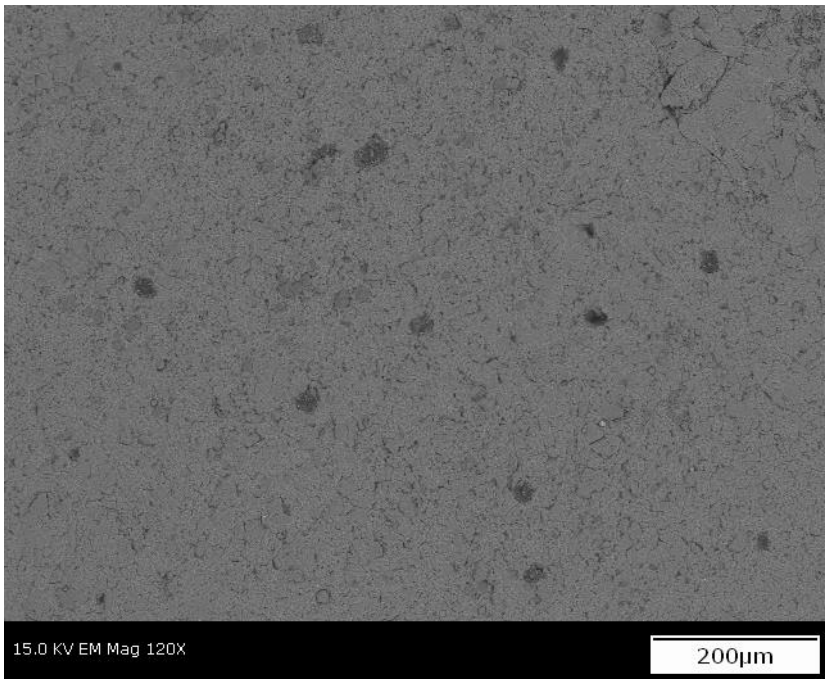

Figure 6.10: Backscatter image with locations of organics being the darker circles

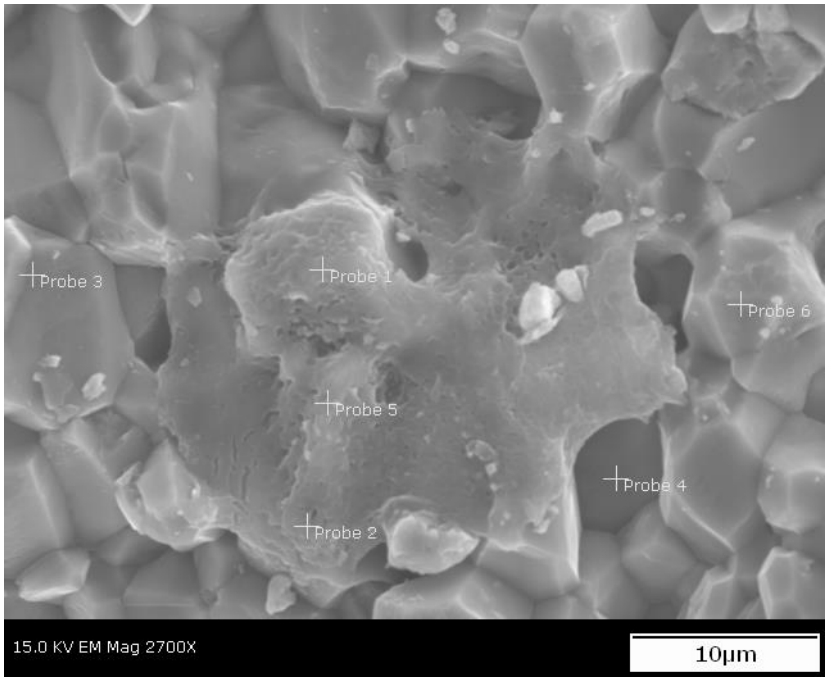

Figure 6.11: Organics found within the backscatter image (Fig. 6.10) above that has an amorphous shape and characteristic curvilinear slits.

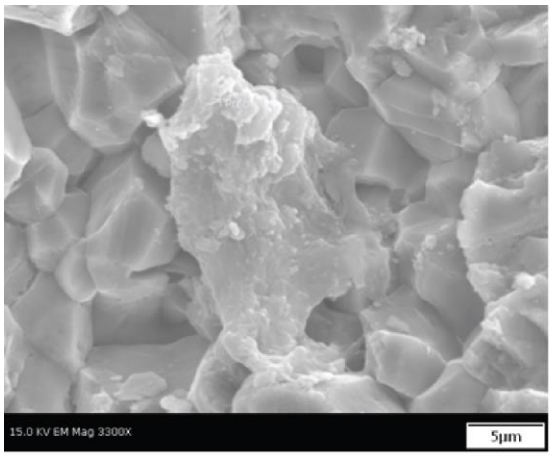

A)

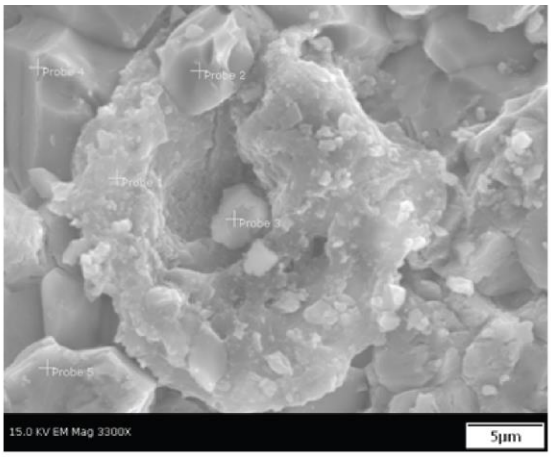

B)

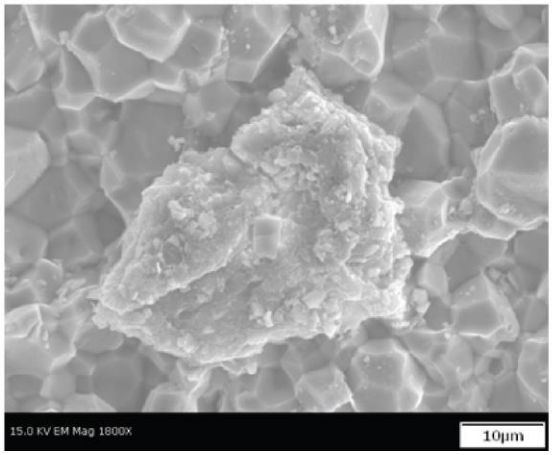

C)

Figure 6.12: Three different examples of a second form of organics with curvilinear margins and variable topography.

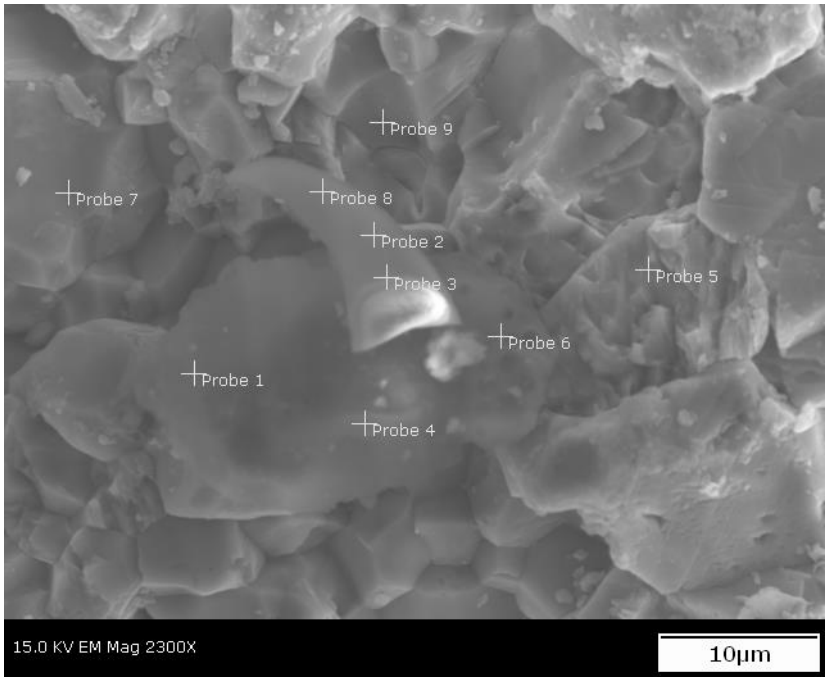

Figure 6.13: Smooth, elliptical carbon piece with an overlying rod of silica rich material. The smooth carbon piece is ~35 µm across.

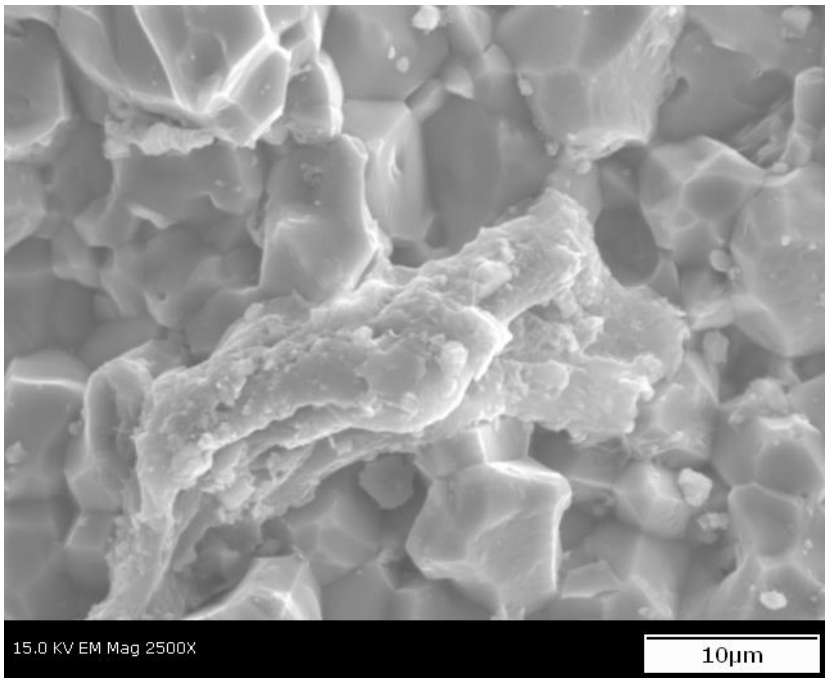

Figure 6.14: Combination of elongate rod and mounded form of organics with curvilinear boundaries between fragments of stacked organics. This morphology may be due to movement during sample slab preparation.

Sample Type C

Four distinct forms of organics occur in Type C concretions within this slab. The first fragment of organics appears to have ripped holes within it, similar to slits, but more widely

split (Fig. 6.15). An electron backscatter image shows two fragments of organics that represent two of the other forms (Fig. 6.16). The second noted form is a smooth (not mounded) circular, bowl-shaped fragment with minor slits that was found in association with some mottled organic forms (Fig 6.17). Three fragments of a third form of organics were found that are a form, mixed between the flat and rounded forms; there is some topography similar to the rounded forms, but also smooth regions as well. All fragments of the third form appear within aligned calcite grains that appear deformed around the organic feature (Fig. 6.18).

The final form found on this sample was only found in sample C. This form is a thin (~0.5 μm in diameter) sheet of organics that is at least 2.2 mm long (Fig. 6.19). The sheet was chemically analyzed at various locations along its length to confirm a carbon peak (Fig. 6.20). Additionally, probes were taken transecting the sheet and there were high iron and potassium feldspar grains on one side and high calcium on the other side. This finding indicates matrix material to one side of the sheet and calcite to the other side of the structure (Fig. 6.21).

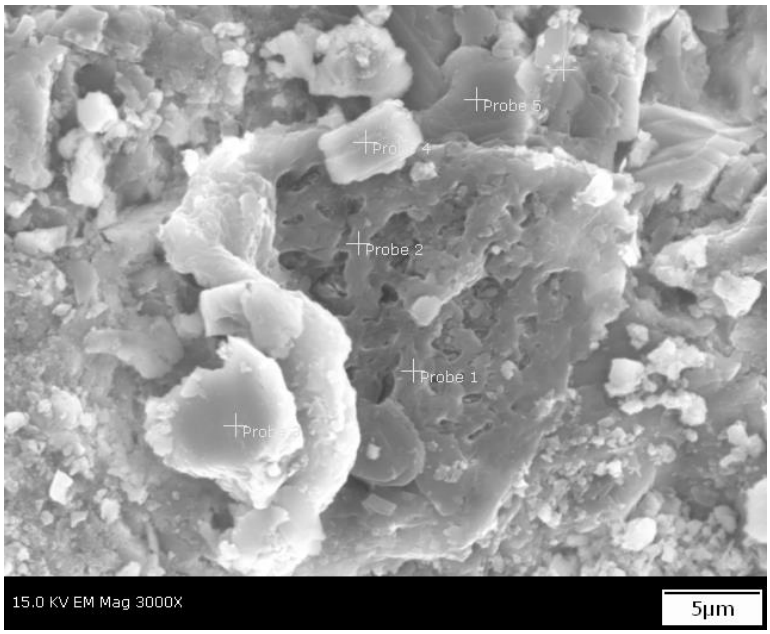

Figure 6.15: First fragment of organics identified with numerous ripped holes (darker pits) within it.

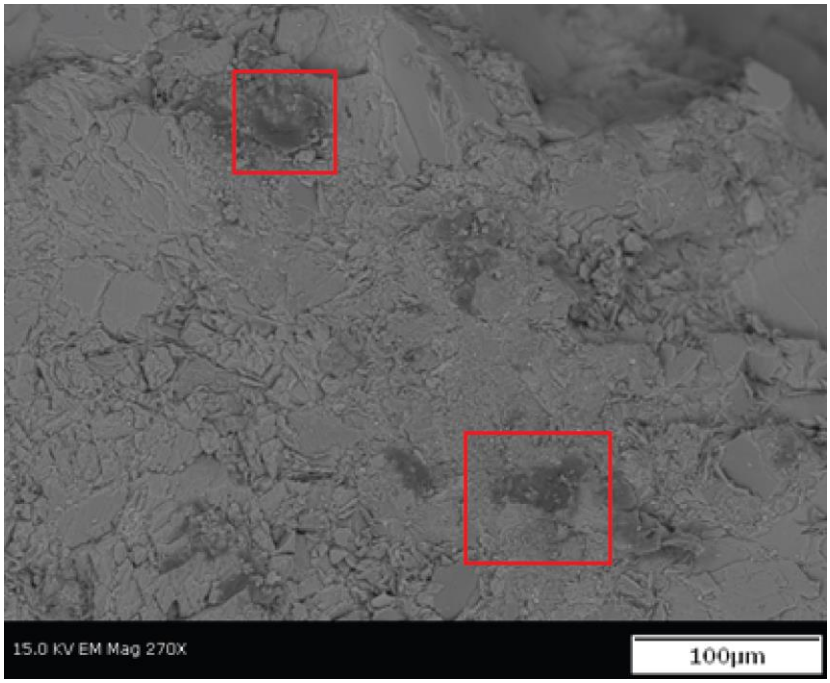

Figure 6.16: Electron backscatter image of two forms of organics described in figures 6.17 and 6.18. The location of the two forms have been boxed in red.

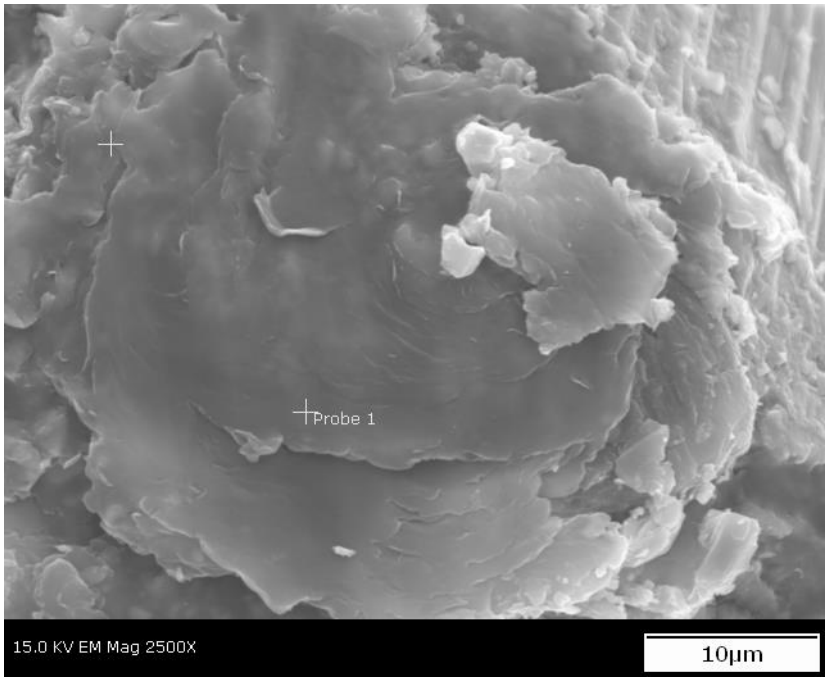

Figure 6.17: Smooth circular, bowl shaped fragment of organics with minor linear slits.

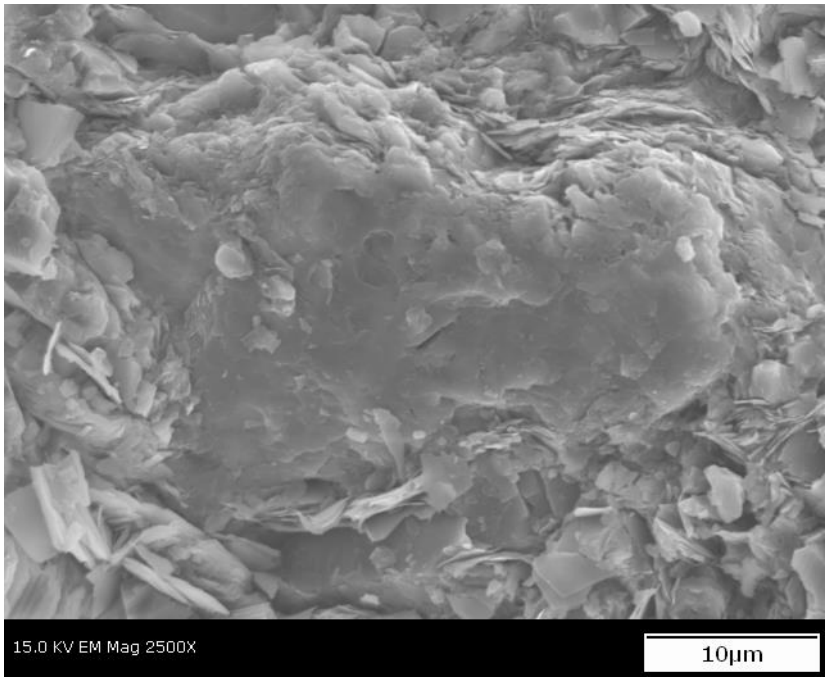

Figure 6.18: Alignment of grains along the margin of an amorphous carbon fragment.

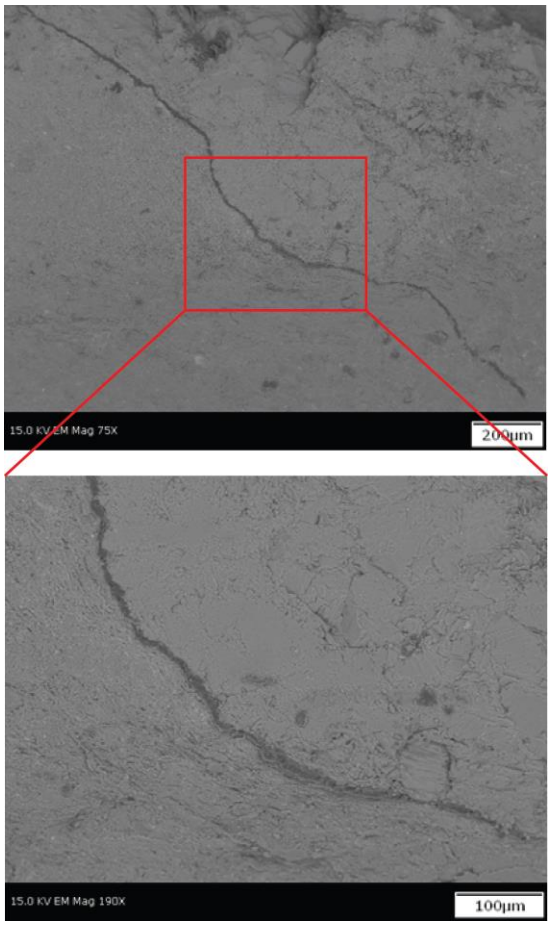

Figure 6.19: An electron backscatter image of the thin sheet of organic material identified as the curvilinear dark grey feature. The lower box is an expanded view of the central portion of the sheet.

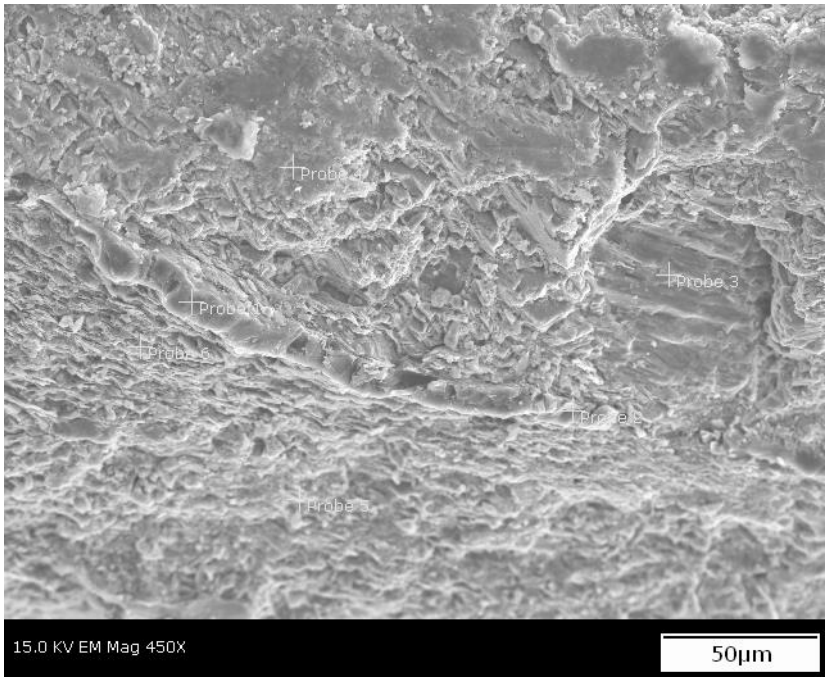

Figure 6.20: A probe within the line of carbon material was analyzed and confirmed a carbon signature.

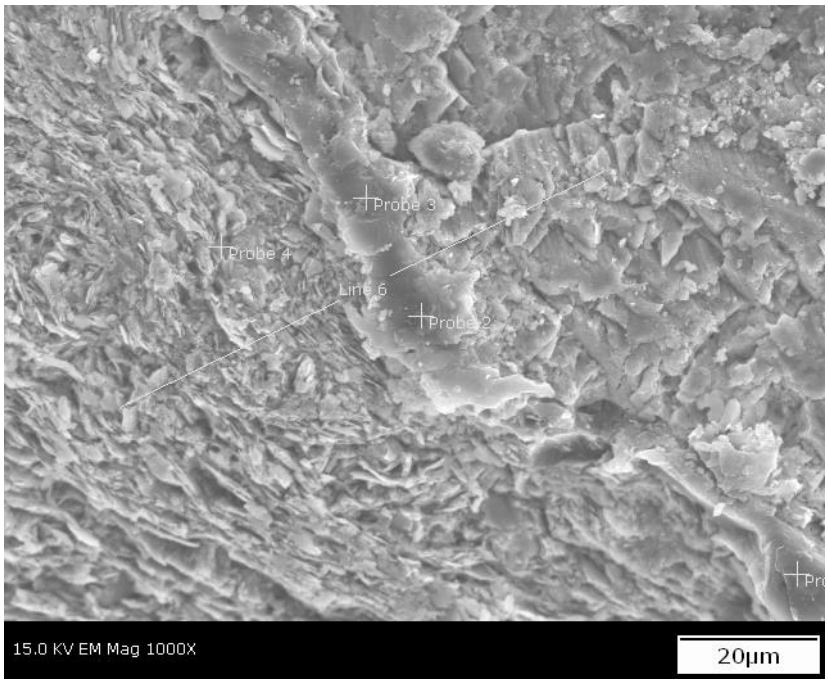

Figure 6.21: Transect of the carbon sheet confirmed high iron and potassium feldspar grains to the left of the sheet and calcite grains to the right of the sheet.

Sample Type D

Many of the forms of organic material found in concretion Type D resemble forms seen in other slabs. One form of organics in this type resembles the intermediate stage between the smooth and rounded form noted in sample C, and is circular with sharp margins

within quartz and potassium feldspar grains (Fig. 6.22). Another form of organics appears folded which could be due to disturbance during slab preparation (Fig. 6.23).

The remaining forms found in this sample were identified in an electron backscatter image that captured four different forms (Fig. 6.24). The first form resembles the ripped pieces seen in sample Type C, but to a lesser extent of tearing (Fig. 6.25). The second form appears smooth with some torn pieces (Figs 6.26). Form three appears to be another intermediate form between smooth and rounded, but with a thin fiber connecting the organic structures (Fig. 6.27). The final form was rod shaped and found within a fractured quartz grain (Fig. 6.28). There were a few areas with multiple forms of organics preserved next to one another, which was unique because organic pieces were often found as singular isolated fragments (Fig. 6.29).

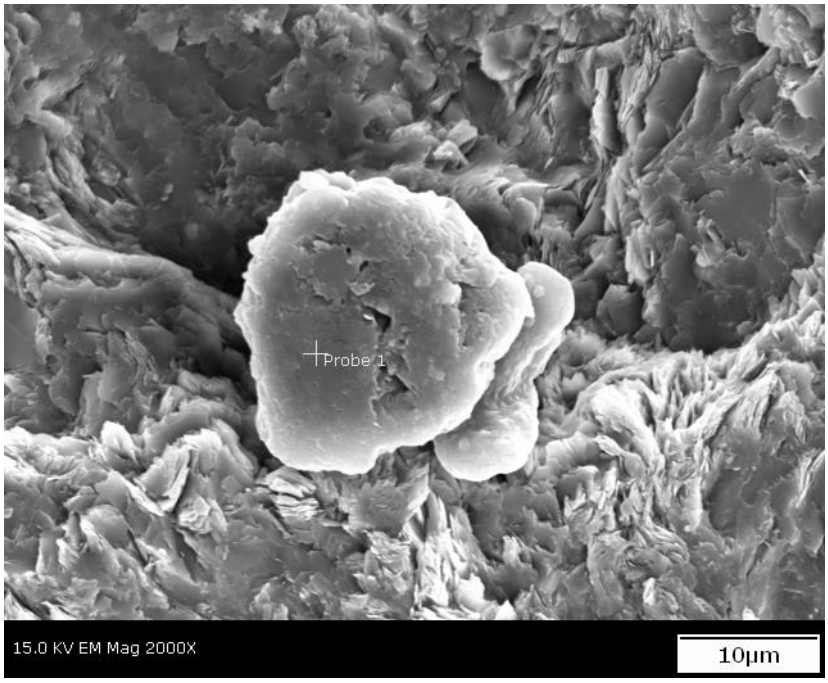

Figure 6.22: Circular form of organics with sharp boundaries found within quartz and potassium feldspar grains. Probe points mark areas where chemical data was gathered to confirm the presence of carbon.

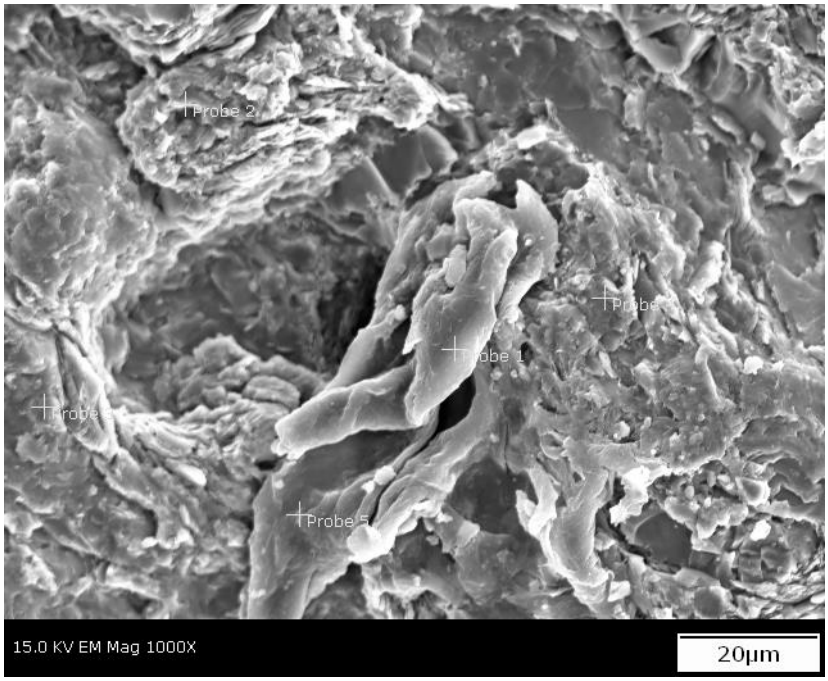

Figure 6.23: Organic fragment that appears layered upon itself. Probe points mark areas where chemical data was gathered to confirm the presence of carbon.

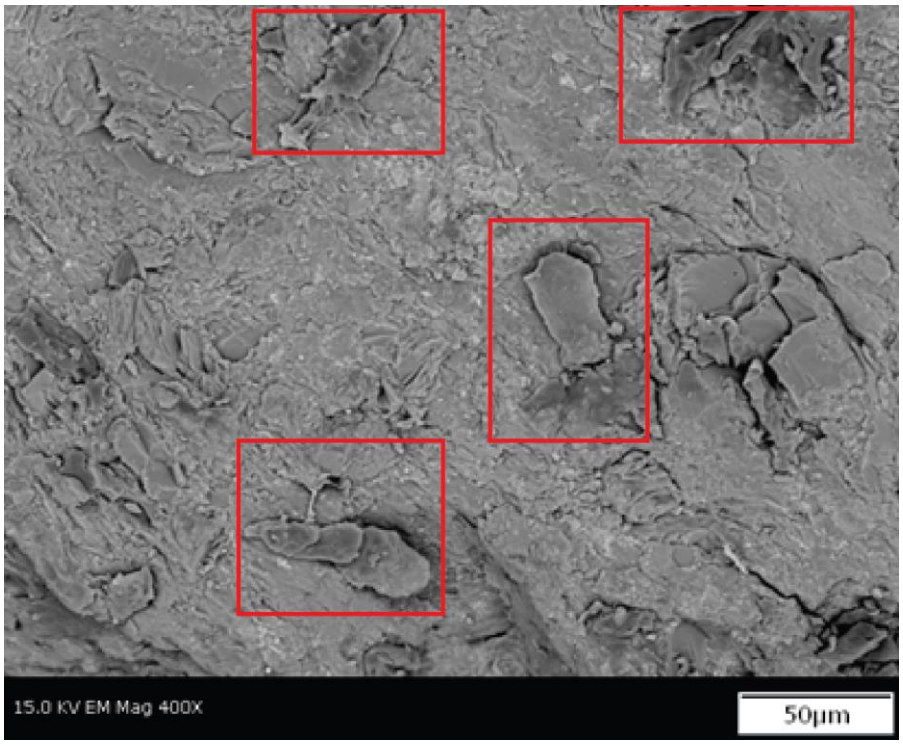

Figure 6.24: Electron backscatter image with several fragments of organics, which are shown within red boxes.

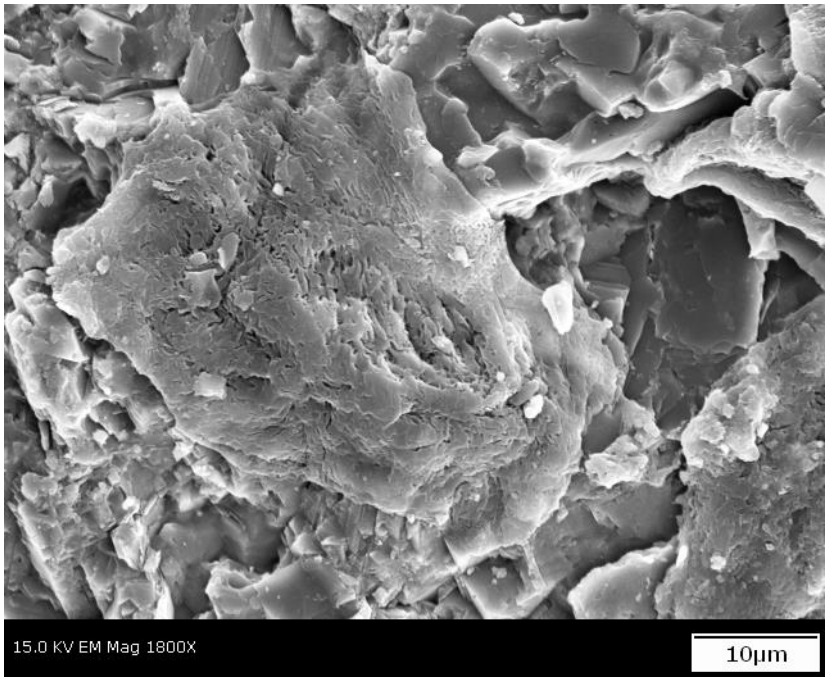

Figure 6.25: Organics form that resembles those from sample C with less tearing. Slits within the sample appear as darker curvilinear shapes within the fragment.

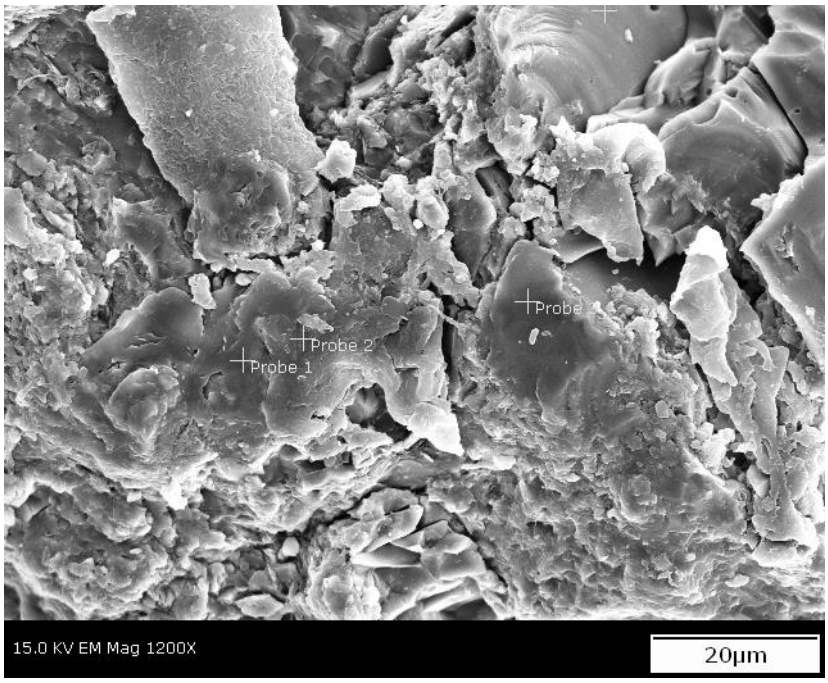

Figure 6.26: Form two of organics found on this sample contains probe 1 and two within it. This form appears smooth with minor curvilinear tears.

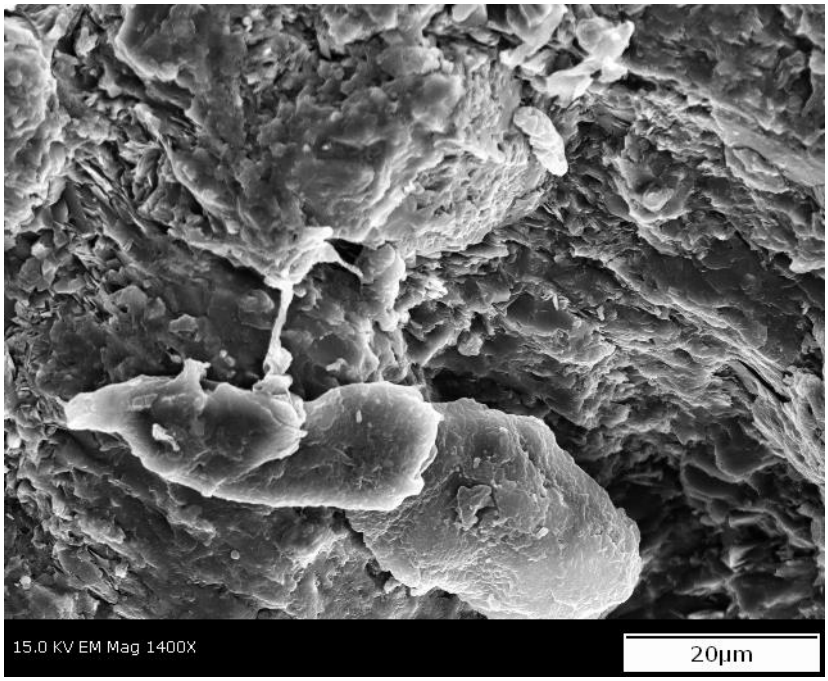

Figure 6.27: Intermediate form between smooth and rounded organics with a thin bright white fiber connecting the two organic masses.

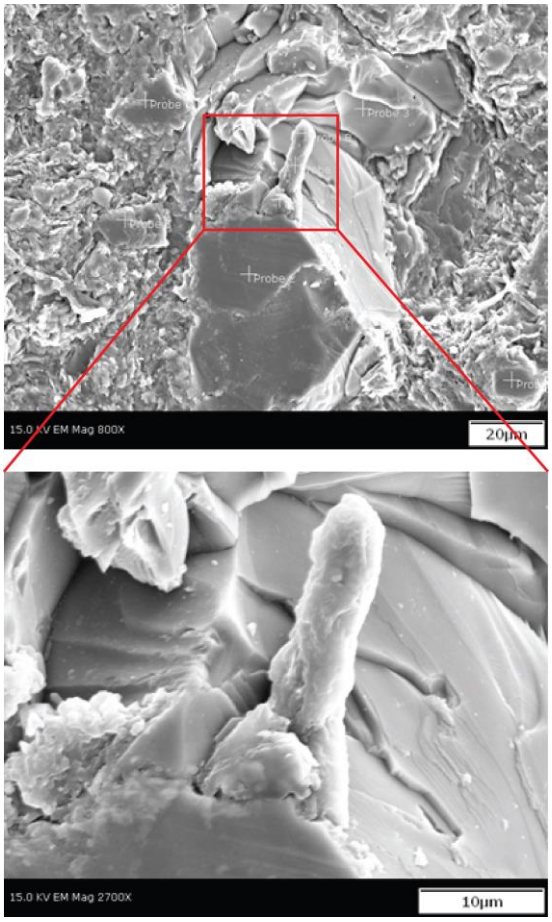

Figure 6.28: Final form of organics that takes on a rod morphology and discovered within a fractured quartz grain. This lends credibility to these carbon fragments coming from the sample as opposed to contamination on the surface of the specimen.

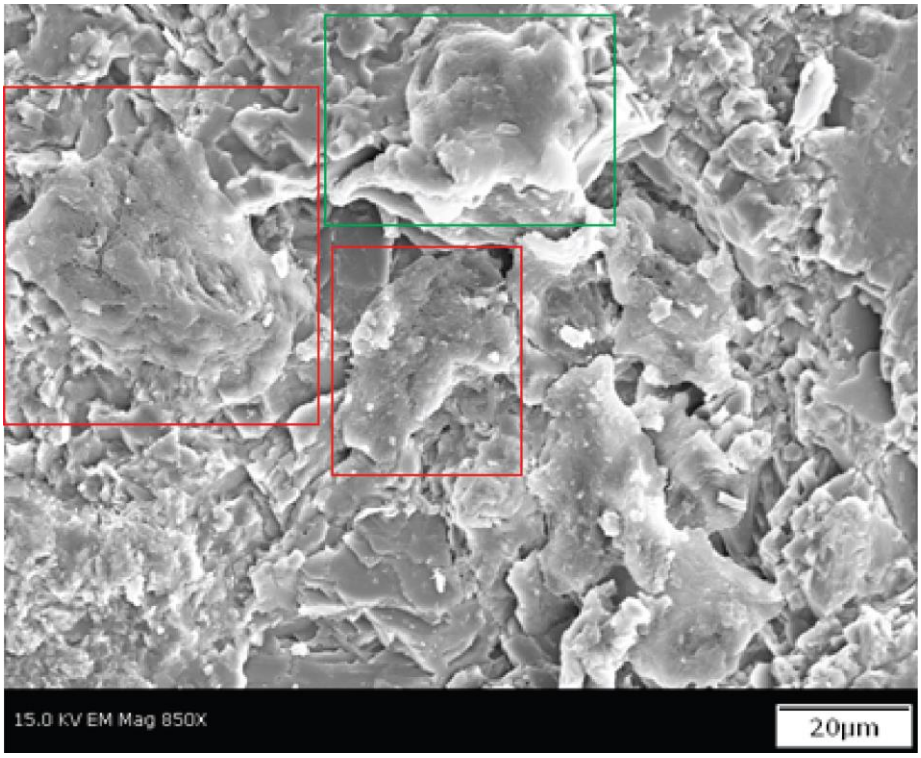

Figure 6.29: A region with multiple forms of organics that are preserved in proximity to one another. The colored boxes outline different form; mottled forms are within red boxes and a smooth form is within a green box.

Chapter 7 : Discussion

While many of the observations made of these calcite nodules could support a number of working hypotheses, there is sufficient evidence from the data collected in the field and in the lab to support the hypothesis that the calcite nodule structures represent biogenic activity within a volcanically-derived sedimentary matrix. The calcite structures from nodule types A-D share common traits that provide support for the hypothesis that the calcite rich outcrops represent the remains of a once-inhabited soil system from 370 million years ago.

The primary goals of this study were to address three objectives:

1) Establish whether the calcite concretions were biogenic or inorganic
2) Establish whether the horizon of interest is a paleosol and determine the genesis of the horizon
3) Describe the stratigraphic distribution of the calcite rich horizon

Calcite Concretions: Biogenic or Inorganic?

Several hypotheses are addressed in this section that may explain the morphology of the calcite concretions noted in this horizon. The first hypothesis is that the calcite cylinders are volcanically-generated pipe amygdules formed by degassing of a cooling lava. While there is a similar morphology to the branching thick cylindrical forms found in these samples to a pipe amygdule, there are several reasons why they are not such structures. Pipe amygdules form in one preferred orientation, while the branching cylinders within this horizon radiate in all directions, as can be seen in cross section (Figure 7.1). The margins of pipe amygdules tend to be quenched and glassy, but the margins of matrix around the calcite nodules preserved in these samples do not show quenched textures necessarily. Lastly, pipe amygdules only occur in lava flows and this unit has been shown to be a pyroclastic deposit (i.e., there is no flow banding present within the matrix of the samples and no crystalline textures are preserved).

Another working hypothesis to explain these curvilinear calcite features is secondary mineral filling of void spaces and cracks. While this may be the case for some of the features (see Appendix 1, description of sample C3) it does not explain all of the calcite features within the samples. The blunt terminations seen in sample D contradict the morphology expected from a filled crack. Fractures would taper towards a sharp point, while the feature on slide D2 has a blunt end that tapers away from that blunt end. There are definite features within some of the nodules on Types A and B that represent secondary filling of void space by calcite spar, but not all of the calcite features can be explained by fractures secondarily filling.

The third working hypothesis is that these structures are preserved rhizoliths. Klappa (1980) outlined several different ways in which rhizoliths can form. While no cell structures of plant tissues are preserved as calcite in these nodules, there are several ways in which rhizoliths can develop without preserving the original cell structure of the plant (Fig. 7.2). Calcite nodules noted in this horizon may have formed by weathering of the material around the root, allowing calcium to be leached from the matrix toward the root during water uptake by the plant (Fig. 7.2F). The matrix material around the root may then have been cemented by calcium carbonate by combination with soil-borne carbon dioxide. The root itself may have decayed to form a void space that was later filled with secondary sparry calcite (Fig. 7.2G). This mode of preservation may also have included fragments of carbon within the regions of sparry calcite. The four different forms of amorphous carbon discovered using SEM provide support for the biogenic nature of these features. Additionally, the sheet of unfragmented, *in situ* carbon found preserved on nodule type C may represent a preserved root hair (~5 μm in diameter). The size of this feature falls within the size range of present day root hairs (~5-20 μm).

Figure 7.1: Red boxes outline areas of the profile where radiating thin branching cylindrical nodules are present. The more circular forms can be visualized as coming out of the page, while the oblate forms are propagating right or left from center.

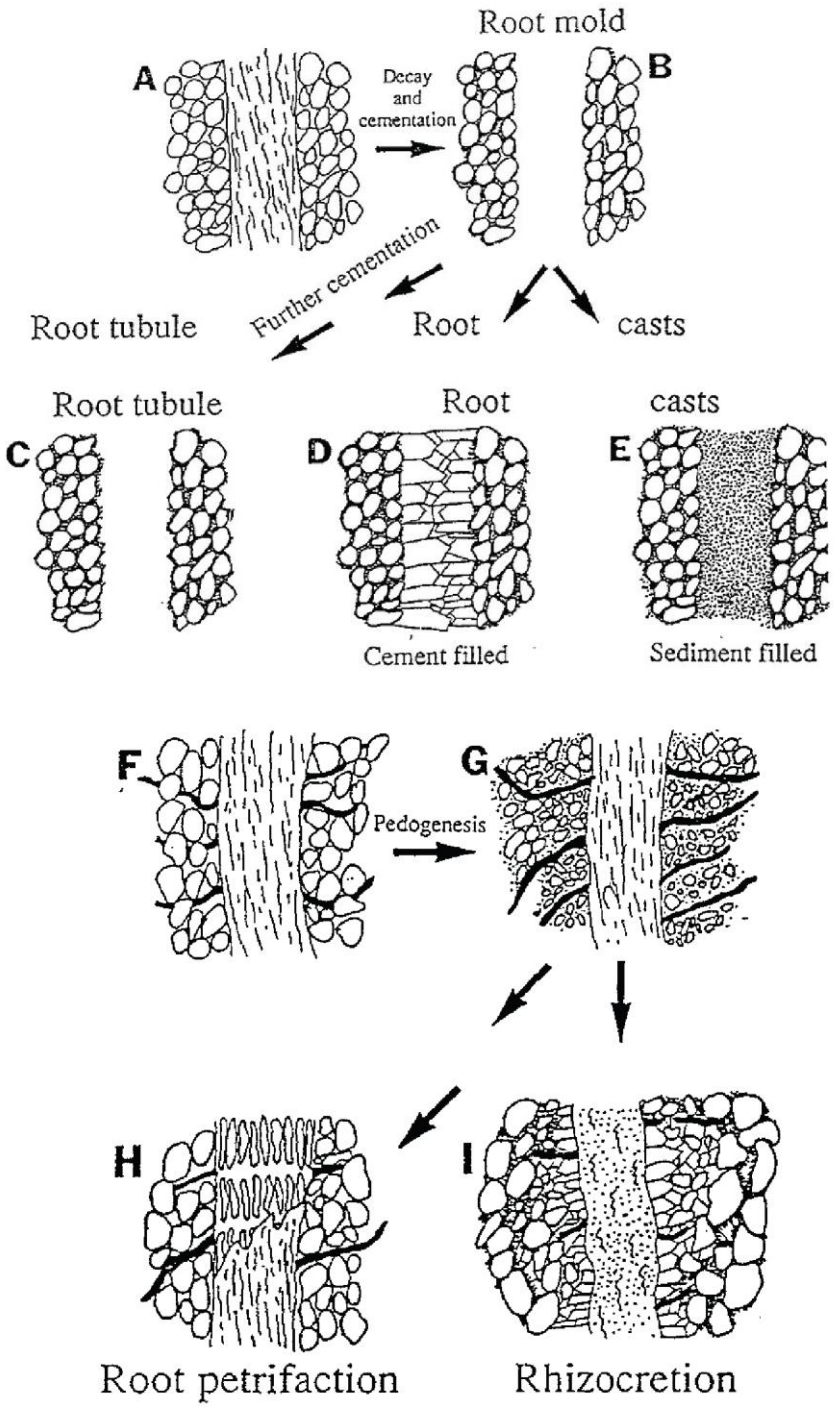

Figure 7.2: Eight different ways in which rhizoliths can form, G and I are the likely scenario for the calcite nodules in this study. G notes the weathering of the material around the root and the progression to I, where that material has cemented and the root has decayed (Klappa 1980).

The Genesis and Nature of the Calcite Rich Horizon

By containing biogenic material associated with rhizoliths, the calcite nodule horizon can be characterized as a paleosol. The pyroclastic nature of the parent material (matrix) was

confirmed by the observational data collected during petrographic work on the samples. Hypotheses about the timing and occurrence of the calcite morphologies are more difficult to establish, but are explained in detail below.

The biogenic material found within all four of the sample types provides evidence to support a biogenic nature to the calcite nodules within the horizon. While most of the carbon forms were isolated amorphous fragments and did not provide preserved cellular structures material, they did suggest an interaction with biologic materials. The presence of one *in situ* sheet of carbon material serves as the most convincing evidence that these nodules may represent rhizoliths within the matrix.

The paleosol is interpreted as having developed within a pyroclastic parent material. The Naragansett Basin, where these outcrops are found, represents a rift basin area with abundant volcanic activity in the late Devonian. The matrix of the calcite horizon is shown to be pyroclastic due to the abundance of angular glass shards that have devitrified to quartz within the coarse matrix of the samples. Additionally the presence of lithic and pumice fragments imply an explosive volcanic origin. The paleosol is considered to have been immature due to the high abundance of angular shards and lithic fragments, which indicate a lack of weathering within the soil. Establishing the timing of emplacement of the roots that formed the rhizoliths within the pyroclastic deposit is a complicated issue.

The timing of the emplacement of the distinct calcite morphologies can be shown, to an extent, by the presence of weathered pits (formerly containing calcite) found in thin sandstone beds above the nodular horizon. These thin sandstone beds represent very immature paleosols that are preserved the first form of calcite nodule to be emplaced within the paleosol. The only form of calcite nodule in the thin sandstone beds are thin branching cylindrical forms (sample type C) noted in the paleosol profile, (Figure 4.1). These structures are interpreted as being the primary structures to form within the developing paleosol and are

shown in the thick horizon to be cross cut by the thick branching cylindrical structures. This relationship provides evidence to indicate the thin branching calcite nodules formed in the paleosol first, and the thick branching structures formed afterward. Due to the repeated vertical occurrence of this primary-secondary nodule relationship in the horizon it can be assumed that the unit represents multiple generations of paleosol development.

In order to form a correlation between the occurrences of distinct morphologies of the calcite nodules to a location within the developing soil, the matrix associated with different morphologies was analyzed in detail. The coarseness of the matrix is interpreted as representing the amount of weathering the soil has undergone in the sample. The fine opaques were interpreted as weathering products within the samples, therefore the higher the percentage of opaques the higher the amount of weathering for the sample. This can then be correlated to a location within a developing soil profile because the more weathered material would be found near the top of the profile. Following this interpretation, samples B and D would be correlated to lower portions of the developing soil, while sample types A and C would be correlated to upper (more weathered) portions of the developing soil (Table 5.1). However, a different interpretation of the distribution of coarse and fine matrix is possible. Due to the volcanic environments in which these sediments were deposited, it is possible that different sources of sediments controlled the grain size (e.g., ash deposit vs. pyroclastic flow) rather than the amount of weathering.

The Stratigraphic Distribution of the Calcite Nodule Horizon

Using the basalt and calcite-bearing units at sites X1 and X2, a lateral correlation can be made between the two sites. The basalt unit thickens to the west from site X1 to site X2 while the opposite is seen in the calcite horizon that thins from east to west. One interpretation for this is that the western site, X2, may represent a local basin or valley that filled with a thick basalt flow. This low region may have previously held a standing body of

water, as evidenced by the basalt pillows at this site. The thinner calcite horizon at this site may be due to influxes of sediment or surface water that destroyed plants or had a sediment accumulation rate too high to develop a soil. The eastern site, X2, may represent a local highland that preserved a thinner basalt flow, but was a more stable environment where plants were less disturbed and able to form a deeper (3 m thick) soil horizon. Overall, it is clear there is a variable thickness to the calcite horizon, which would be expected in the case of highly variable units such as paleosols developing in structurally unstable volcanic regions.

Chapter 8 : Concluding Remarks

This thesis provides a more complete explanation of the calcite-rich horizon of sedimentary rocks within the Devonian portion of the Wamsutta Formation. The first objective was to establish whether the calcite features were biogenic or inorganic. Detailed petrographic descriptions of the samples and SEM analyses provided a means of establishing the biogenic nature of the concretions. The presence of several fragmented forms of carbonized organics was confirmed, and while the origin of the amorphous carbon could not be attributed to a specific plant structure, the abundance of carbon found within the calcite provided evidence to support a biogenic nature. Only sample C showed *in situ*, unfragmented, carbonized remains that could be interpreted as a root hair and supports the hypothesis that these calcite structures are rhizoliths.

Establishing whether the horizon of interest represents a paleosol was supported with the same evidence used to support the first objective as well as additional descriptive analysis of the matrix surrounding the nodules. The biogenic material found within these rocks support that this feature represents a paleosol. There is a primary-secondary relationship between the thin branching cylindrical nodules and thick branching cylindrical nodules that is evident in several localities of the outcrop profile and support multiple generations of soil development. Additionally, the matrix surrounding the nodules was described in detail to provide supporting evidence for the possible environments in which the nodules could have formed. This was done with the assumption that the fine opaques found within the matrix of several samples represented weathering products. This was used to place the more weathered matrix, higher fine opaque, samples (A and C) higher in a developing soil profile than the coarser matrix samples (B and D).

The final objective of this thesis was to describe the stratigraphic distribution of the calcite-bearing horizon. In correlating sites X1 and X2, there was a lateral continuity of the

calcite horizon that thinned to the west at site X2. The thinning of the calcite at site X2 may represent a lowland that filled with more of the basalt flow and was unable to develop a thick soil horizon, due to influx of sediment at that location. Following that logic, site X1 is interpreted to represent the highlands and therefore does not contain as thick of a basalt unit, but a thick (3 m) soil horizon that may have had less sediment influx that allowed plants to root deeper at that site.

Significance

The significance of this deposit is closely tied to the time frame in which it was developed. There are very few preserved root horizons within volcanic deposits from the Late Devonian. Evidence of roots preserved within volcanic deposits is rare and has been found in Yellowstone National Park and around some volcanic mountain ranges in the Cascades. Shallow root systems (<1 m) dominated the Early Devonian and rapidly evolving terrestrial plants developed deeply rooting systems (~1 m +) by the late Devonian (Fig. 8.1). The calcite nodule horizon is found in association with dated Late Devonian rhyolite and falls within the time range for the initial development of early deeply rooted plant ecosystems. This means the calcite nodule horizon preserved at site X1 may represent one of the earliest deeply rooted paleosols.

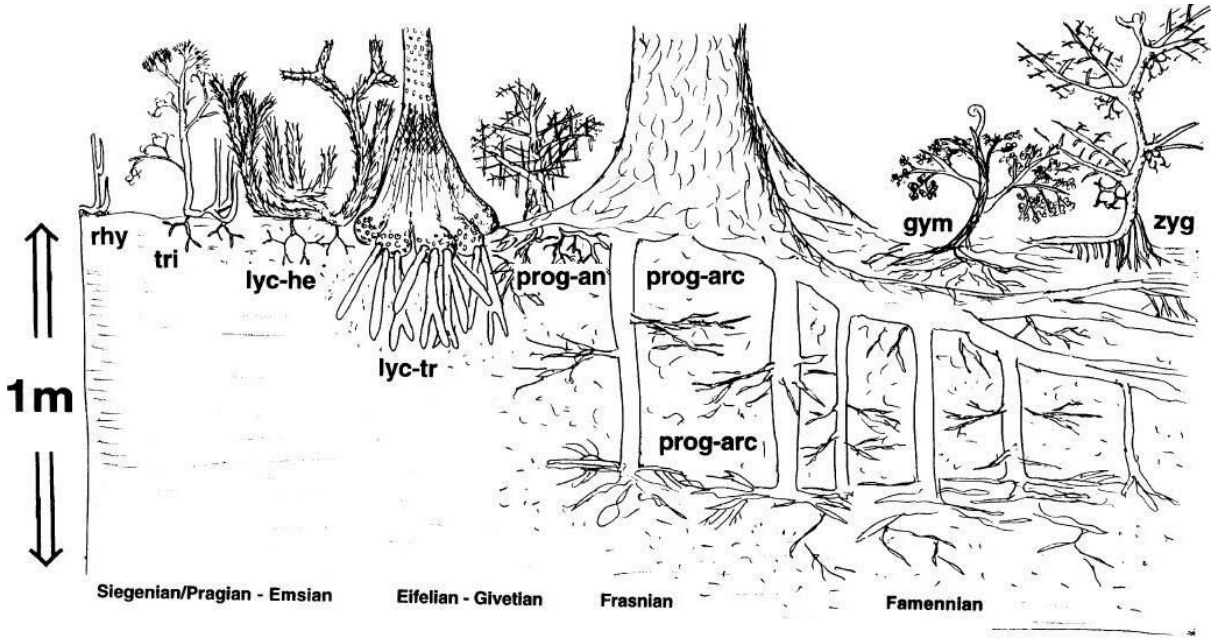

Figure 8.1: Progression of time through the Devonian, from left to right, as root systems become deeper in the Frasnian-Famennian (~374 Ma) (Algeo et al, 2010)

Future Work

Building off of this thesis, more work can be done to link the type of plant that could have been rooting in this horizon to specific nodule morphologies. This would involve further investigation of the samples at SEM magnifications in order to discover additional forms of carbonized organics that may be present within the samples. Additionally, further work with the SEM would greatly strengthen the argument that these structures represent rhizolith features if more *in situ* organics could be found. Another line of investigation would be to further analyze the matrix surrounding the calcite nodules in order to confirm correlations between the nodule types and matrix properties. This data could then be used to more accurately correlate specific morphologies to levels within the paleosol where they may have developed.

References

Algeo, T. and S. E. Scheckler, 2010, Land Plant Evolution and Weathering Rate Changes in the Devonian: Journal of Earth Science, v. 21, Special Issue, 75-78.

Benner, J. S. and Gardulski, A. F., 2010, Phytoturbation below a Late Devonian—Westphalian unconformity in southeastern Massachusetts. Geological Society of America *Abstracts with Programs*, Vol. 42, No. 1, p. 105.

Calder, J. H., 1998, The Carboniferous Evolution of Nova Scotia: Geological Society, London, Special Publications, v. 143, 261-302.

Cazier, E. C., 1987, Late Paleozoic Tectonic Evolution of the Norfolk Basin, Southeastern Massachusetts: The Journal of Geology, v. 95, 55-73.

Klappa, C. F., 1980, Rhizoliths in terrestrial carbonates: classification, recognition, genesis and significance: Sedimentology, v. 27, 613-629.

Lyons, P. and W. C. Darrah, 1978, A late Middle Pennsylvanian flora of the Narragansett basin, Massachusetts: Geological Society of America Bulletin, v. 89, 433-438.

Maria, A. and O. D. Hermes, 2001, Volvanic Rocks in the Narragansett Basin, Southeastern New England: Petrology and Significance to Early Basin Formation: American Journal of Science, v. 301, 286-312.

Mosher, S., 1983, Kinematic History of the Narragansett Basin, Massachusetts and Rhode Island: Constraints on Late Paleozoic Plate Reconstructions: Tectonics, v.2, 327-344.

Murray et al., 2004, Tectonostratigraphic Relationships and Coalification Trends in the Narragansett and Norfolk Basins, New England: Journal of Geodynamics, v. 37, 583-611.

Thompson, M. and O. D. Hermes, 2003, Early Rifting in the Narragansett Basin, Massachusetts-Rhode Island: Evidence from Late Devonian Bimodal Volcanic Rocks: The Journal of Geology, v. 111, 597-604.

Appendix I:

Thin Sections from Sample A

A1

The sample A1 has elongate lobes of calcite that are separated by thin lenses of matrix ranging from 0.26 mm at the thickest and 0.1 mm at the thinnest areas (Fig. A.1). The slide is dominated by calcite lobes (80%) while the matrix makes up 20% of the slide (Table 5.1). The matrix is primarily fine-grained opaque minerals with various larger grains of quartz (up to 0.1 mm across). The grains within the matrix range from a few angular clasts to rounded clasts and are dominated by subangular quartz grains. The quartz grains appear to be isolated within the fine matrix. Most of the quartz grains display wavy undulatory extinction.

In plane polarized light there is clear alignment of the long axis of dark fine-grained minerals parallel to quartz grain margins within the matrix (Fig. 5.3A). Some of the larger quartz clasts have reddish brown inclusions within their grains that remain a dark brown in cross-polarized light (Fig. A.2A). A similar amorphous brown inclusion is seen in several localities near the margin of the massive calcite lobes along the sediment seam. Additionally, this dark brown material is noted within seams of sediment encroaching into the calcite lobes (Fig. A.2B). There are rare spots where the brown material looks to be staining in an elliptical form, approximately 0.05 mm across (Fig. A.2A).

The massive calcite lobes are relatively homogeneous. The texture and size of the calcite grains within the lobes varies according to location. Along the margins of the lobes where there is contact with matrix there are medium sized grains of calcite (~ 0.1 mm), which are larger than the micritic grains (average 0.0125 mm across) and smaller than the sparry calcitic grains (average 0.25 mm across). This sample does not contain any sparry calcite, and the largest medium sized grains visible in this sample are 0.05 mm across. The medium sized calcite grains occur as interlocking subhedral grains of calcite that form curvilinear structures

through the micritic lobes. There is a change in grain size along the margins of the calcite lobes, showing a rough gradation from medium to micritic grains as you move deeper within the lobe.

Some of the interlocking coarser curvilinear calcitic regions form elliptical, circular, and horseshoe-shaped features within the calcite lobe (Fig. A.2C). There are regions where these features encircle darker grains. Observation of the darker grains under higher magnification showed tightly packed extremely small micritic grains of calcite and some circular black spots. The micritic calcite appears deeper within the calcite lobe, inside of the medium grain calcitic boundary, that separates the micritic grains from the matrix.

There are abundant transitional zones between the calcite lobe and matrix, where thin lenses of matrix intertongue with fine-grained calcite (Fig. A.2D). Transitional zones are evident where the lobes pinch out into the matrix, and are also visible along the lobes separated by thin layers of sediment (~ 0.1mm across). The exception to the homogeneity of the calcitic lobes is the brown inclusions and staining in some areas and numerous engulfed quartz grains and sediment pockets entrenched within the micritic lobes of calcite (Fig. 5.2). The micritic lobes of calcite are separated from the matrix by medium coarseness calcite grains.

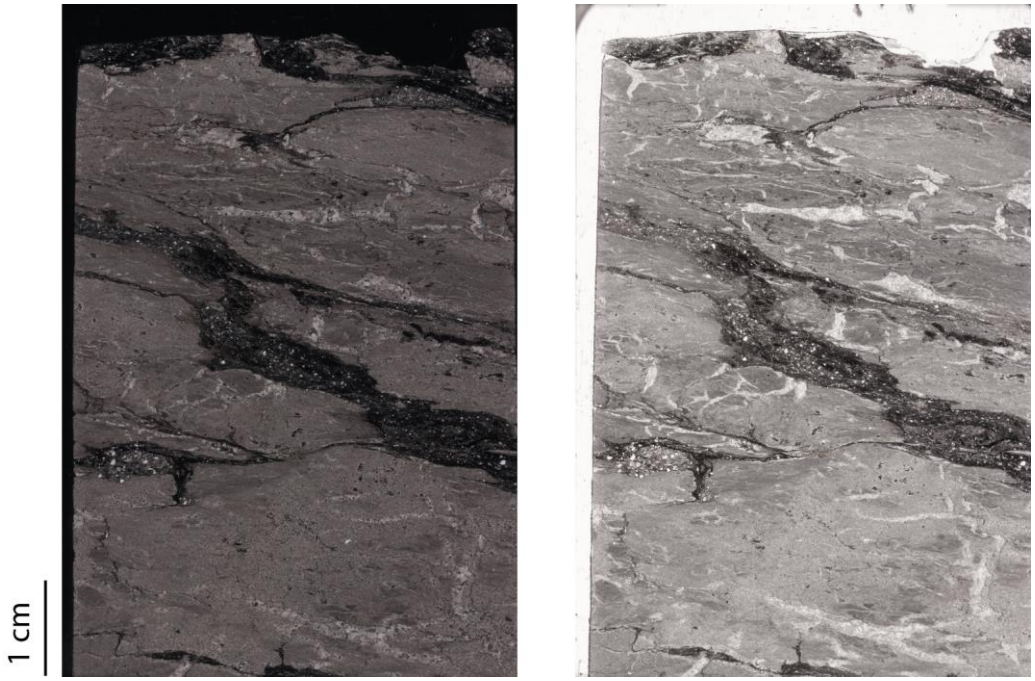

Figure A. 1: Scan of thin section for sample A1, which is shown in cross polars on the left and plane polarized light on the right.

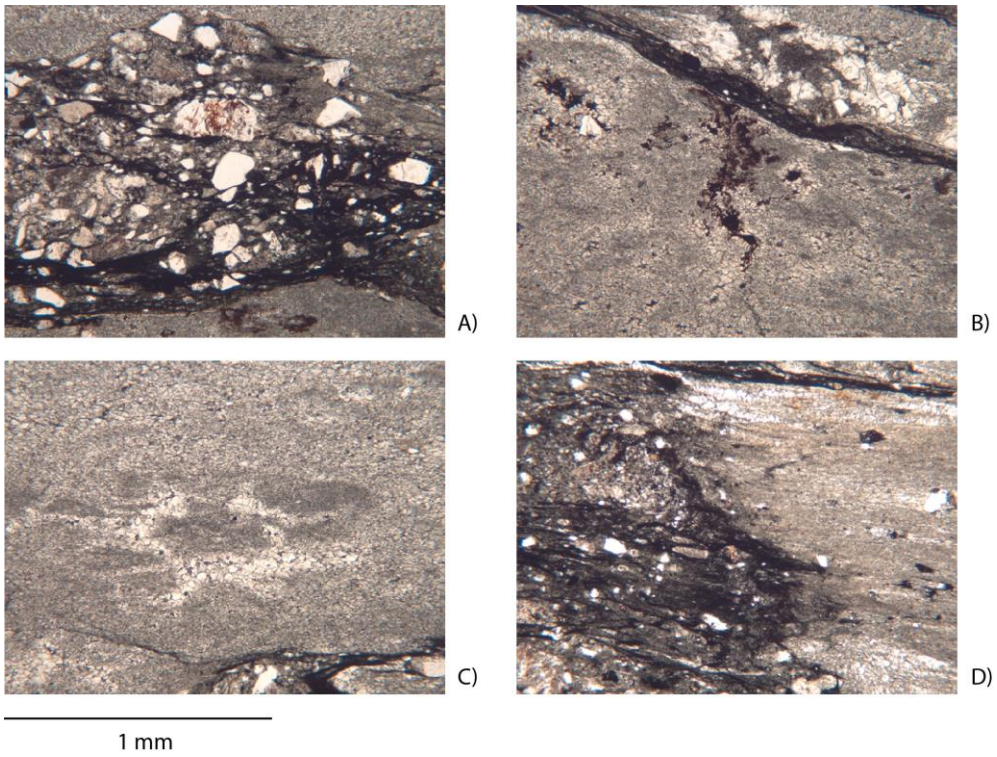

Figure A. 2: A) Brown staining on a quartz grain as well as elliptical forms of brown staining within the micritic calcite at the bottom of the photograph, B) Amorphous brown staining within a crack inside of the micritic calcite nodule, C) Elliptical form filled with medium calcite within a micritic nodule, D) Transitional zone of intertonguing matrix and micritic calcite.

A2

Sample A2 has elongate lobes of calcite that are separated by thin lenses of matrix ranging from 0.5 mm at the thickest and 0.025 mm at the thinnest areas (Fig. 5.1). The slide is dominated by calcite (85%) while the matrix makes up 15% of the slide (Table 5.1B). The matrix is primarily larger grains of quartz (0.19mm) within an opaque fine sediment. The grains within the matrix range from a few angular smaller clasts to large (~ 0.19mm) rounded clasts (Fig. A.3A). The matrix forms curvilinear paths between the lobes of calcite. The grains are subhedral and make up the bulk of the matrix in the bottom half of the slide separating the two lobes of calcite. These quartz grains are very numerous within the fine matrix and most of the grains display undulatory extinction. There are also small, highly birefringent grains within the matrix that are likely pyroxene or olivine (Fig. A.3A). The sediment appears to be primarily volcanically derived minerals (plagioclase, quartz, pyroxenes, olivines).

In plane polarized light, dark fine-grained minerals are aligned around quartz grains and other grains within the matrix. Some of the larger quartz clasts have reddish brown inclusions that remain dark brown in cross-polarized light. A similar amorphous brown staining occurs in several localities within the calcite lobes that are surrounded by micritic calcite grains (Fig. A.3B). The brown areas tend to be stretched within seams of medium grained calcite. Isolated brown segregations reach lengths of ~ 0.625 mm across, and can form aggregates of several smaller spherical structures that coalesce into a larger feature (Fig. A.3B).

The calcite lobes in this sample contain many intrusions by matrix material and there are engulfed quartz grains located very close to the matrix intrusions. Additionally, there are several areas with pockets of fine opaque matrix material within micritic calcite lobes. The slide contains 63% micritic (~0.0125 mm across) calcite, 7% medium coarseness calcite

(~0.1 mm across), and 15% sparry calcite (~0.25) (Table 5.1B). The sparry calcite forms interlocking masses of subhedral calcite grains that form curvilinear structures and ellipsoids. The sparry calcite regions show abrupt transitions to micritic calcite at the margins of these curvilinear and ellipsoid features. There are many circular and ellipsoid masses of medium grained calcite within the micritic lobes (Fig. 5.3C). Many of the medium grained regions are sinusoidal lines that form "W" shaped structures (Fig. 5.3B). There are regions where the circular features encircle darker grains under cross-polars that are tightly packed, extremely small micritic grains of calcite with some circular black spots (fine-grained sediment) (Fig. 5.3C). The micritic texture starts inside of the medium grained calcite that forms on the margin of the lobes of calcite, appearing as a border around the lobes separating the micritic grains from the sediment.

The lobes on this slide have numerous intrusions of sediment that create the appearance of many smaller lobes of calcite. There are many transitional zones between the calcite lobes and matrix that contain diffuse boundaries and lenticular strips of matrix intertonguing with fine grained calcite (Fig. 5.3D). The transitional zones are typically seen where the lobes appear to pinch out into the matrix, but also occur between the lobes separated by thin layers of matrix (~ 0.1mm across).

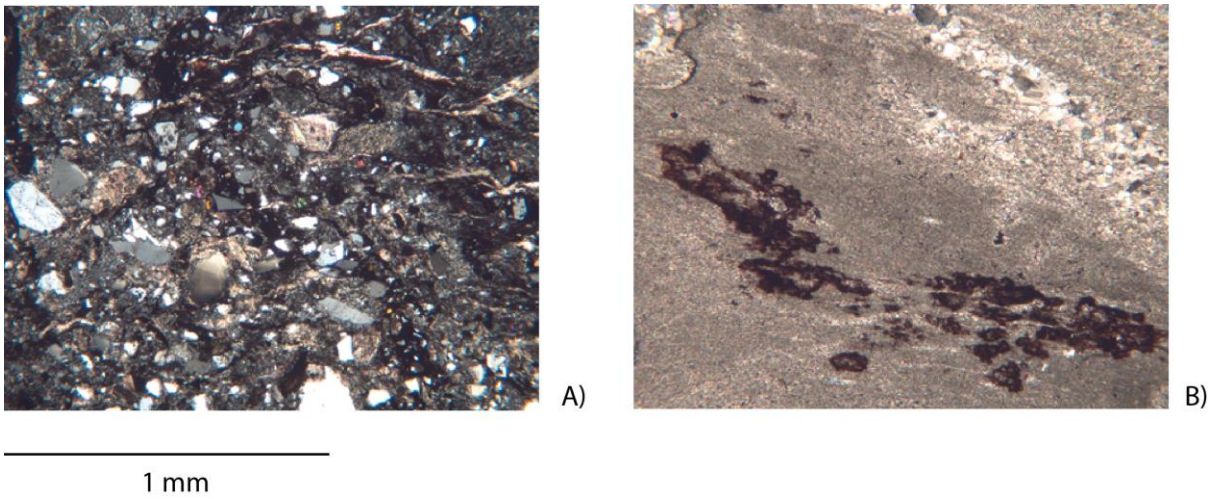

Figure A. 3: A) Matrix that contains small highly birefringent grains, typically green or pink, as well as abundant quartz grains, B) Amorphous brown staining within micritic calcite inside of a nodule.

Thin Sections from Sample B

B1

Sample B1 has one large and one smaller nodular calcite region within coarse matrix (Fig. 5.4). The matrix in this sample is composed of some larger subangular quartz grains (~ 0.5mm) and abundant smaller angular quartz grains (~ 0.025mm) that exhibit undulatory extinction. There are also grains of calcite within the matrix. The small amount of opaque fine material within the matrix forms bands that wrap around clusters of interlocked finer grained quartz and isolated grains of quartz (Figs. A.4). There are a few highly birefringent grains (olivines and pyroxenes) within the matrix and some isotropic grains (oxides).

In plane polarized light the matrix appears to be a coarser grained fabric than the fine opaque fabric of sample A. Within the nodule of calcite there are thin circular and linear structures that are visible because they are medium grained calcite within the mainly micritic nodule. There are euhedral quartz grains (~0.15 mm across) deep within the nodule separated from the sediment that could have been early inclusions during formation of the nodule.

The margin around the large nodule of calcite appears fractured and many of the calcite grains appear to have been incorporated into the matrix, which could be due to shear

or rotation of the nodule within the matrix. Along the nodular margin, within the matrix, a quartz grain was observed to have five small seams of interlocking microcrystalline calcite grains (Fig. 5.6D). The margin along the smaller nodule has more coarse grain matrix inclusions. The calcite grains that rim this nodule appear to be warped by the large grains within the matrix, and could be due to compaction. One of the included grains has a brown stain coating and an associated green high relief grain (epidote or chlorite) (Fig. 5.5).

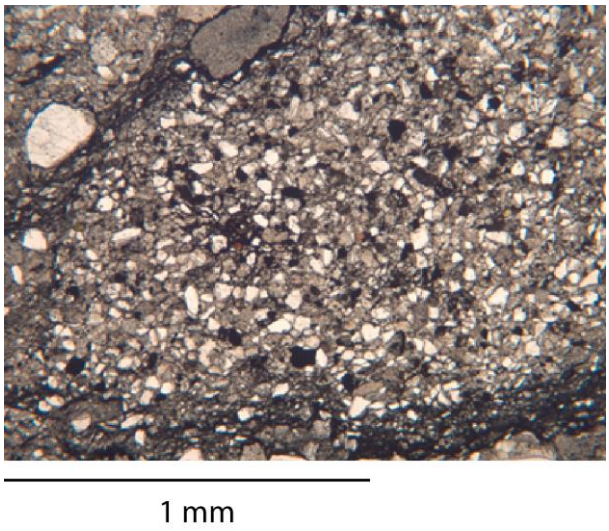

Figure A. 4: Minor fine opaques form bands around a cluster of interlocking fine grains of quartz.

B2

Sample B2 has one distinct band of calcite-rich material that forms a sigmoidal pattern that is massive on the sides and thins in the middle of the slide where it is split by a line of sparry calcite (Fig. A.5). The margins between the calcite regions and the sediment are not distinct in all areas of the slide and calcite is found in the sediment surrounding the calcitic regions. The calcite nodules are predominately micritic with entrenched quartz grains and curvilinear forms of medium grained calcite within it.

The matrix in this sample is entirely coarse grains that lack fine opaques and makes up 35% of the slide (Table 5.1). The matrix is predominately small, subrounded quartz grains that are ~0.04 mm across and contain larger subangular to rounded quartz grains that are up to ~0.5 mm across. There are highly birefringent well-rounded grains within the matrix that

are often ~0.025 mm across but can reach lengths of ~0.125 mm in the longer rod and elliptical forms (Fig. 5.6A). There are abundant sparry calcite grains within the sediment around the margins of the calcite nodular regions. Domains are present within the matrix, and areas with coarse matrix are separated by thin lamellar streaks of fine matrix. The quartz grains within this sample exhibit undulatory extinction and often have inclusions or gas bubbles on their surface. One corner of the slide contains grains that appear shard-like with very sharp triangular terminations. This sample does not contain distinct boundaries between the matrix and calcite on the upper half of the slide; therefore the matrix contains regions of sparry and medium grained calcite aggregates within it.

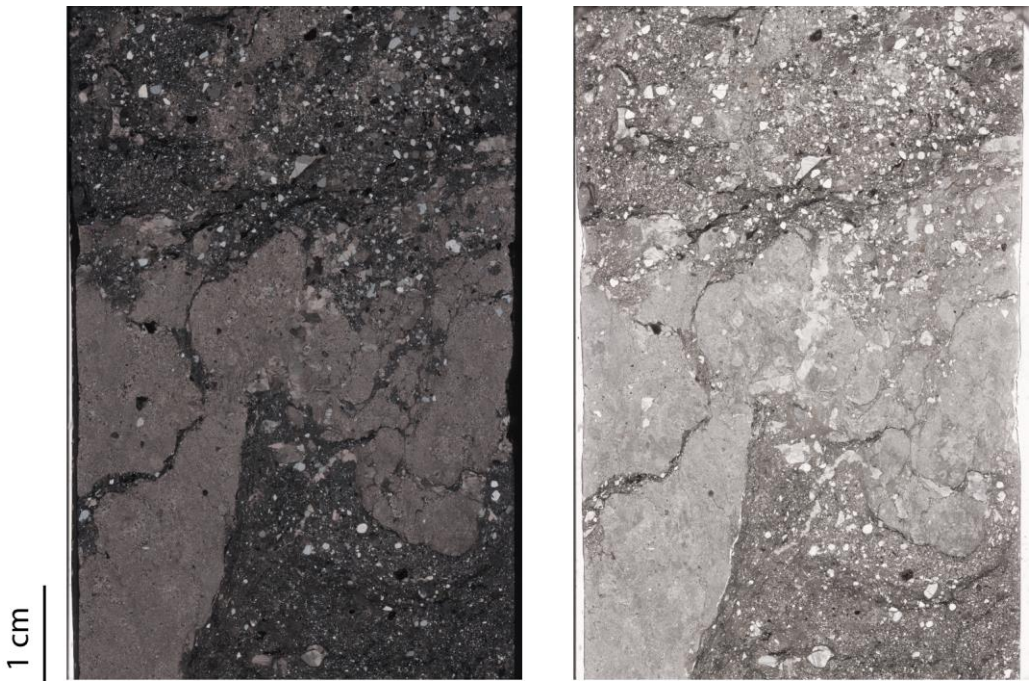

Figure A. 5: Scan of thin section for sample B2, which is shown in cross polars on the left and plane polarized light on the right.

B3

Sample B3 has one distinct region of calcite that makes up 80% of the slide (Table 5.1). Thin zones of finer matrix separate the calcite region into different areas, but the mass remains connected overall (Fig. A.6). 45% of the slide is made up of micritic calcite that occurs in a majority of the nodule and fills inside of a region of massive sparry calcite. The

massive sparry calcite crystals within the central region form a semi-circular “horseshoe” shape around micritic calcite. Some incorporated finer matrix is included in the “horseshoe” region as well as small rounded quartz grains, and highly birefringent grains. The sparry calcite grains in this region are ~1.25 mm across. This region also has medium grained calcite within the nodular structure that stand out because they are lighter than the micrite and smaller than the sparry calcite on the sample. There are numerous inclusions of small ~0.06 mm rounded quartz grains that have undulatory extinction. In figure 5.10A, there is a circular dark core within a lighter rim of fine-grained microcrystalline quartz (~0.044 mm across) with a dark fibrous rim on the outside of this feature. The darker regions of micritic calcite have a pinkish color on the thin section, which may be an iron oxide coating.

The matrix in this sample is coarse and composed of mainly sub-round quartz grains (~0.1 mm) that support some larger quartz clasts (~0.25 mm). Most of the quartz grains within this sample show undulatory extinction and often have inclusions and small bubbles that form tracks on their surfaces. The sediment makes up 20% of the slide and contains regions of sparry calcite as well as isolated grains of calcite. There are trace amounts of highly birefringent rounded grains within the matrix that are up to ~0.0375 mm across. Within the matrix there is a light brown clast (in plane polarized light) that may be a pumice fragment, and was ~0.43 mm across (Fig. 5.6B). The margin between the matrix and calcite is not well defined and there are no visible intertonguing transition zones between the matrix and calcite nodule.

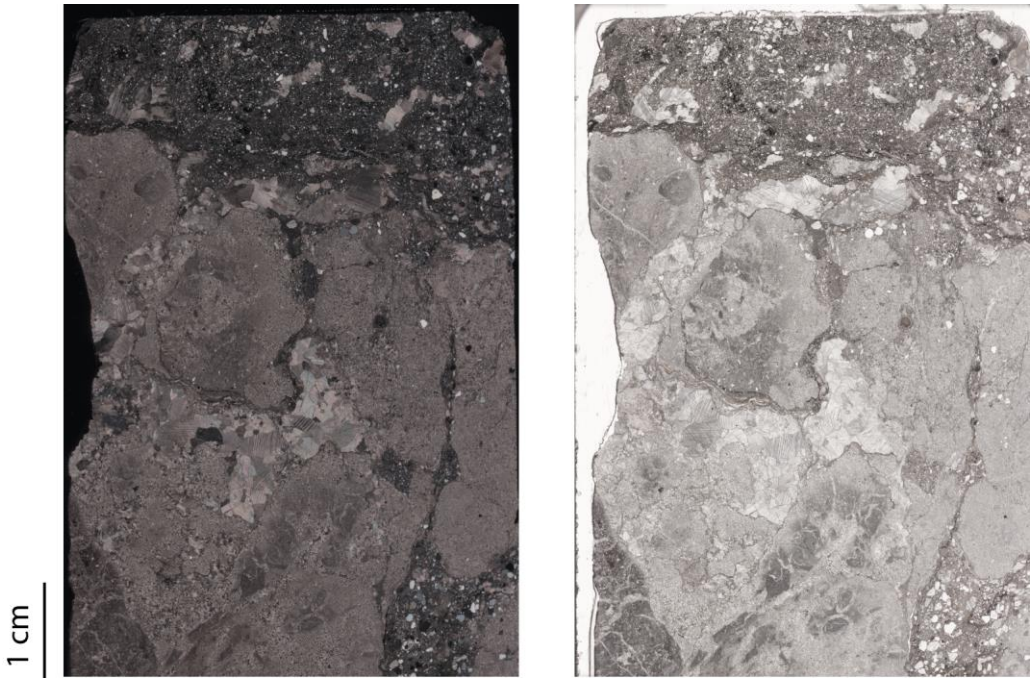

Figure A. 6: Scan of thin section for sample B3, which is shown in cross polars on the left and plane polarized light on the right.

Thin Sections from Sample C

C1

Sample C1 contains nodular calcite that has numerous seams of fine-grained matrix and grades into an anastomosing channel like structure of sparry filled calcite cylinders (Fig. A.7). The slide contains 75% calcite, and 40% of the slide is micritic calcite within the nodular region of calcite (Table 5.1). There are semi-circular horseshoe shapes within the micritic calcite that are filled with sparry calcite grains (Fig. A.8A). Regions within the nodules appear to be medium grained calcite domains, and the micritic calcite has bands of brown and dark grey material within the nodule (Fig. A.8B). Additionally, the bands show elongate and pinching out lenticular features. The slide also contains isolated curvilinear cylinders (~0.9 mm across) filled with sparry and medium grained calcite.

Minor, small (~0.06 mm) rounded quartz grains are found incorporated within the micritic texture that exhibit undulatory extinction. The margins between the calcite and matrix are abrupt in some regions and more transitional in others. Transitional regions border

over half of the calcite nodule. The transitional texture between the fine-grained matrix and sparry calcite is unique in that it is not the intertonguing texture seen on other sample slides and consists of polygonal sparry calcite filled cylinders that isolate regions of fine matrix.

The matrix on this slide is fine-grained opaque's that contain minor rounded quartz grains (~0.025 mm across). In plane polarized light the matrix appears as elongate regions of dark brown grains that warp around clusters of slightly larger fine grains within the matrix (Fig. A.8C). The matrix is blocked off into distinct pockets of matrix outlined by finer opaques. Several isolated sparry calcite grains are found within the matrix, some of which have inclusions of matrix material within their structures. The matrix is somewhat marbled in texture between fine matrix clusters and opaques.

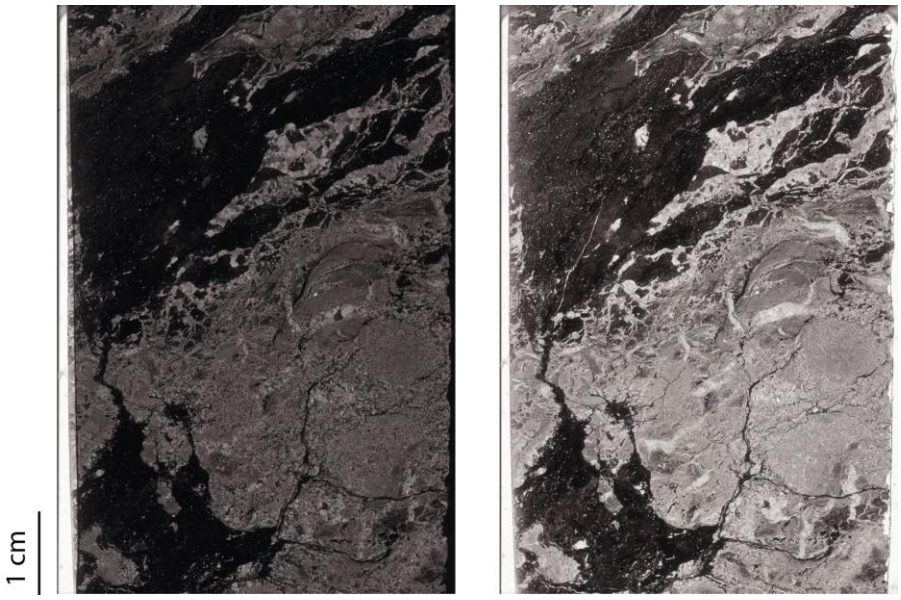

Figure A. 7: Scan of thin section for sample C1, which is shown in cross polars on the left and plane polarized light on the right.

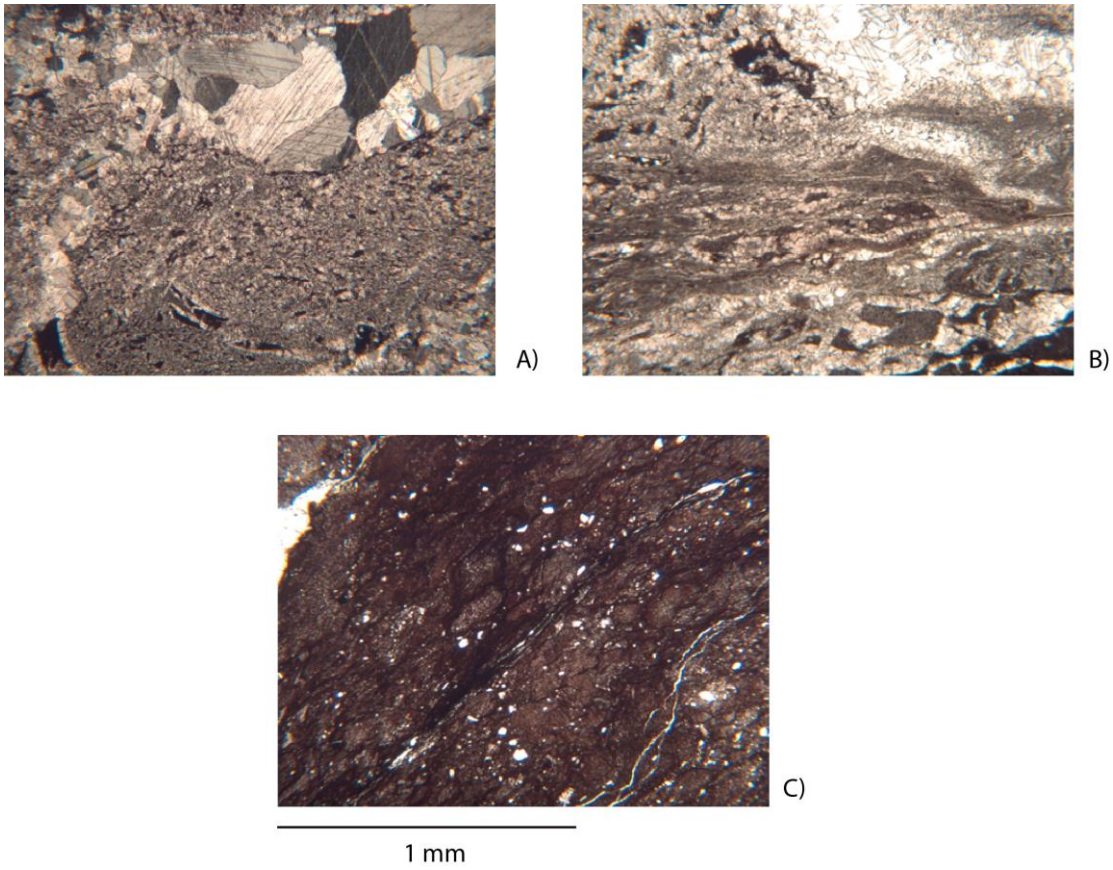

Figure A. 8: A) A portion of the semi-circular horseshoe shape within the micritic calcite that is filled with sparry calcite grains, B) Area within the nodule where the micritic calcite has bands of brown and dark grey material, C) Elongate regions of dark brown grains that warp around lighter brown clusters within the matrix.

C2

Sample C2 contains one band of micritic calcite and one curvilinear cylinder of sparry calcite within a fine-grained matrix (Fig. 5.7). This slide contains 30% calcite, half of which is micritic calcite (Table 5.1). The micrite band of calcite on the slide has frequent small inclusions of sediment within the margins of the band. This calcite region has a transitional zone of anastomosing polygonal cracks filled with calcite that isolate rectangles of matrix between them (Fig. A.9A). In the central portion of the calcite band are several larger inclusions of fine sediment that are ringed by medium grained calcite grains that grade into the micritic sized calcite fabric (Fig. A.9B). The margins of the band of calcite that do not

contain the anastomosing transitional zone instead have medium grained calcite creating a distinct border between the calcite and fine matrix (Fig. A.9B). There are minor, small (~0.025 mm) subangular quartz inclusions within the micrite band (Fig. A.9C).

The curvilinear cylinder contains minimal inclusions of sediment and is almost entirely sparry calcite. The margins between the calcite and sediment are distinct and no gradation or transition is visible. Moving further down the length of the feature, the calcite contains matrix inclusions and anastomosing polygonal channels of calcite that are separated by pockets of matrix.

The matrix that makes up 70% of this slide contains small (~0.025 mm) rounded quartz grains that exhibit undulatory extinction. The quartz grains are aligned within the matrix in long regions that are separated by fine grained matrix lacking any small (~0.025 mm) quartz grains. Isolated rounded calcite grains that appear within the matrix are surrounded by a dark black halo of sediment ~0.025 mm that lightens into a dark brown as you move away from the grain (Fig. A.9D). The matrix contains minimal small (~0.025 mm across) highly birefringent rods, which are infrequently trapped within the calcite band. In plane polarized light the matrix appears dark brown with thin seams of black running through it that appear to align between the dark brown regions creating the appearance of flow structures (Fig. 5.8C).

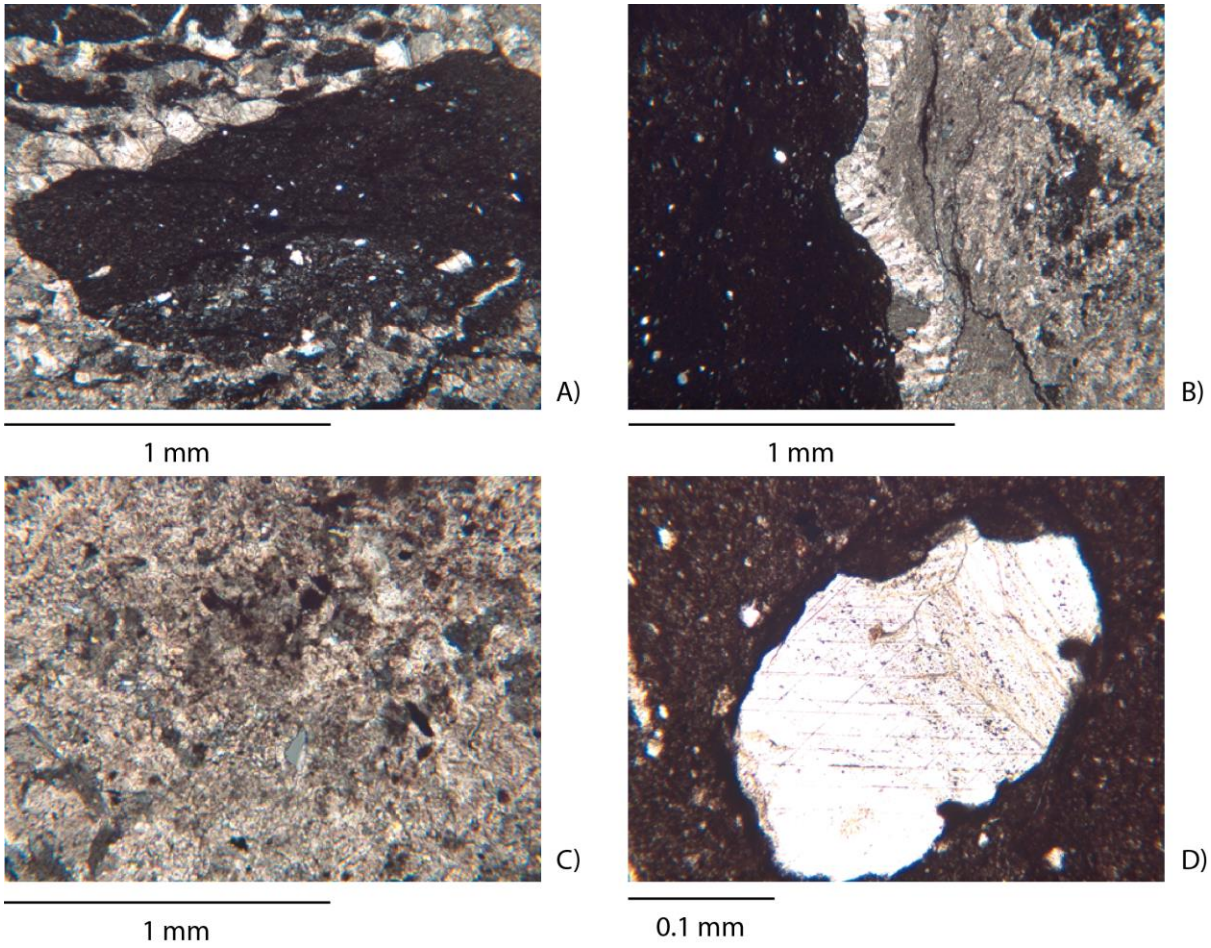

Figure A. 9: A) Pocket of sediment and anastomosing polygonal cracks filled with calcite that isolates rectangles of matrix, B) Pocket of sediment bordered by medium grains of calcite within a calcite nodule, C) Small, grey angular quartz inclusion within a micritic nodule, D) Isolated calcite grain within the matrix that has a dark halo of sediment around it.

C3

Sample C3 contains the most calcite out of the three samples of type C, 80% (Table 5.1). Most of the calcite rich regions have sediment within the nodules or pockets of sediment that appear within polygonal calcite cylinders. Most of the calcite on the slide is medium grained with minor pockets and curvilinear cylinders filled with sparry calcite (Fig. A.10). There are minor quartz inclusions within the micritic fabric of the nodules and some dark red hematite staining as well. There are minimal rounded features that are filled with medium grained calcite that are distinct. Most of these features are curvilinear s or u-shaped channels within the micrite (Fig. A.11A).

The matrix on this slide is made up of fine (~0.025 mm across) grains of rounded quartz that have undulatory extinction. In thicker bands between calcite nodules, the matrix is a dark grey with more small quartz inclusions than within the seams of matrix that run within the nodules which are opaque with few inclusions. A unique transition zone appears as a grey structure with oblong elliptical pockets of dark sediment within it (Fig. A.11B). A fracture separates this from the neighboring calcite nodule region and it is unclear whether the grey region is calcite. One feature of interest is a (~0.05 mm wide) thin linear seam of medium grained calcite that cross cuts the calcite nodule and matrix on the slide. The calcite within the linear seam is more coarse grained and does not contain any inclusions. Within the calcite nodule are several radial calcite spherulites that form around small microcrystalline quartz or calcite grains (Fig. 5.8D). Some of the radial spherulites appear more development than others (Fig. 5.8A). Most of the margins between the calcite and matrix are a medium grain border of calcite, or anastomosing channels of calcite and matrix (Fig. 5.8B).

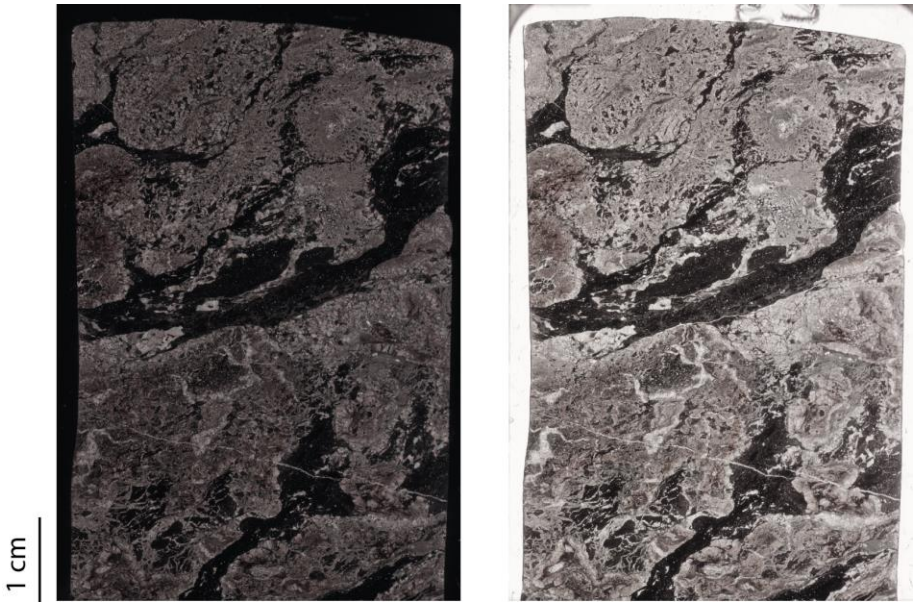

Figure A. 10: Scan of thin section for sample C3, which is shown in cross polars on the left and plane polarized light on the right.

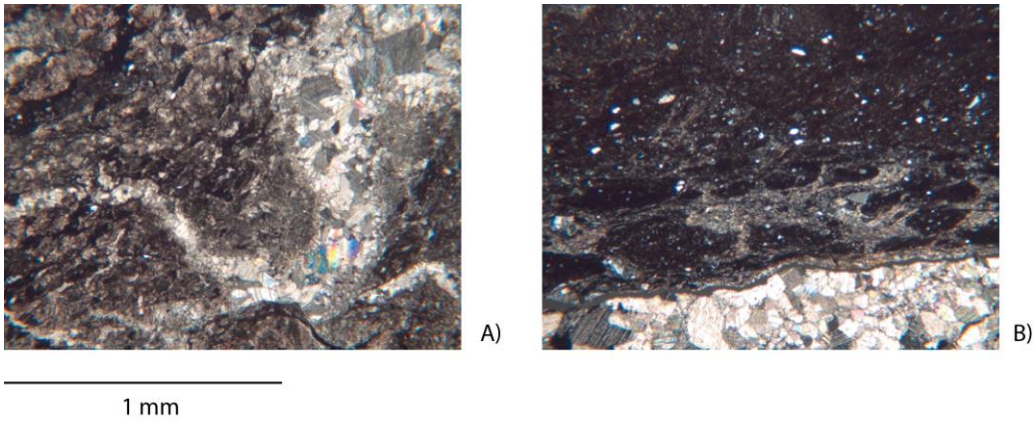

Figure A. 11: A) Curvilinear u-shaped channel filled with medium grained calcite within the micritic nodule, B) Unique transition zone of oblong elliptical pockets of dark sediment outlined in grey minerals.

Thin Sections from Sample Type D

D1

Slide D1 contains mostly sediment (70%) and a few linear bands and circular nodules of calcite (Table 5.1). The calcite is predominately medium coarseness with some sparry calcite and minor micritic calcite. The calcite occurs in discontinuous bands that are broken up by the matrix that separates the circular nodules from the linear bands (Fig. A.12). Within the calcite bands are small, engulfed, rounded and angular quartz grains. The margins of the calcite contain some small highly birefringent grains.

This matrix is coarse grained and predominately made up of quartz grains that range from ~0.025 mm to ~0.19 mm across. Most of the quartz grains are angular and exhibit undulatory extinction. While the matrix consists of small grains, the abundance of these small grains provides an overall coarse appearance to the matrix. There are small (~0.06 mm across) rounded isotropic grains within the matrix and (~0.025 mm across) highly birefringent rounded elliptical shapes and rods. Also, a small lithic fragment was found within the matrix (Fig. A.13A). There are a few circular brown grains within the sediment that are ~0.38 mm across. The matrix is not homogenous across the slide and there are domains of dark brown opaques with well-sorted small (~0.0125 mm across) sub-rounded grains of quartz that are packed between thin curvilinear calcite features (Fig. A.13B). There

are zones of dark yellow and grey that appear near transition areas between calcite and matrix. The areas are visible in plane-polarized light as pale brown moderate to low relief regions with abundant small black dots (Fig. A.13C). Under cross-polars, the region appears as mixed lines of dark orange/brown and black that go extinct at once at different points of rotation (ie. all the dark orange go extinct at the same time and all the black parts go extinct at the same time). The bimodal extinction makes the region stand out as a unique texture that could be a weathering or alteration product.

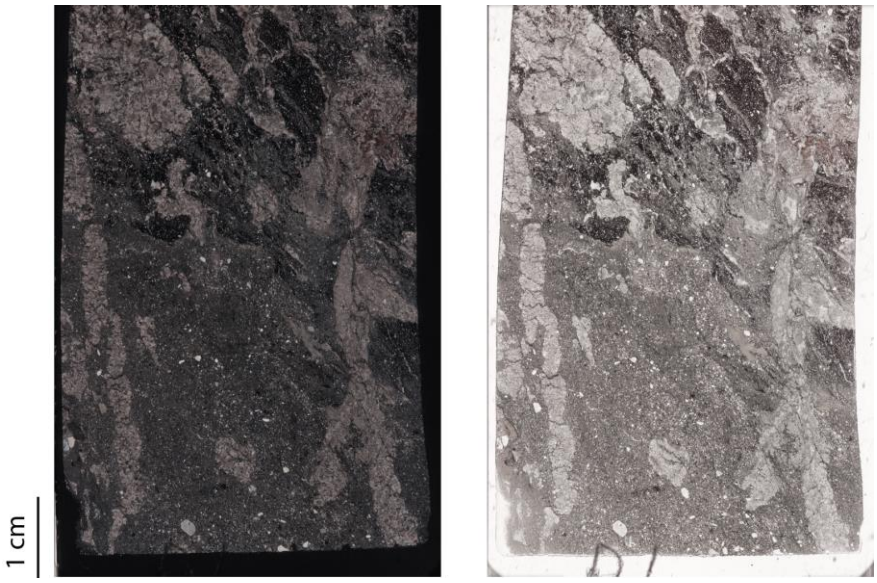

Figure A. 12: Scan of thin section for sample D1, which is shown in cross polars on the left and plane polarized light on the right.

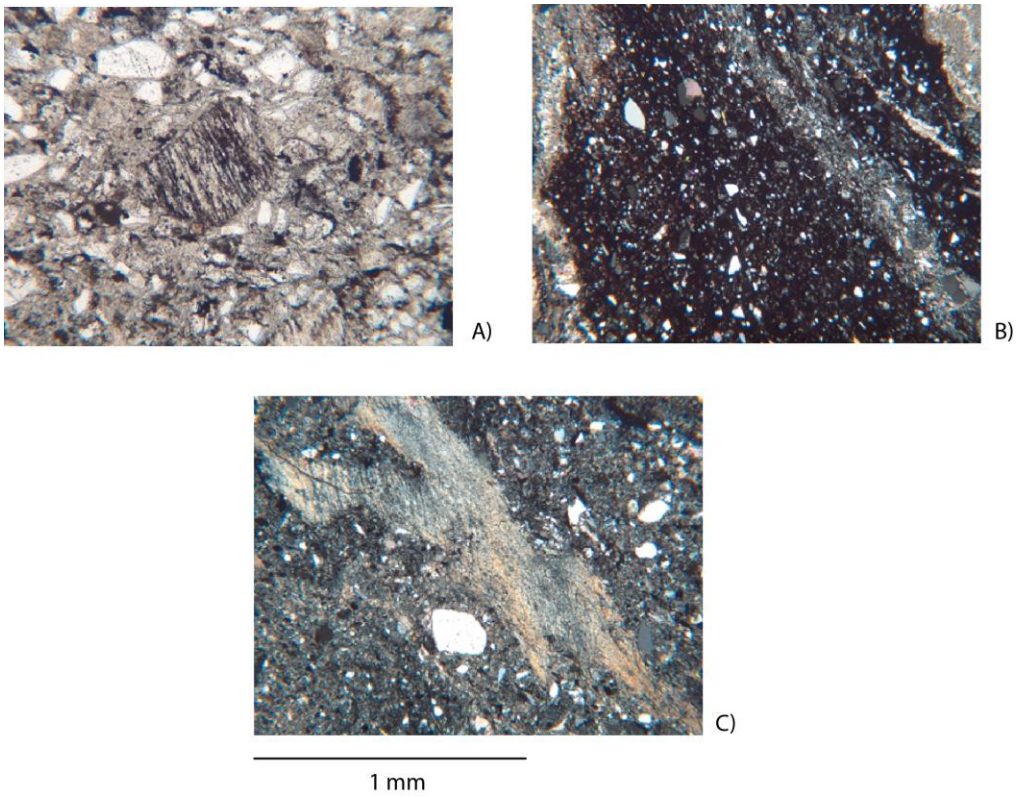

Figure A. 13: A) Possible lithic fragment discovered within the matrix of the sample, located in the center of the photograph, B) Coarse matrix with subroanded grains of quartz and domains of brown opaques, C) Pale brown region is seen in the center of the photograph in plane polarized light with associated grey region.

D2

The calcite on sample D2 is predominately sparry calcite and some medium grained calcite with no micritic calcite on the sample. There is palisade arrangement of the sparry calcite in an arcuate form on several areas of the slide (Fig. 5.9). There are several areas with large concentric grains of calcite that form spherulite structures of calcite (Fig. 5.10B). The calcite nodule has large sparry grains on one side, where it interacts with the transitional thread zoning seen in sample D1. Continuing a transect across the calcite nodule, the grains grade from spar to medium sized calcite and gradually transition into the matrix which is not as sharp of a boundary as the sparry palisade arrangement of calcite on the other side. The blunt stubby cylindrical calcite feature on the slide terminates in a rounded shape that tapers away from the rounded end. This calcite feature contains frequent larger sub angular quartz

grains (~0.5 mm) within the margins of its structure and smaller (~0.025 mm) grains deeper within the calcite area (Fig. 5.10A).

The matrix of this sample has a high number of shard shaped angular quartz grains within it (devitrified glass). Within the matrix are also a number of smaller sub rounded and sub angular quartz grains, all of which have undulatory extinction. There are only a few discrete domains of fine opaques with no small grain inclusions. There are small (~0.025 mm across) acicular rods of highly birefringent grains within the sediment that are not found as inclusions within the sparry calcite regions (Fig. 5.10C).

As in slide D1, a unique texture is visible in plane polarized light as pale brown moderate to low relief regions with abundant small black dots within the sediment that appears more frequently on this slide, occurring along a crack that visible goes through a majority of the slide and ends in sparry calcite (Fig. A.14). Under cross-polars, the region appears as mixed threads of dark orange/brown and black that go extinct at once at different points of rotation (ie. all the dark orange go extinct at the same time and all the black parts go extinct at the same time). This bimodal extinction makes the region stand out as a unique texture that could be due to weathering or alteration of the original composition.

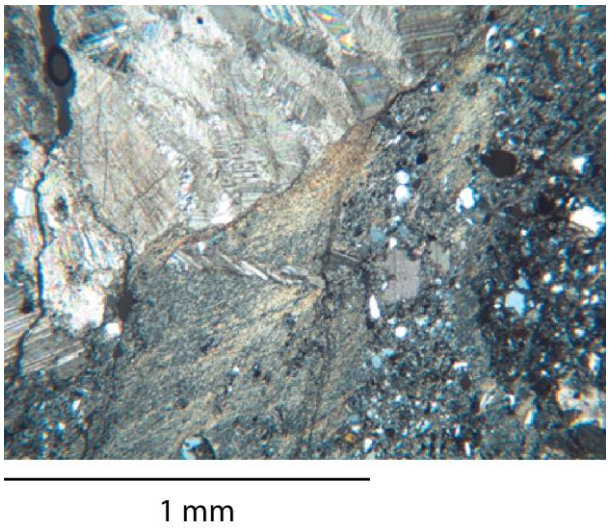

Figure A. 14: Pale brown region is seen in the center of the photograph in plane polarized light.